UNIVERSITY OF
LINCOLN

The Visualisation of Interactions between *Acinetobacter baumannii* and the Antimicrobial Peptides: Colistin Sulphate, Bicarinalin and BP100

By Marcus Eales

Supervised by Dr Clare Miller and Dr Lorna Lancaster

A thesis submitted in partial fulfilment of the requirements for the degree of MSc Biochemistry and Molecular Biology by Research

December 2015

Abstract

It is estimated that there are over 700,000 deaths annually worldwide due to multi-drug resistant (MDR) bacterial infections and by 2050 this is predicted to rise to 10 million. One of these MDR organisms is *Acinetobacter baumannii*, an opportunistic pathogen implicated in pneumonia, meningitis and septicaemia. It is especially difficult to treat due to its ability to become rapidly resistant to a wide range of antimicrobials and persist due to its ability to form biofilms. Biofilms are sessile communities of bacterial cells, attached to surfaces and embedded within a protective polysaccharide matrix, making them 10-1000 times more resistant than their planktonic form.

Antimicrobial peptides (AMPs) are a diverse group of polypeptides that are present in nearly all living things as part of the innate immune system. They are being extensively researched as potential alternatives to classical antibiotics. The objective of this research project was to compare the bactericidal and biofilm activity of two synthetic nature inspired antimicrobial peptides, bicarinalin and BP100, with colistin sulphate. Colistin sulphate is an antimicrobial peptide, currently used as a last resort treatment of *A. baumannii* infections.

The bacteriostatic and bactericidal effects of colistin sulphate, bicarinalin and BP100 on *A. baumannii* 19606 were assessed using microbiological assays and the consequences of peptide action was visualised on single cells of *A. baumannii* using atomic force microscopy (AFM). The changes in the roughness and area of the cell surface at increasing peptide concentrations were determined to quantify the effect of the three different peptides.

The effect of the peptides on biofilm formation was investigated by determining the minimum biofilm inhibition concentration (MBIC) and on preformed biofilms using the biofilm removal assay. Peptide action on the biofilms was visualised by scanning

electron microscopy (SEM) and confocal laser scanning microscopy (CLSM). The nucleic acid stain SYTO9 was used with CLSM to visualise and quantify biofilm bio-volume reduction at increasing concentrations of peptide.

Bactericidal results showed concentrations of 0.5 μg/ml for colistin sulphate and 4 μg/ml for both bicarinalin and BP100. Biofilm removal assay results highlighted that at higher concentrations, both bicarinalin and BP100 had significantly greater biofilm removal potential than colistin sulphate. At peptide concentrations of 1024 μg/ml, biofilm reduction was only circa 50% for colistin sulphate but 65% and 83% for the AMPs bicarinalin and BP100 respectively. At 2048 μg/ml, the highest concentration analysed, BP100 eradicated 95% of the biofilm, nearly twice that of colistin.

AFM illustrated dramatic changes in cell size and membrane conformity when treated with peptides of concentrations at and above the MBC. SEM images showed the decrease in biofilm presence and cellular changes as peptide concentration increased. CLSM images and bio-volume quantification, with increasing peptide concentrations, further reinforced the evidence that bicarinalin and BP100 were more effective than colistin against *A. baumannii* biofilms at high concentrations. At a concentration of 1000 μg/ml, bicarinalin and BP100 removed approximately 50-55% of the biofilms, twice as much as colistin, a trend consistent with the biofilm removal assay results.

The results demonstrated the potential for AMPs as therapeutic alternatives to the currently used treatment against *A. baumannii* infections. Compared to colistin sulphate, bicarinalin and BP100 had generally better removal potential against *A. baumannii* biofilms.

Certificate of Originality

This is to certify that I am responsible for the work submitted in this thesis, that the original work is my own, except as specified in the acknowledgements and in references, and that neither the thesis nor the original work contained therein has been previously submitted to any institution for a degree.

Signature:

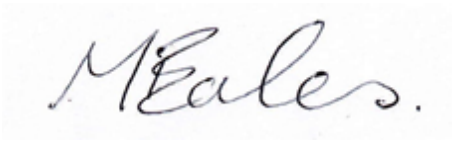

Marcus Eales

Acknowledgements

I would like to give my express gratitude to Dr Clare Miller for her valuable support, advice and guidance throughout this project.

I am also very grateful to Dr Lorna Lancaster for her counsel and encouragement.

My thanks to Martyn Balmont for training me on the confocal laser scanning microscope and also to Dr Enrico Ferrari for training me on the atomic force microscope.

My thanks to Mike Shaw and Philip Skipper for their help with the scanning electron microscope sample preparation.

I am indebted to Dr Richard Walshaw and the Leeds Electron Microscopy & Spectroscopy Centre at the University of Leeds for allowing the use of their scanning electron microscope.

I am very grateful to Laura Pearson for her help using the IBM SPSS 21 software.

Finally, I would like to thank Jane Morris for her company, help and encouragement in the laboratory.

Contents

1 Introduction

1.1 Project Objectives

By 2050, deaths due to antimicrobial resistant (AMR) infections are predicted to rise from 700,000 to 10 million a year worldwide. It is estimated that over the next 35 years, 300 million people will die globally due to AMR infections (O'Neill, 2014). The abuse of currently used antimicrobials and the paucity of novel antimicrobials progressing successfully through clinical trials is a serious concern. The continuous evolution of bacterial resistance mechanisms have led to the prospect of patients dying from minor cuts, childbirth and elemental surgery within the next few decades (Rossolini *et al.*, 2014).

This project involves the opportunistic pathogen *Acinetobacter baumannii* responsible for various infections such as pneumonia, septicaemia, wound infections and meningitis (Maragakis and Perl, 2008). It is clinically important due to its ability to become rapidly resistant to a wide range of antimicrobials and also to persist on clinical surfaces by forming biofilms. Biofilms are structured consortia of bacteria embedded in a self-produced polymer matrix consisting of polysaccharide, protein and DNA, leading to a significantly increased tolerance to antimicrobials (Høiby *et al.*, 2010).

The aim of the research project is to investigate the effectiveness of specific antimicrobial peptides (AMPs) against *A. baumannii* which may be useful alternatives to currently used antibiotics. AMPs are a diverse group of polypeptides that are present in nearly all living things as part of the innate immune system (Lakshmaiah *et al.*, 2015). They are being researched as potential alternatives to classical antibiotics due to their ability to kill multi-resistant (MDR) bacteria (Li *et al.*, 2012). The project

examines the activity of two little researched antimicrobial peptides, bicarinalin and BP100. Bicarinalin is a peptide isolated from ant venom (Rifflet *et al.*, 2012; Téné *et al.*, 2014), and BP100 is a synthetic hybrid of two peptides derived from bee venom and the haemolymph of a moth (Manzini *et al.*, 2014; Alves *et al.*, 2010). The effectiveness of these peptides was compared to the currently used antibiotic colistin sulphate which is commonly used as a last resort treatment for multi-drug resistant *A. baumannii* infections (Falagas *et al.*, 2010; Potron *et al.*, 2015).

The methodology involved using microbiological assays and advanced visualisation techniques such as Scanning Electron Microscopy (SEM), Confocal Laser Scanning Microscopy (CLSM) and Atomic Force Microscopy (AFM).

To investigate the effectiveness of bicarinalin and BP100 compared to colistin sulphate against planktonic *A. baumannii* cells, the minimum inhibitory concentration (MIC) and minimum bactericidal concentration (MBC) were determined. The consequence of interactions between each of the three antimicrobials and the bacterial cells was visualised at increasing concentrations (normalised to the MBC) using the AFM. The effects on the cell were also quantified by measuring the change in cell roughness and surface area at increasing concentrations for each antimicrobial.

The minimum biofilm inhibitory concentration (MBIC) was determined to assess the ability of *A. baumannii* to form a biofilm in the presence of increasing concentrations of the three AMPs. The relative effectiveness of each peptide against preformed biofilms was quantitatively investigated at increasing peptide concentrations using the biofilm removal assay. The consequence of interactions between each of the antimicrobials and the *A. baumannii* biofilms was also visualised at increasing concentrations using the SEM and CLSM. The effects on the biofilms were also quantified, using CLSM, by measuring the bio-volume of a biofilm with the CLSM at increasing concentrations for each antimicrobial.

1.2 Project Outline

The fundamental theory and a summary of previous research are described in **Chapter 2**. The characteristics of *A. baumannii*, including the formation of its biofilms, are examined. The nature and antimicrobial mechanisms of the antibiotic, colistin sulphate and the two peptides, bicarinalin and BP100, are also discussed. The visualisation techniques used (AFM, SEM and CLSM) and the advantages and limitations of each microscope are compared.

Chapter 3 discusses the materials and methods used. Tests were carried out to identify *A. baumannii* and its growth curve was determined to ensure reliable and practical assay techniques. Each experiment required a preliminary calibration to ensure a standard initial viable cell count of $5x10^5$ colony forming units (CFU)/ml and hence consistent comparisons between the results. The methods and sample preparations are described in detail to permit further repeats of the experiments and independent validations of the results. The assay methods are explained to determine the MIC, MBC, to grow the biofilms and hence to determine the MBIC and biofilm removal with increasing peptide concentration. The preparation and visualisation techniques are described for the AFM, SEM and CLSM including the methodologies used to determine cell surface roughness, cell surface area and bio-volume of the biofilm. All experiments were repeated several times to achieve reliable results and the statistical analyses are also discussed.

Chapter 4 describes the results of the microbiological assays and microscopic analysis. The MIC, MBC and MBIC are determined for the three AMPs. The results of the microscope visualisations are presented showing the effects on individual cells of *A. baumannii* and on *A. baumannii* biofilms when subjected to increasing peptide concentrations. For each antimicrobial, the cell surface area and roughness were quantified using AFM and biofilm bio-volume was quantified with CLSM. As the

measurements were made several times over a number of different experiments, the statistical confidence was indicated by error bars and statistical tests.

Chapter 5 discusses the results and makes recommendations for further research.

Further details of the identification techniques and results are included in the **Appendix**.

2 Fundamental Theory

2.1 Antimicrobial Resistance

Since the discovery of the antibiotic Penicillin by Alexander Fleming in 1928, healthcare and medicine have been revolutionised. Antibiotics have allowed complicated surgeries and treatment such as caesarean sections, chemotherapy, joint replacements and organ transplants to become commonplace in clinical practice. As a result, they have contributed to the increase of the average life span worldwide (Rossolini *et al.*, 2014).

However, antimicrobial resistant (AMR) infections currently claim at least 50,000 lives each year in Europe and USA and hundreds of thousands in other parts of the world. It is estimated that, over the next 35 years, 300 million people will die globally due to AMR infections. By the year 2050 there could be as many as 10 million deaths attributed to AMR each year worldwide (O'Neill, 2014). In financial terms, the consequences of AMR is also considerable. By 2050, the world's Gross Domestic Product (GDP), is estimated to be reduced by 2-3.5%, equating to a loss of about £65 trillion (O'Neill, 2014).

2.1.1 The Current Dilemma

One of the main problems in the treatment of bacterial infections is that, unlike most other drugs used in clinical treatment, antibiotics lose their efficacy over time. This means new antibiotic classes need to be discovered constantly as bacteria mutate to become resistant against the older classes. The period from the 1930s to the 1960s has been termed the 'golden era' of antibiotic research when most of the currently administered classes of antibiotics were discovered (**Figure 2.1.1**). From the 1970s to

2000 the antibiotic pipeline dried up. However, more recently twenty-two new antibiotics have been introduced associated with five new classes; linezolid (2000), daptomycin (2003), retapamulin (2007), fidaxomicin (2010) and bedaquiline (2012) (**Figure 2.1.1**). The introduction of bedaquiline was accelerated through clinical trials to help treat tuberculosis (Butler *et al.*, 2013; Rossolini *et al.*, 2014a).

Although the launch of these recent novel antibiotic classes is a reason for short term optimism, they are all limited to the treatment of Gram-positive infections while it is the Gram-negative infections caused by pathogens such as *Pseudomonas aeruginosa*, *Acinetobacter baumannii* and those of the *Enterobacteriaceae* family, that are in more urgent need of new therapies (Butler *et al.*, 2013; Rossolini *et al.*, 2014).

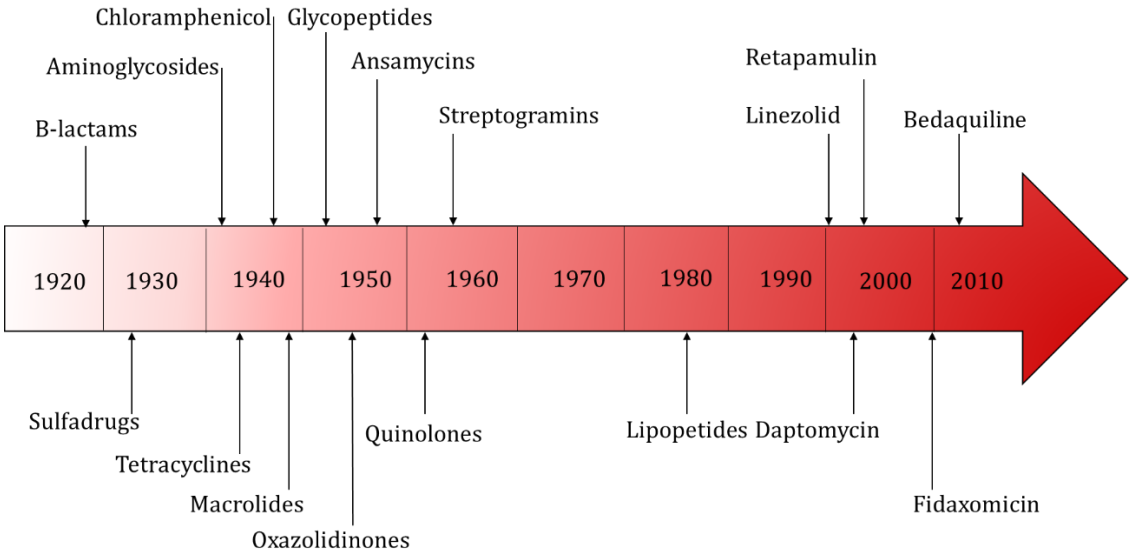

Figure 2.1.1- Timeline of the Antibiotics from 1920s to present day *(Lewis, 2012; Butler et al., 2013)*

2.1.2 Origins of Antibiotic Resistance

The appearance of multi-drug resistant (MDR) strains of bacteria arises through several different mechanisms such as alterations of the antibiotic target, changes in cell

permeability, efflux pumps within the cell membrane and the expression of resistance genes obtained from other cells by horizontal gene transfer (Rodríguez-Rojas *et al.*, 2013).

Some antibiotics have been found to increase the mutation rate by promoting mutations within the bacteria. The induction of stress responses causes oxidative damage through the production of reactive oxygen species. This results in damage to cellular proteins, DNA and lipids which could lead to mutagenesis (Rodríguez-Rojas *et al.*, 2013).

2.1.3 Combating Antimicrobial Resistance

As antimicrobial resistance becomes more problematic globally, it is vital to promote national and international policies to tackle the problem. It is essential to increase antimicrobial resistance awareness within the health and agricultural sectors and with the education of the general public. This would lead to a reduction in demand for antibiotic treatment, the unnecessary waste or discarding of antibiotics into the environment and reduction of antibiotic usage in agriculture and livestock (Rossolini *et al.*, 2014).

This increased awareness must also include healthcare staff and more stringent guidelines regarding prescription allocation by GPs. This will be helped by better diagnostics, reducing the dissemination of MDR organisms by surveillance of MDR strains, antimicrobial stewardship programs and infection control practices (Rossolini *et al.*, 2014; O'Neill, 2015). Optimising the currently available antimicrobial therapy regimens with effective dosing, drug combinations and local rotating of drug usage will also help to control antimicrobial resistance (Rossolini *et al.*, 2014).

Better focused financial incentives or benefits for pharmaceutical companies would encourage them to invest more into antibiotic discovery and development programs as well as suitable alternatives to antibiotics such as antimicrobial peptides, polymers, vaccines and phage therapy (O'Neill, 2015; Rossolini *et al.*, 2014). In 2008, a change in the framework of phase III clinical trials by the US Food and Drug Administration (FDA), has made it more financially beneficial to consider investing in the development of new antibiotics whereas previously high costs and poor returns deterred many large pharmaceutical companies from conducting effective antibiotic research (Butler *et al.*, 2013).

2.2 *Acinetobacter baumannii*

This research project investigated the effects of three antimicrobial peptides on one specific species of the bacterial genus *Acinetobacter* which is a cause of many deaths especially in hospital environments (Isa *et al.*, 2014).

Acinetobacter baumannii is an opportunistic Gram-negative, strictly aerobic, oxidase-negative coccobacillus (Giamarellou *et al.*, 2008; Abbott *et al.*, 2013). Most Acinetobacter species are clinically irrelevant and ubiquitously found in the environment such as the normal microbiota of human skin, animals, water and soil (Abbott *et al.*, 2013). However, *A. baumannii* is found almost exclusively in the hospital environment and is particularly prevalent in intensive care units and burns units; it has been reported to be responsible for between 2-10 % of all Gram-negative hospital infections (Isa *et al.*, 2014).

A. baumannii is is closely related phenotypically to other *Acinetobacter* species such as *A. calcoaceticus*, *A. pittii* and *A. nosocomialis*. As a result, it is very difficult to distinguish between the four species with phenotypic tests, so together they have been grouped together as the *A. calcoaceticus-A. baumannii* complex (Abbott *et al.*, 2013; Toh *et al.*, 2015).

2.2.1 Clinical Relevance

Acinetobacter baumannii is the most clinically relevant species of the *Acinetobacter* genus and, due to the emergence of MDR strains, it is recognised as a major opportunistic pathogen by its inclusion as a member of the 'ESKAPE' group. This group includes *Enterococcus faecium*, *Staphylococcus aureus*, *Klebsiella pneumonia*, *Acinetobacter baumannii*, *Pseudomonas aeruginosa* and *Enterobacter* species. This

group causes the majority of hospital acquired infections and collectively requires new innovative practices to combat their pathogenesis, transmission and resistance (Boucher *et al.*, 2009; Rice, 2008).

A. baumannii is able to persist in the environment for long periods of time due to its ability to grow at a wide temperature and pH range, survive in both moist and dry conditions and exploit different energy sources. Environmental sources of outbreaks of *A. baumannii* such as curtains, door handles, mops and medical equipment have highlighted its ability to colonise and persist for long periods outside the human body (Isa *et al.*, 2014; Maragakis and Perl, 2008). This persistence, along with intrinsic resistance to many antimicrobials, enables the pathogen to cause widespread epidemic infections within the hospital setting (Maragakis and Perl, 2008).

A. baumannii has been implicated in a wide variety of hospital infections. Two with the highest mortality rates are ventilator associated pneumonia and septicaemia (Isa *et al.*, 2014). Other infections include meningitis, endocarditis, skin and soft tissue infections, urinary tract infections and wound infections (Maragakis and Perl, 2008; McConnell *et al.*, 2013).

Risk factors for *A. baumannii* infection include old age, use of mechanical ventilation during treatment, weakened immune system as a result of chemotherapy, prolonged hospital stay (especially in intensive care units), invasive procedures such as surgery and intravascular catheters, alcoholism, heavy smoking and underlying illnesses such as, diabetes mellitus, AIDS, and renal diseases (Isa *et al.*, 2014; Maragakis and Perl, 2008).

2.2.2 Virulence and Pathogenesis

No one virulence factor has been found to be solely responsible for the clinical success of *A. baumannii* but a variety of virulence factors have been identified suggesting a multifactorial strategy for virulence.

There are four main areas of virulence factors in *A. baumannii*:

1. Outer Membrane proteins and Lipopolysaccharide
2. Iron Acquisition Systems
3. Lypolytic Enzymes
4. Biofilm Formation

It has been suggested that the **outer membrane protein** OmpA (Omp36) has roles in bacterial avoidance of immune systems such as complement mediated killing by interacting with inhibitors of the alternative complement pathway within the human body. The protein is believed to induce apoptosis in epithelial cells, through release of pro-apoptotic molecules such as cytochrome, and assisting in biofilm formation and surface motility (McConnell *et al.*, 2013).

A. baumannii is a Gram-negative organism which means its cell wall consists of a thin peptidoglycan layer and a protective outer membrane made up of phospholipids and lipoproteins as shown in **Figure 2.2.1** (Silhavy *et al.*, 2010; Cabeen and Jacobs-Wagner, 2005).

The **lipopolysaccharide (LPS)** is the main constituent of the outer leaflet of the outer cell membrane and consists of three components: O-antigen repeats and core oligosaccharides anchored to the phospholipid layer by the third component lipid A. Lipid A has been described as an endotoxin and shown to be a potent inducer of pro-inflammatory cytokine expression in human monocytes (Isa *et al.*, 2014).

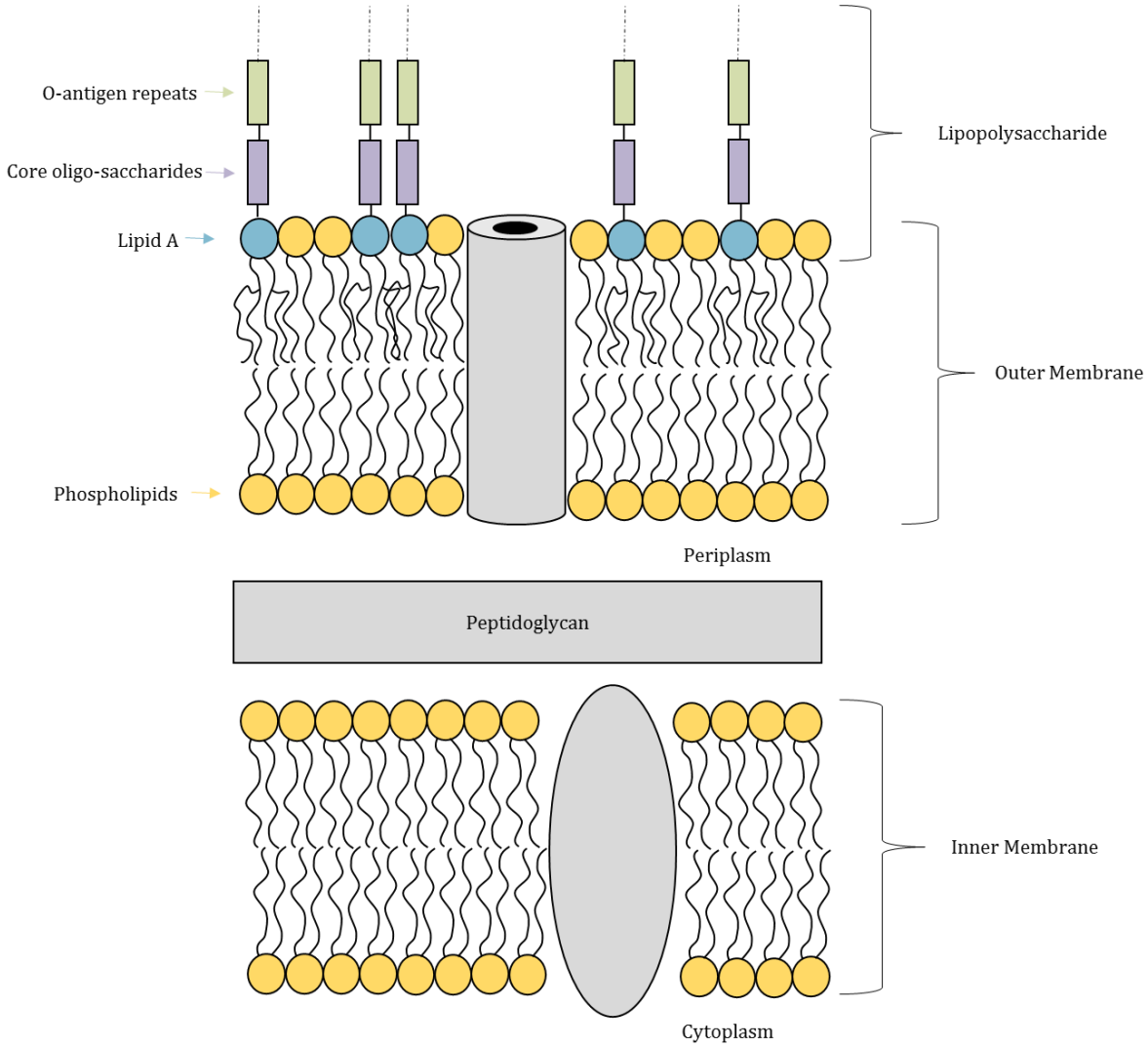

Figure 2.2.1- ***Cell membrane and Gram negative wall of A. baumannii,*** *showing the inner membrane, peptidoglycan layer, outer membrane and lipopolysaccharide leaflet components (Cabeen and Jacobs-Wagner, 2005).*

Iron acquisition systems are important virulence factors in *A. baumannii* by allowing it to survive and persist in limited iron conditions within the human host where most iron is sequestered by haemoglobin, transferrin and lactoferrin (Gordon and Wareham, 2010; Gaddy *et al.*, 2012; Eijkelkamp *et al.*, 2011).

Lypolytic enzymes such as phospholipases C and D, have been implicated in epithelial cell invasion by cleavage of phospholipids present in host cell membranes and survival in human serum (Isa *et al.*, 2014; McConnell *et al.*, 2013).

Biofilms can be defined as a structured consortium of bacteria, embedded in a self-produced polymer matrix composed of polysaccharide, protein and DNA (Høiby *et al.*, 2010). This ability for *A. baumannii* to form biofilms is one of the main reasons why it is so prevalent in the clinical setting. The nature, formation and clinical relevance of *A. baumannii* biofilms are further explained in **Section 2.3**.

2.2.3 Resistance Mechanisms

The intrinsic resistance to certain antibiotics includes the presence of an outer membrane, which limits the access of antimicrobial to intracellular targets (Poole, 2001), and the presence of certain enzymes. The acquisition of genes from transferable plasmids, transposons and integrons can lead to acquired resistance. The resistance mechanisms of *A. baumannii* fall into three categories:

1. Antimicrobial-inactivating enzymes
2. Changes in the antimicrobial target or cellular function due to mutations/gene transfer.
3. Reduced access to bacterial targets

Antimicrobial inactivating enzymes: *A. baumannii* contains genes, many of which are acquired by horizontal gene transfer, enabling it to synthesise enzymes that confer resistance against a wide range of antibiotics. β-lactams, such as penicillin, carbapenems and cephalosporins, are all related by the presence of the β-lactam ring (seen in penicillin in **Figure 2.2.2**). They exert their bactericidal activity by interfering with the cell wall and nucleic acid synthesis and inhibiting protein synthesis and metabolic pathways. *A. baumannii* is able to synthesise β-lactamases; enzymes that are able to cleave amide and ester groups conferring resistance against many of this

antibiotic group. Other genes acquired by *A. baumannii* encode for enzymes include (Camp & Tatum, 2010; Bonomo & Szabo, 2006; Maragakis & Perl, 2008):

- AmpC cephalosporinases which confer resistance to broad spectrum cephalosporins.
- Acetyltransferases, nucleotidyl-transferases and phosphotransferases that promote resistance to fluoroquinolones and members of the quinolone class.
- Aminoglycosides, another class of antibiotic that includes gentamicin and amikacin.

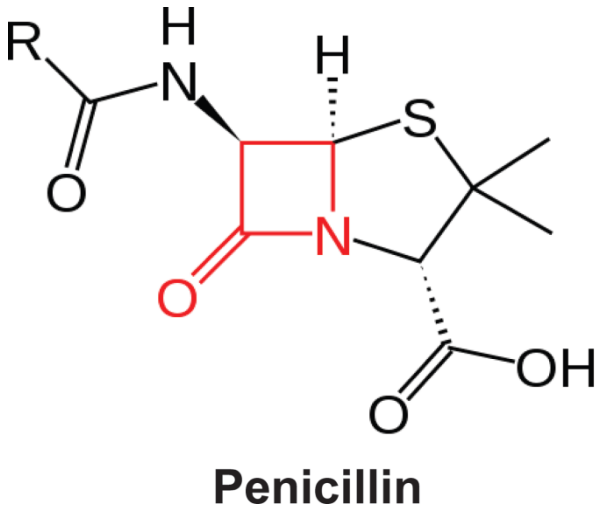

***Figure 2.2.2- Diagram of the β-lactam ring within penicillin**, (highlighted in red) (Zeng and Lin 2013).*

Mutations in genes within the bacteria, or acquired from other bacteria, can lead to alterations in antimicrobial bacterial targets, such as on the lipopolysaccharide layer of the outer membrane. This results in a reduced affinity for the antimicrobial target or an alteration in up-regulating cellular functions such as the production of efflux pumps. These pumps have the ability to actively expel β-lactams, aminoglycosides and quinolones from the cell (Camp and Tatum, 2010; Bonomo and Szabo, 2006; Maragakis and Perl, 2008).

Reduced access: outer membrane proteins (OMPs) and porins transport antimicrobial agents into the periplasmic space enabling them to access targets such as penicillin-binding proteins. A loss of these transport proteins reduces the concentration of antimicrobials, such as carbapenems, entering the cell allowing β-lactamases to break down the antimicrobial (Camp and Tatum, 2010; Bonomo and Szabo, 2006.; Maragakis and Perl, 2008).

2.2.4 Current Therapies

Due to the increasing resistance rates of *A. baumannii,* treatment is becoming progressively more difficult. Current antibiotic treatments include the following:

- The β-lactam class, carbapenems including meropenem and imipenem remain the treatment of choice.
- β-lactamase inhibitors such as sulbactam are also used due to their potent activity against many *A. baumannii* strains.
- Tigecycline, a glycylcycline antibiotic, has been used (Kassamali *et al.*, 2015).
- Colistin sulphate, a member of the polymyxin family, is used as a last resort treatment. Its effectiveness against *A. baumannii* was analysed in this research project and more information about its specific mechanism of action and *A. baumannii*'s mechanisms of resistance are further explained in **Section 2.4.4** (Maragakis and Perl, 2008).

2.3 Biofilms

A biofilm can be defined as a structured consortium of bacteria embedded in a self-produced polymer matrix consisting of polysaccharide, protein and DNA (Høiby *et al.*, 2010). Biofilms have been shown to have an increased tolerance to antimicrobials, of about 10-1000 times that of planktonic forms, although the cells themselves still show the same susceptibility when a biofilm is disrupted (Bjarnsholt, 2013; Høiby *et al.*, 2010; Mah *et al.*, 2003).

Biofilm growth can occur on biotic surfaces such as teeth and lungs and abiotic surfaces such as prosthetic joints, catheter and stents. As a result, biofilms have been implicated in persistent, chronic infections such as dental plaques, tuberculosis, otitis media, osteomyelitis (Høiby *et al.*, 2010). 65-80% of all infections are thought to be biofilm related (Van Acker *et al.*, 2014).

2.3.1 Formation of Biofilms

Biofilm formation is a multistage process consisting of four phases as summarised in **Figure 2.3.1**:

1. Attachment of planktonic cells to an interface
2. Formation of micro-colonies
3. Maturation of the biofilm
4. Detachment of cells from the biofilm

For *A. baumannii* to initially adhere to a surface, it forms pili via the CsuA/BABCDE usher-chaperone assembly system; this is regulated by the two component BfmS/BfmR system with a sensor kinase encoded by bfmS and a response regulator encoded by

bfmR (Gaddy *et al.*, 2009; Longo *et al.*, 2014). The outer membrane protein, OmpA, is also thought to have a role in the attachment to certain surfaces (Longo *et al.*, 2014). The extracellular polysaccharide poly-β-(1, 6)-N-actylglucosamine (PNAG), encoded from the pgaABCD operon, is thought to be involved in intercellular binding within the biofilm (Brossard and Campagnarl, 2012; Longo *et al.*, 2014).

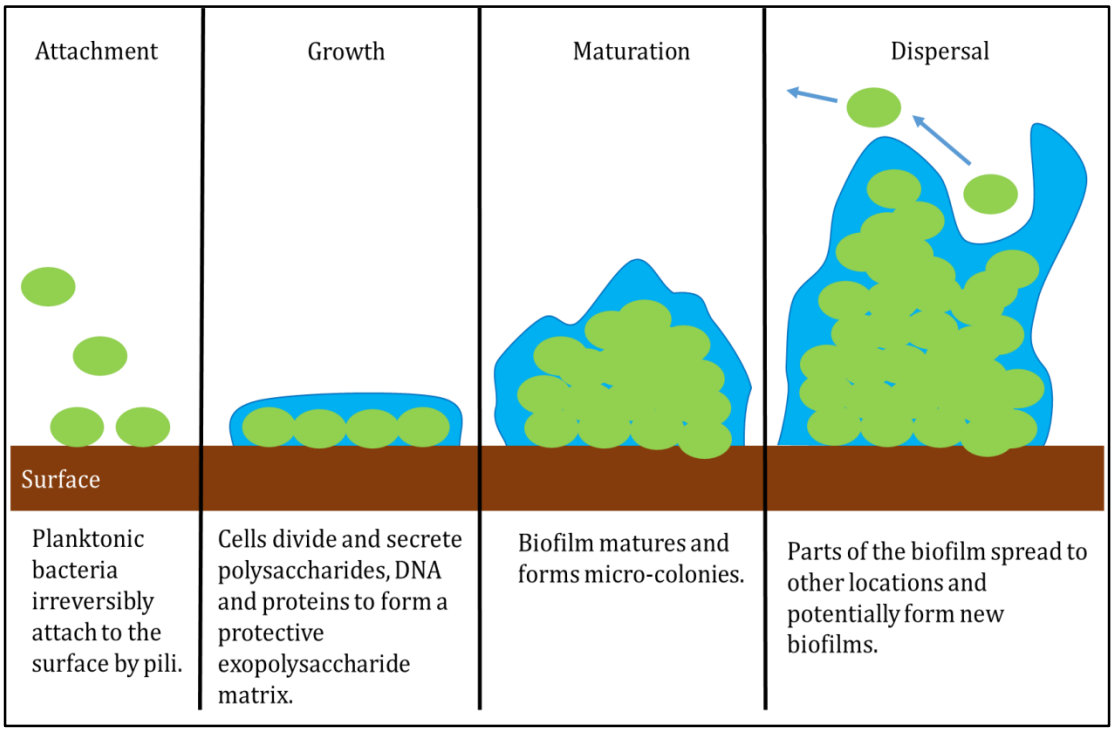

Figure 2.3.1-The lifecycle of a biofilm. *Four stages are illustrated: attachment, growth, maturation and dispersal* (Donlan and Costerton, 2002; Høiby *et al.*, 2010).

The biofilm-associated protein (Bap) is believed to have a role in biofilm maturation and maintenance by increasing the cell surface hydrophobicity which is thought to help the binding to normal human bronchial, epithelial and neonatal keratinocyte cells. Bap is also necessary for the formation of water channels and 3D micro-colony formation (Brossard and Campagnarl, 2012; Lin, 2014). Cell to cell signalling in Gram-negative bacteria is usually mediated by the production of *N*-acyl-homoserine lactone (AHL) signalling molecules. *A. baumannii* contains the abaI gene which encodes for an AHL

molecule AbaI which is believed to have a role in quorum sensing (Bhargava *et al.*, 2010; Niu *et al.*, 2008).

2.3.2 Antimicrobial Resistance in Biofilms

Biofilms have been shown to help bacteria survive in the environment and protect them from host immune systems and antimicrobial agents. Several mechanisms are considered to be involved in biofilm tolerance and resistance:

1. Changes in the chemical microenvironment within the biofilm leading to sub-populations within the biofilm.
2. Higher mutation rate and horizontal gene transfer.
3. Upregulation of efflux pumps.

Changes in chemical microenvironment: oxygen and nutrient levels decrease from the surface of the biofilm to the inner layers. As a result, some bacteria within the biofilm exhibit stationary phase physiology with slow metabolic and growth rates. Some antibiotics, such as β-lactams, require metabolically active cells to exert their bactericidal activity (Høiby *et al.*, 2010). However, other research has demonstrated that bacteria with higher metabolic activity are more resistant against colistin as bacteria in the inner layers of the biofilm were killed and those on the outer layers survived (Nuri *et al.*, 2015; Donlan and Costerton, 2002).

Mutation rate: the increase in mutation frequency and horizontal gene transfer within a biofilm involves the reduced expression of DNA repair genes and an elevation in oxidative stress (Nuri *et al.*, 2015).

Efflux pumps have been shown to confer antimicrobial resistance in many bacteria in both planktonic and biofilm states and also to be upregulated when in a biofilm (Nuri *et al.*, 2015).

2.4 Antimicrobial Peptides

With over 2400 catalogued, antimicrobial peptides (AMPs) represent a diverse group of polypeptides. They are commonly short in length (15-50 amino acids), usually amphipathic and have a net positive charge. AMPs are involved in the innate immune system of practically all living things including plants, invertebrates, fish, and mammals (Li *et al.*, 2012; Lakshmaiah *et al.*, 2015).

2.4.1 Natural Function

The primary function of AMPs involves killing pathogenic organisms such as bacteria, fungi, parasites and viruses. They also have a role in the induction of angiogenesis, wound repair, chemotaxis of immune cells to sites of inflammation, and the neutralization of endotoxins or septic effects of bacterial molecules such as lipopolysaccharide. AMPs can be present within primary barriers, preventing the colonisation of tissues by bacteria, fungi and viruses; they are also within phagocytes, as part of granules, to enhance phagocytosis (Jenssen *et al.*, 2006; Guaní-Guerra *et al.*, 2010).

2.4.2 Antimicrobial Mechanism

AMP characteristics consist of a net cationic charge, the ability to assume a range of secondary structures such as α-helices or β-sheets and being amphipathic, by containing both hydrophilic and hydrophobic regions (Brogden, 2005). A key difference in the composition of bacterial membranes compared to eukaryotic membranes is the presence of a net negative charge, instead of a neutral charge. This results in greater affinity of cationic peptides binding to bacterial cells (Laverty *et al.*, 2011). The first interaction between the peptide and bacterial cell surface is thought to be electrostatic attraction due to the difference in charge (Brogden, 2005). When the peptides attach to the cell surface, they interact with the membrane's lipid bilayers exerting their bactericidal effects by:

1. Membrane disruption leading to cell lysis
2. Formation of transient pores resulting in the transportation of peptides into the cell to interact with intracellular targets

Hydrophilic positively charged domains of the AMPs interact with the negatively charged microbial surface and head groups of the phospholipids to cause cell penetration (Li *et al.*, 2012). There are four commonly described modes of membrane interaction of AMPs:

1. The Toroidal Pore Model
2. The Carpet Model
3. The Barrel Stave Model
4. The Aggregate Channel Model

The toroidal pore model (**Figure 2.4.1**) involves the peptide binding and inserting itself perpendicularly into the cell membrane by electrostatic interactions between the phospholipid head of the bilayer and the hydrophilic regions of the peptide. This leads

to a positive curvature of the bilayer so the peptides and lipid head groups both line the pore (Maria-Neto *et al.*, 2015).

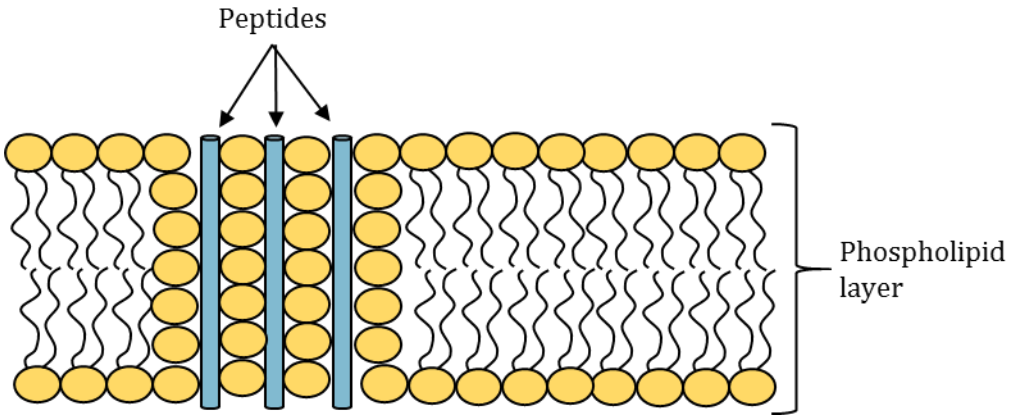

Figure 2.4.1-Simplified image of the toroidal pore model. *Pores are composed of peptides and phospholipid head groups causing local change of membrane thickness.*

In the **carpet model** (**Figure 2.4.2**), the AMPs cover the cell surface, until a threshold concentration is achieved; micelles are formed along with the formation of pores through the membrane (Laverty *et al.*, 2011; Li *et al.*, 2012; Nguyen *et al.*, 2011; Maria-Neto *et al.*, 2015).

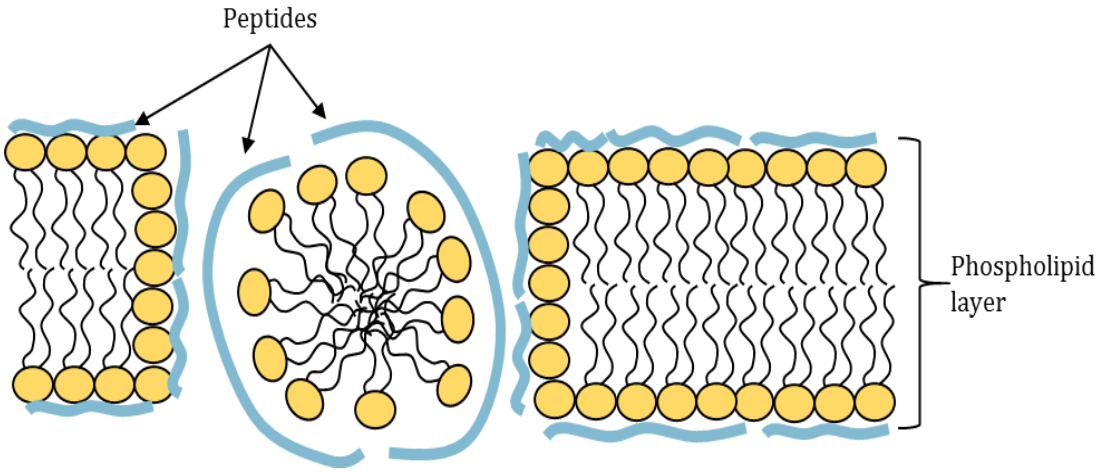

Figure 2.4.2-Simplified image of the carpet model. *The AMP breaks off membrane lipids into micelle-like structures.*

The barrel stave model (**Figure 2.4.3**) is similar to the toroidal pore model whereby the peptides insert themselves perpendicularly into the membrane and form barrel-like clusters creating transmembrane pores. This can result in cell death by leakage of cellular contents and loss of polarisation across the membrane (Laverty *et al.*, 2011; Li *et al.*, 2012; Nguyen *et al.*, 2011; Maria-Neto *et al.*, 2015).

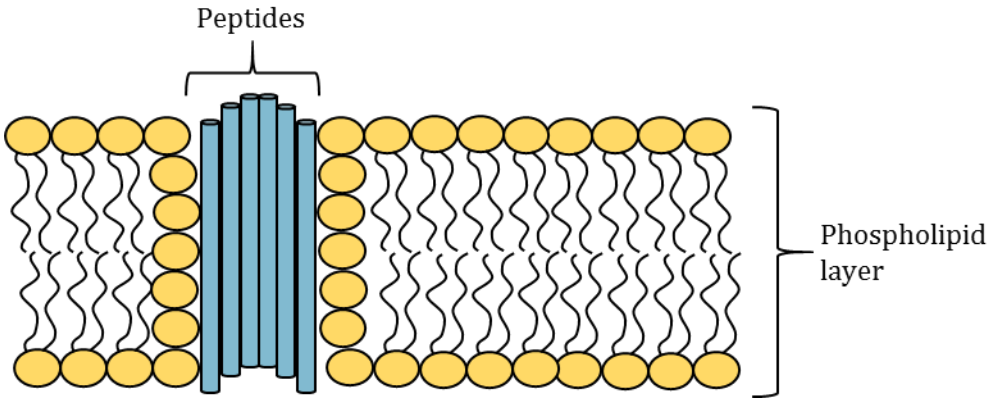

Figure 2.4.3-Simplified image of the barrel stave model. *Peptides form lined pores across the membrane.*

The aggregate channel model involves competitive displacement of cations Mg^{2+} and Ca^{2+} within the lipopolysaccharide resulting in membrane destabilisation (Li *et al.*, 2012).

Along with interacting with the bacterial cell membrane, AMPs have been shown to interact with intracellular targets. By binding to DNA, RNA and proteins, they interfere with cell wall synthesis, nucleic acid synthesis, protein synthesis and enzymatic activity (Brogden, 2005; Li *et al.*, 2012).

2.4.3 Advantages and Disadvantages of AMPs

Most AMP action is a result of the initial electrostatic interaction between the positive domains of the AMP and the negative bacterial surface. The bacteria will therefore need

to extensively alter the properties of their membrane, not just specific receptors often seen in classical antibiotic resistance, to become less susceptible to AMPs (Li *et al.*, 2012).

The advantages of AMPs include:

1. Rapid onset killing.
2. Broad-spectrum activity.
3. Bactericidal activity.
4. Specific targets/receptors on the cell surface not needed for bactericidal activity.
5. Potentially low levels of induced resistance.
6. Concomitant broad anti-inflammatory activities (Gordon and Romanowski, 2005).

There have been reports of resistance against antimicrobial peptides and the resistance mechanisms have been found to be similar to the mechanisms against antibiotics. These mechanisms include alterations in the net surface charge, alterations in lipid A, changes in outer membrane protein production, production of proteolytic enzymes and role of membrane transporters (Brogden, 2005).

Disadvantages of AMPs include:

1. Cytotoxicity.
2. Susceptibility to proteolytic degradation.
3. Liable to change depending on environment such as pH.
4. Cost of manufacturing and synthesis.
5. Intrinsic resistance (Gordon and Romanowski, 2005).

Most current AMP drugs undergoing clinical trials are for topical infections due the cytotoxicity through systemic treatment (Lakshmaiah Narayana and Chen, 2015). The production costs of antimicrobial peptides is also a significant barrier if these peptides are to become widely used (Seo *et al.*, 2012).

2.4.4 Colistin sulphate

Colistin sulphate, otherwise known as polymyxin E, is a member of the cationic, cyclic polypeptide antibiotic group known as the polymyxins and is produced by the soil bacterium *Bacillus polymyxa* (Adams *et al.*, 2009). This group contains five members, polymyxin A-E, but only two, polymyxin B and E, are used in clinical treatment and differ only by D-phenylalanine in polymyxin B being replaced by D-leucine in polymyxin E (Laverty *et al.*, 2011).

Polymyxins are active against many Gram-negative bacteria such as *A. baumannii*, *P. aeruginosa*, *Salmonella*, *Shigella*, *Klebsiella* and *Enterobacter* species. They are not active against Gram negative or Gram positive aerobic cocci, Gram positive aerobic bacilli, anaerobes, fungi and parasites (Falagas and Kasiakou, 2005).

Colistin sulphate was discovered in 1949 and used therapeutically during the 1950s but was believed to have significant side effects such as nephrotoxicity, mainly acute tubular necrosis, and neurotoxicity associated with vertigo and ataxia. As a result the intravenous use was restricted to treatment for lung infections caused by MDR Gram-negative bacteria in cystic fibrosis patients (Karageorgopoulos and Falagas 2008).

Colistin sulphate is now currently used as a last resort treatment due to the emergence of MDR Gram-negative bacteria such as *A. baumannii* which are resistant to carbapenems, cephalosporins and aminoglycosides and the paucity of therapeutic treatment alternatives (Falagas and Kasiakou, 2005; Potron *et al.*, 2015).

2.4.4.1 Antimicrobial Mechanism

In treatment, colistin sulphate can be administered orally or topically and targets the cell membrane of Gram-negative bacteria. Electrostatic interactions account for the first interactions between the cationic polypeptide of colistin and the anionic endotoxic component of the lipopolysaccharide (LPS), lipid A (Moffatt *et al.*, 2010; Falagas and Kasiakou, 2005). Colistin uses the aggregate channel model as described in **Section 2.4.2** whereby it displaces the cations Mg^{2+} and Ca^{2+} which normally stabilise the LPS layer. This results in permeability changes in the membrane, leading to cell content leakage and ultimately cell death (Falagas and Kasiakou, 2005).

Colistin sulphate has a molecular weight of 1155.4 g/mol and its structure includes two distinct hydrophobic regions, the N-terminal fatty acyl chain and the Phe-Leu segment as shown in orange in **Figure 2.4.4**. The hydrophilic cycloheptapeptide ring includes three positively charged amine residues, shown in green. The colistin peptide is folded such that the hydrophobic and hydrophilic components form two distinct faces resulting in structural amphipathicity. This allows the interaction with constituents of the lipopolysaccharide such as lipid A where the hydrophobic regions interacts with the lipid A fatty acyl chains while the hydrophilic residues face in the opposite way towards the aqueous environment. (Velkov *et al.*, 2010; Rhouma *et al.*, 2015).

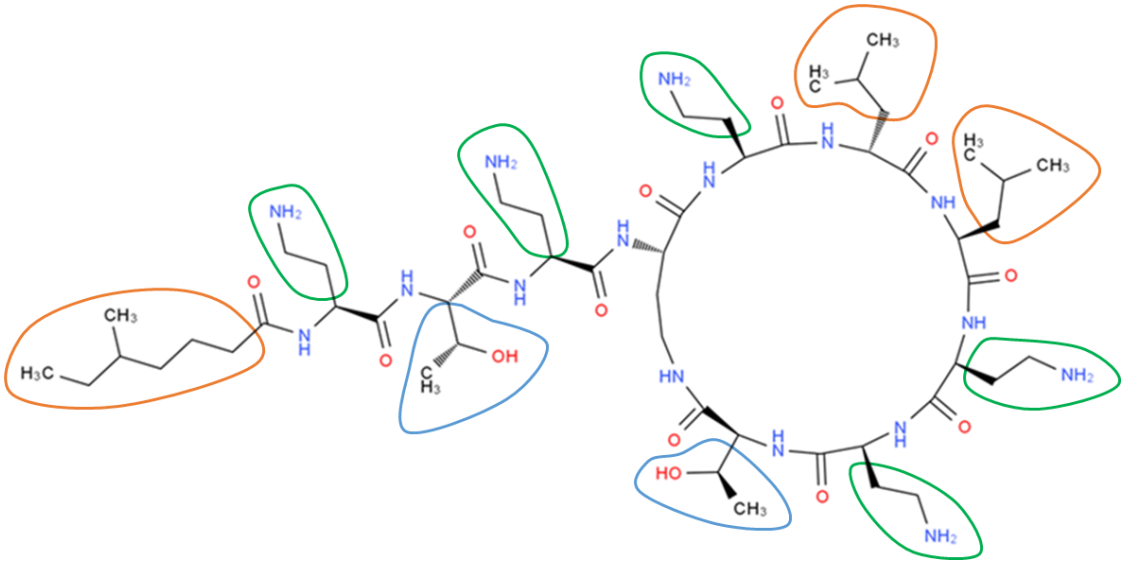

Figure 2.4.4-Structure of Colistin sulphate. *Molecular formula of $C_{52}H_{98}N_{16}O_{13}$ (Chembase, 2014). Orange annotations indicates hydrophobic residues, blue indicates hydrophilic regions and green indicates polar groups (Velkov et al., 2010).*

2.4.4.2 Resistance

A. baumannii resistance to colistin sulphate is believed to be the result of two main mechanisms:

1. The first involves mutations in the genes, lpxA, lpxC or lpxD, that affect the encoding enzymes responsible for lipid A biosynthesis. These mutations lead to subsequent inability to produce lipid A and LPS (Moffatt *et al.*, 2010; Potron *et al.*, 2015; Durante-Mangoni *et al.*, 2015).
2. The second mechanism involves mutations in the genes, pmrA and pmrB, that encode the PmrAB two-component system which is involved in environmental sensing of Fe^{3+}, Mg^{2+} and pH. Changes in this system can lead to altered gene expression resulting in lipid A modification (Adams *et al.*, 2009).

Modifications to lipid A can lead to the reduction or elimination of the initial charged electrostatic interaction between the colistin sulphate and lipid A. This can also reduce

the negative charge of the LPS and therefore lowering its affinity to colistin *(Moffatt et al.*, 2010).

The result of reduced levels, or complete loss of LPS, decreases the anionic charge of the outer membrane of the bacterial cell and therefore decreases the affinity of the cationic charged polypeptide of colistin. Hetero-resistance of *A. baumannii* against colistin could be due to the presence of cells that have random mutations in these key genes (Moffatt *et al.*, 2010).

2.4.4.3 Relation to this Project

Colistin sulphate is a currently used as antimicrobial treatment of last resort against *A. baumannii* infections. In this project its effectiveness was compared with the AMPs bicarinalin and BP100 against both planktonic cells and biofilms of *A. baumannii*.

2.4.5 Bicarinalin

Bicarinalin is an amphipathic, C-terminally amidated, novel antimicrobial peptide derived from the venom of the myrmicine ant, *Tetramorium bicarinatum* (Rifflet,*et al.*, 2012).

It consists of a sequence of 20 amino acid residues (KIKIPWGKVKDFLVGGMKAV) with a molecular weight of 2213.78 g/mol. Ant venom is an area of research interest that has, to date, been poorly studied compared to other animal venoms although other AMPs have been identified in other ant genera such as the ponericins from *Pachycondyla goeldii* and pilosulin from *Myrmecia pilosula* (Rifflet *et al.*, 2012).

Figure 2.4.5-Vial containing bicarinalin as white lyophilised conforms*. Created by GenScript. 97.7% purity and structure was confirmed by high performance liquid chromatography (HPLC)*

Rifflet (2012) evaluated the antibacterial activity of bicarinalin using a synthetic replicate against *Staphylococcus aureus* and *Staphylococcus xylosus* in comparison to melittin, another AMP, and standard antibiotics ampicillin and tetracycline. They found bicarinalin had similar antibacterial activity against *S. aureus* but was more potent than melittin and tetracycline against *S. xylosus*.

Bicarinalin also has the advantage of weak haemolytic activity compared to melittin against erythrocytes which has been a significant obstacle for using AMPs in treatment against antibiotic-resistant pathogens. It also highlighted that bicarinalin had similar antibacterial activity as other AMPs such as defensin, pilosulin and scolopin but was generally less haemolytic. (Rifflet *et al.*, 2012).

Tene (2014) further tested the bacteriostatic and bactericidal effects of bicarinalin against *Cronobacter sakazakii* and four species of *Enterobacter*: *E. cloacae*, *E. aerogenes*, *E. hormaechei* and *E. cloacae* while comparing the results with melittin, ampicillin and tetracycline. Bicarinalin was found to be more potent than melittin and

the other antibiotics against all of the bacteria tested by Tene (2014.) Bicarinalin is considered to be a promising candidate for treatment against resistant bacterial strains and other potential applications such as dried food and cosmetics (Téné *et al.*, 2014; Rifflet *et al.*, 2012).

2.4.5.1 Antimicrobial Mechanism

It is believed that bicarinalin's antibacterial mechanism is similar to other AMPs, with its cationic charge, as a result of lysine residues, naturally attracted to the anionic charged bacterial cell surface. This interaction leads to the local disruption of the bacterial surface (Rifflet *et al.*, 2012).

In **Figure 2.4.6** the helix wheel for bicarinalin is shown and elucidates bicarinalin's amphipathicity which is a characteristic of antimicrobial peptides. All the hydrophobic residues apart from Ile and Val are on one side of the helix while the hydrophilic amino acid residues are located on the opposite side. (Rifflet *et al.*, 2012).

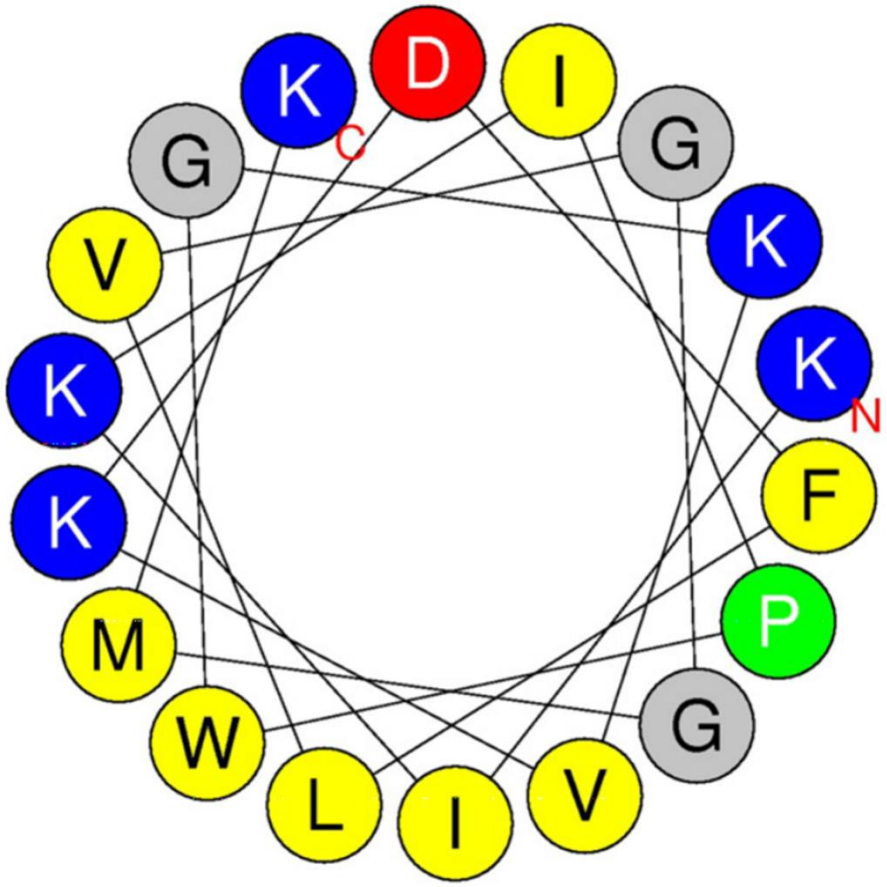

Figure 2.4.6-Helix wheel of Bicarinalin. *Hydrophobic residues shown as green and yellow circles, positively charged as blue circles, hydrophilic residues as grey and red circles, (Rifflet et al., 2012).*

2.4.5.2 Relation to this project

Bicarinalin was chosen for this project because it has been shown to have higher antimicrobial potency compared to currently used antibiotics; it is not cytotoxic at bactericidal doses and has proven activity against Gram-negative bacteria. There is also no evidence in the literature of it ever being tested against *A. baumannii* (Téné *et al.*, 2014; Rifflet *et al.*, 2012).

2.4.6 BP100

BP100 is a short C-amidated undecapeptide peptide consisting of eleven amino acid units (KKLFKKILKYL) and a molecular weight of 1420.88 g/mol. It was originally made through combinatorial chemistry involving two peptides, cecropin A and melittin (Alves *et al.*, 2010).

Cecropin A is a member of the well-researched AMP family, the cecropins, first isolated from the giant silk moth *Hyalophora cecropia*. The cecropin family, although susceptible to protease degradation, do not exhibit cytotoxic effects against human erythrocytes (Badosa *et al.*, 2007; Ferre *et al.*, 2009).

Melittin is a 26 amino acid, haemolytic alpha helical peptide first purified from the European honeybee in 1958 (Hou *et al.*, 2015). Melittin has been shown to have high antibacterial activity. However, on its own, its strong cytotoxic action, makes it unsuitable for applications in antibiotic treatment (Pott *et al.*, 2015).

Figure 2.4.7 Vial containing BP100 as white lyophilised conforms. *Created by GenScript. 98.4% purity and structure was confirmed by high performance liquid chromatography (HPLC)*

To circumvent cercropin A's susceptibility to proteolytic degradation and melittin's high cytotoxicity, they were combined to produce a derivative, BP100. BP100 exhibits low susceptibility to protease degradation and low cytotoxicity against erythrocytes and fibroblasts (Manzini *et al.*, 2014). BP100's bactericidal activity has been established to be highly active, discerning Gram-negative bacteria including plant pathogens such as *Erwinia amylovora*, *Pseudomonas syringae* and *Xanthomonas azonopodis* (Ferre *et al.*, 2009) and the human pathogen *Escherichia coli* (Alves *et al.*, 2010).

2.4.6.1 Antimicrobial Mechanism

It is believed that BP100 interacts with the bacterial cell membrane by its electrostatic attraction to the negatively charged LPS layer. (Alves *et al.*, 2010).

The helix wheel as shown in **Figure 2.4.8** indicates the presence of positively charged Lys residues on one side of the peptide (pentagons) and on the opposite side there are hydrophobic residues (diamonds). BP100, consisting of only 11 amino acids, is not long enough in length to transverse the span of the phospholipid bilayer to form transmembrane pores. The carpet model model is therefore considered as the most likely mechanism of action as shown in **Figure 2.4.2**. (rzlab, 2016; Wadhwani *et al.*, 2014).

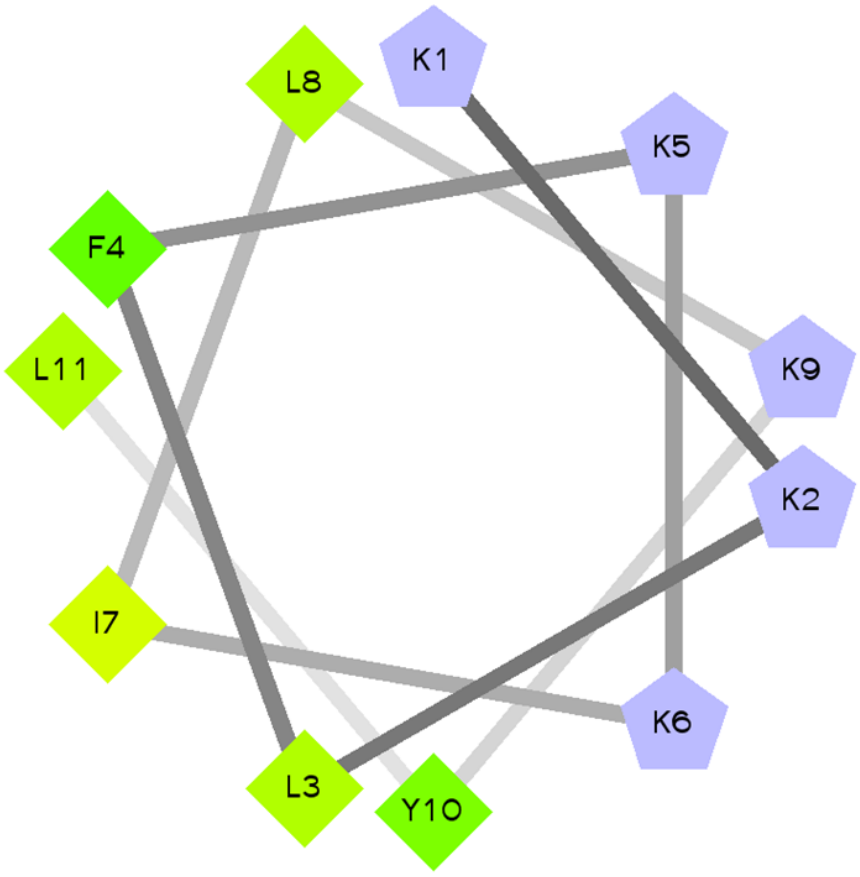

Figure 2.4.8-Helix wheel of BP100. *Hydrophobic: diamond high (green) low (yellow), Positive charge: pentagons (rzlab, 2016).*

2.4.6.2 Relation to this Project

BP100 was chosen because of its high bactericidal activity against Gram-negative plant pathogenic bacteria and *Escherichia coli* and its low cytotoxic activity (Alves *et al.*,

2010; Güell *et al.*, 2012; Badosa *et al.*, 2007). There is also no evidence in the literature of it ever being tested against *A. baumannii*.

2.5 Visualisation Techniques

This project used three microscopes, the atomic force microscope (AFM), scanning electron microscope (SEM) and the confocal laser scanning microscope (CLSM) to investigate the effect of the three antimicrobial peptides: colistin sulphate, bicarinalin and BP100 on *Acinetobacter baumannii* planktonic cells and biofilms.

2.5.1 Atomic Force Microscopy

The AFM was first invented in 1986 and since has become widely used in biomedical research such as virology, microbiology, biomaterials, nanotechnology and genetics. (Chang *et al.*, 2012) Its ability to map surfaces at micrometre to nanometre resolution and used in tandem with conventional microscopes has allowed in-depth analysis and detailed imaging at a molecular level (Chang, *et al.*, 2012; Longo and Kasas, 2014).

The bacteriostatic and bactericidal concentrations of the peptides on planktonic *A. baumannii* cells were determined through microbiological assays. In this project the consequence of this activity was then visualised using the AFM.

2.5.1.1 Fundamentals of AFM Operation

The AFM consists of four parts:

- a probe that consists of a cantilever with a sharp tip mounted on the end, made of silicon or silicon nitride (**Figure 2.5.1**)
- a piezo scanner that drives the cantilever

- a laser diode
- a detector

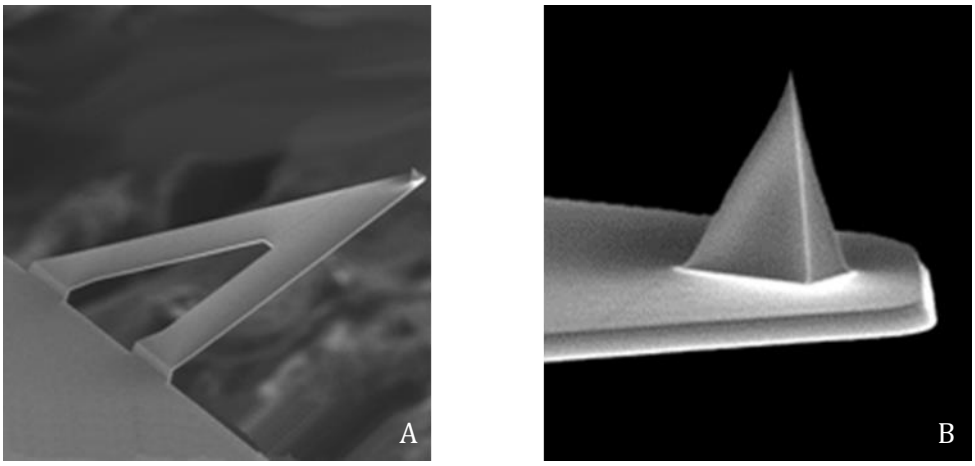

Figure 2.5.1- SEM Images of the cantilever and tip. *Image A shows AFM cantilever and tip while image B shows close up of silicon tip. (Bruker, 2015).*

There are two main modes of AFM: contact mode and non-contact mode. In contact mode, the tip of the probe is brought into contact with the sample or bacterial surface and is dragged or scanned over the required surface area in a raster pattern. Surface features cause the displacement of the cantilever which is measured by the detector through the deflection of the laser beam reflected from the back of the cantilever. The laser deflection is plotted and a topographic image of the sample surface is produced (Chang *et al.*, 2012) (**Figure 2.5.2**).

Non-contact mode allows the measurement of attractive forces such as van der Waals or dipole interactions between the tip and the bacterial surface. This involves oscillating the cantilever above the surface of the bacterial surface and measuring the alterations in amplitude or frequency of the cantilever (Chang *et al.*, 2012).

Contact mode has the inherent problem that lateral forces applied on the sample surface can cause damage and move loosely attached objects (Kaemmer, 2011). To circumvent this problem, a newer type of contact mode, “PeakForce Tapping” was

made. This requires the cantilever to oscillate, resulting in the tip touching the surface for a short amount of time and then being lifted up again. This mode has a drawback in that the interaction force between the tip and the sample surface is fixed during scanning which may lead to damage to the sample along with false imaging (Kaemmer, 2011).

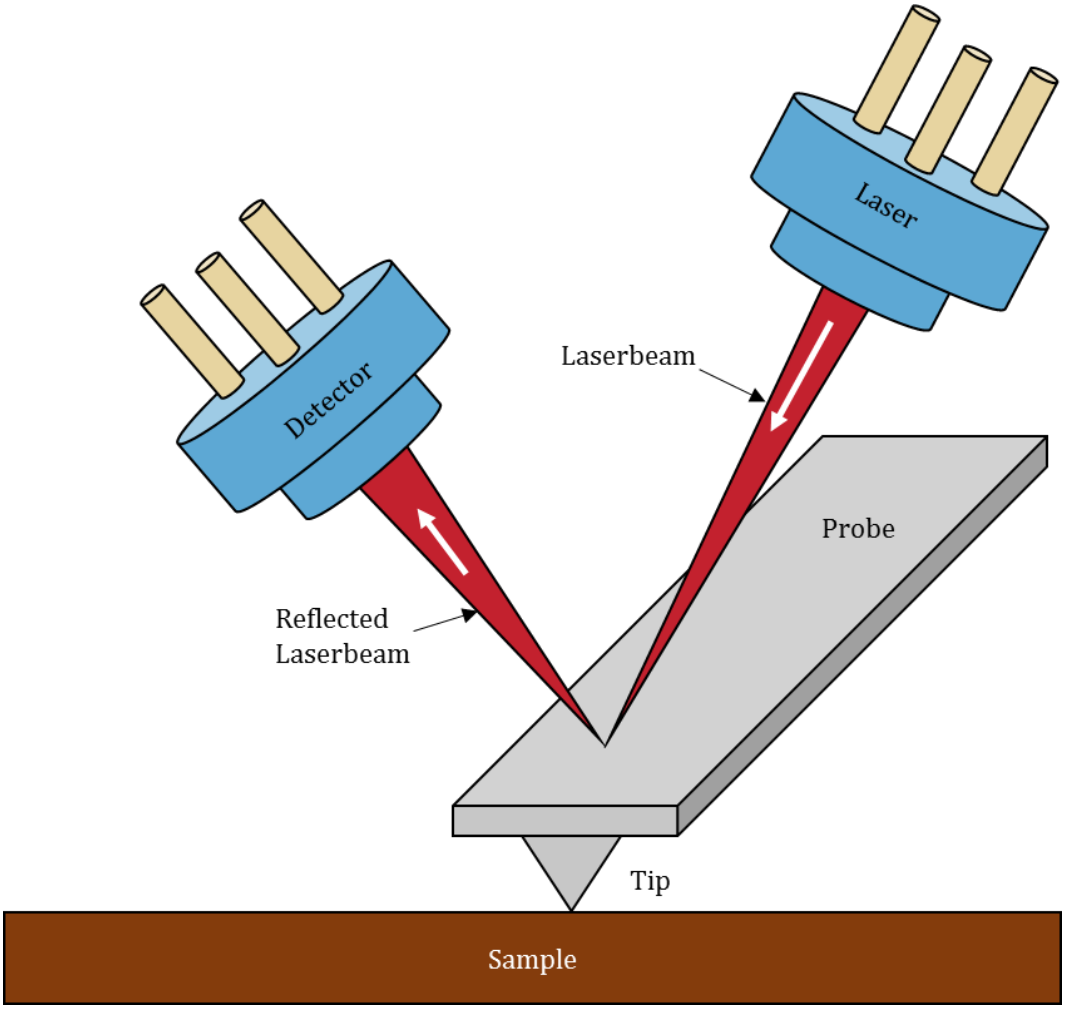

Figure 2.5.2-Simplified image of AFM setup. *A laser beam is directed onto the back of the probe while the probe is moving up and down on the sample. The beam is then reflected into the detector and an image of the surface topography is produced (Bruker, 2011).*

In this project the "PeakForce Tapping" mode was used with "ScanAsyst" software. The programme includes an algorithm that automatically adjusts all critical parameters

such as gain, scan-rate and z-limit in real-time to optimize imaging. This is especially important for samples that have both soft and hard areas such as bacterial cells fixed on glass slides (Kaemmer, 2011) as used in this project.

2.5.1.2 Advantages and Limitations

The AFM has numerous advantages over conventional electron and optical microscopes. The first is the simplicity of sample preparation. It also does not require the use of fluorescent dyes as in the CLSM (**Section 2.5.3**) or vacuuming or metal coating as required in the scanning electron microscope (**Section 2.5.2**). The bacterial cell samples can be grown on, or suspensions can be pipetted onto, flat surfaces such as graphite, silicon, glass slides or modified surfaces such as poly-lysine coated surfaces. This ensures, during preparation, there is little disruption to the samples. The samples can also be visualised in liquid as well as in air permitting the analysis of samples within their physiological buffer solutions. The resolution of AFM scanning enables the visualisation of samples at nanometre or micrometre scales (Chang *et al.*, 2012).

The AFM has become a valuable and widespread tool in imaging studies but as with all equipment there are limitations. The primary limitation is that the AFM is only able to obtain surface information from samples so other microscopes, such as transmission electron microscopes, optical microscopes and fluorescence microscopes, are also used in conjunction (Chang *et al.*, 2012).

2.5.2 Scanning Electron Microscopy

The SEM was used to visualise the effects of a range of peptide concentrations on biofilms. The concentrations were determined at which the peptides removed the majority of the biofilm grown by *A. baumannii*; the effects of this activity was then visualised using the scanning electron microscope.

2.5.2.1 Fundamentals of SEM Operation

From the electron gun, located at the top of the SEM, accelerated electrons are fired at a sample (**Figure 2.5.3**). These electrons pass through electromagnetic lenses forming a focused spot, potentially 2 nm in diameter, of electrons that is scanned over a sample (Zhou *et al.*, 2007; Güell *et al.*, 2012; Kaláb *et al.*, 2008).

Secondary electrons are formed when a primary electron dislodges an electron from the sample surface. Secondary electrons have low energy levels which mean they can only be detected when they are dislodged near the surface of the sample. These electrons are reflected into the secondary electron detector where is signal is produced. (Zhou *et al.*, 2007).

The signals are processed and translated into pixels creating a 2D impression of the sample surface morphology. The SEM is under a vacuum, usually below 10^{-6} Torr, to remove any air molecules that would impede the electron beam as well as the secondary electrons travelling to the detector (Zhou *et al.*,2007; Alhede *et al.*, 2012).

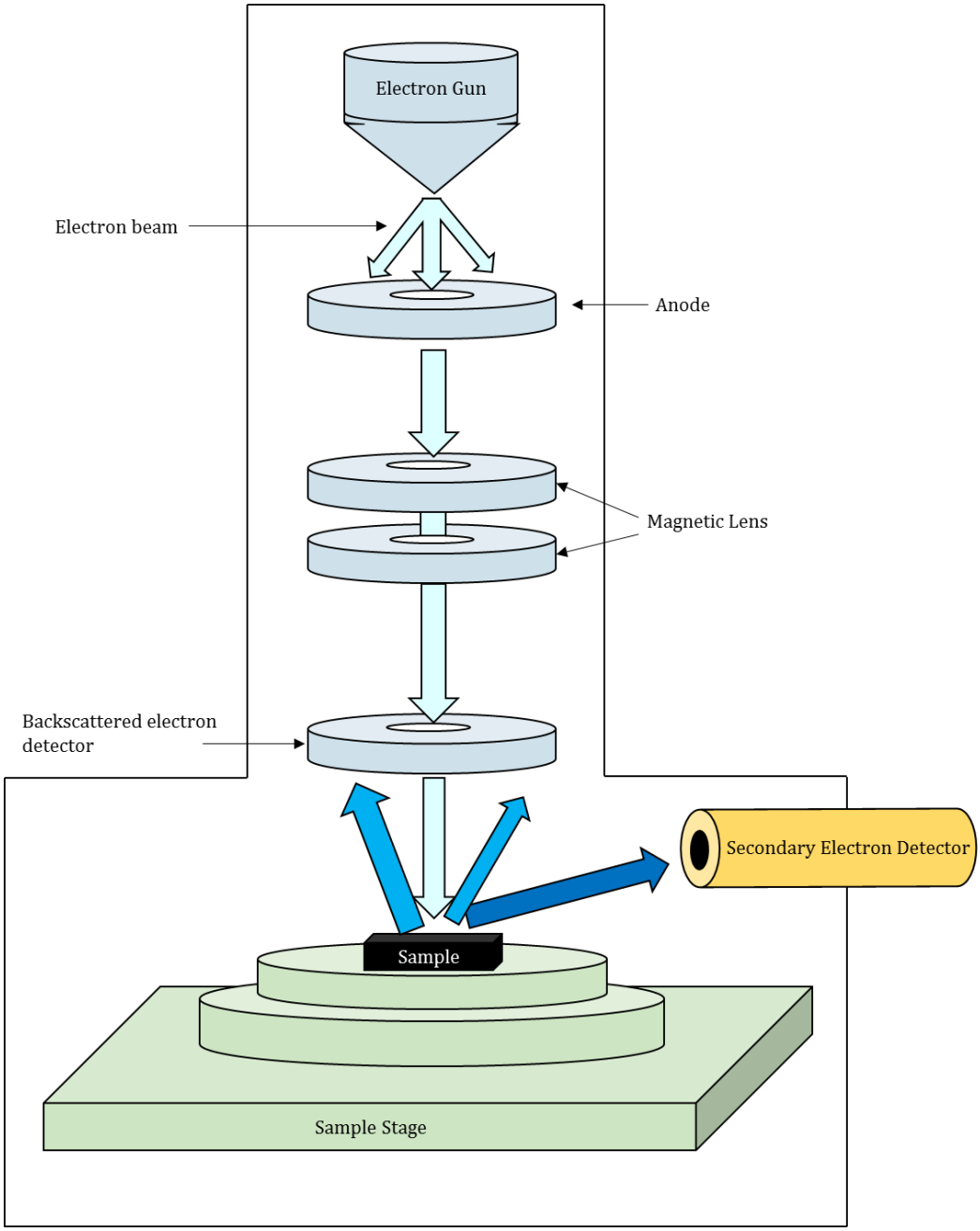

Figure 2.5.3-Simplified image of SEM setup. *Accelerated electrons are fired at a sample and pass through an anode and magnets which creates a narrow focused spot of electrons. Secondary electrons are released from the sample and are detected by a detector which creates an image of the sample surface* (Alhede *et al.*, 2012).

Most bacterial sample preparation for SEM work includes the use of a buffer such as sodium cacodylate and a fixative such as glutaraldehyde. The buffer is used to produce an isotonic solution for the sample and to protect the sample from becoming acidic. The glutaraldehyde is used to preserve the structure of the sample tissues when within a

vacuum. The specimen is dehydrated with increasing concentrations of methanol to remove any water. The sample is then mounted and coated in a thin layer of conductive metal such as gold, carbon or platinum which is usually applied via the sputter coating method (Kaláb *et al.*, 2008; Alhede *et al.*, 2012).

2.5.2.2 Advantages and Limitations

The SEM is able to produce high resolution, high magnification images of the sample surface. It is relatively easy to operate and sample preparation is straightforward although time consuming. The primary limitations of the SEM are that only the surface topography of the sample can be analysed and limited quantitative data can be obtained during or after the imaging. The preparation of the sample, in the case of bacteria, involves dehydration, and can cause alterations in morphology and structure and only dead samples can be visualised (Alhede *et al.*, 2012).

2.5.3 Confocal Laser Scanning Microscopy

The concept of the confocal laser scanning microscope (CLSM) was developed in the 1950s with the first commercial instrument appearing in 1987. However, it was not until the late 1990's when the CLSM began to be widely used (Claxton *et al.*, 2006; Lavrentovich, 2012) .

In this project the CLSM was used to analyse the biofilm produced by *A. baumannii* by creating 3 dimensional images by a process of Z stacking. The samples were visualised by staining with the nucleic acid fluorochrome, SYTO9. The biofilm was quantified by calculating the bio-volume of the biofilm after it had been subjected to increasing concentrations of each of the three peptides, colistin sulphate, bicarinalin and BP100.

2.5.3.1 Fundamentals of CLSM Operation

The confocal microscope uses a laser for the light source and acousto-optic tuneable filters (ATOFs) to select specific excitation wavelengths. The laser passes through a dichroic mirror which selectively transmits light of a chosen wavelength (**Figure 2.5.4**). This light is reflected into the back focal plane of the objective lens which in turn focuses the laser light at a specific point on a sample which is stained with the fluorochrome (Claxton *et al.*, 2006).

When a photon from the laser beam is absorbed by a fluorophore, an electron within the sample is excited by entering a higher, unstable energy state. The electron is in this higher energy state for a few nanoseconds then falls back to the original ground state. As it falls, light is emitted as a characteristic wavelength (Claxton *et al.*, 2006; Lavrentovich, 2012).

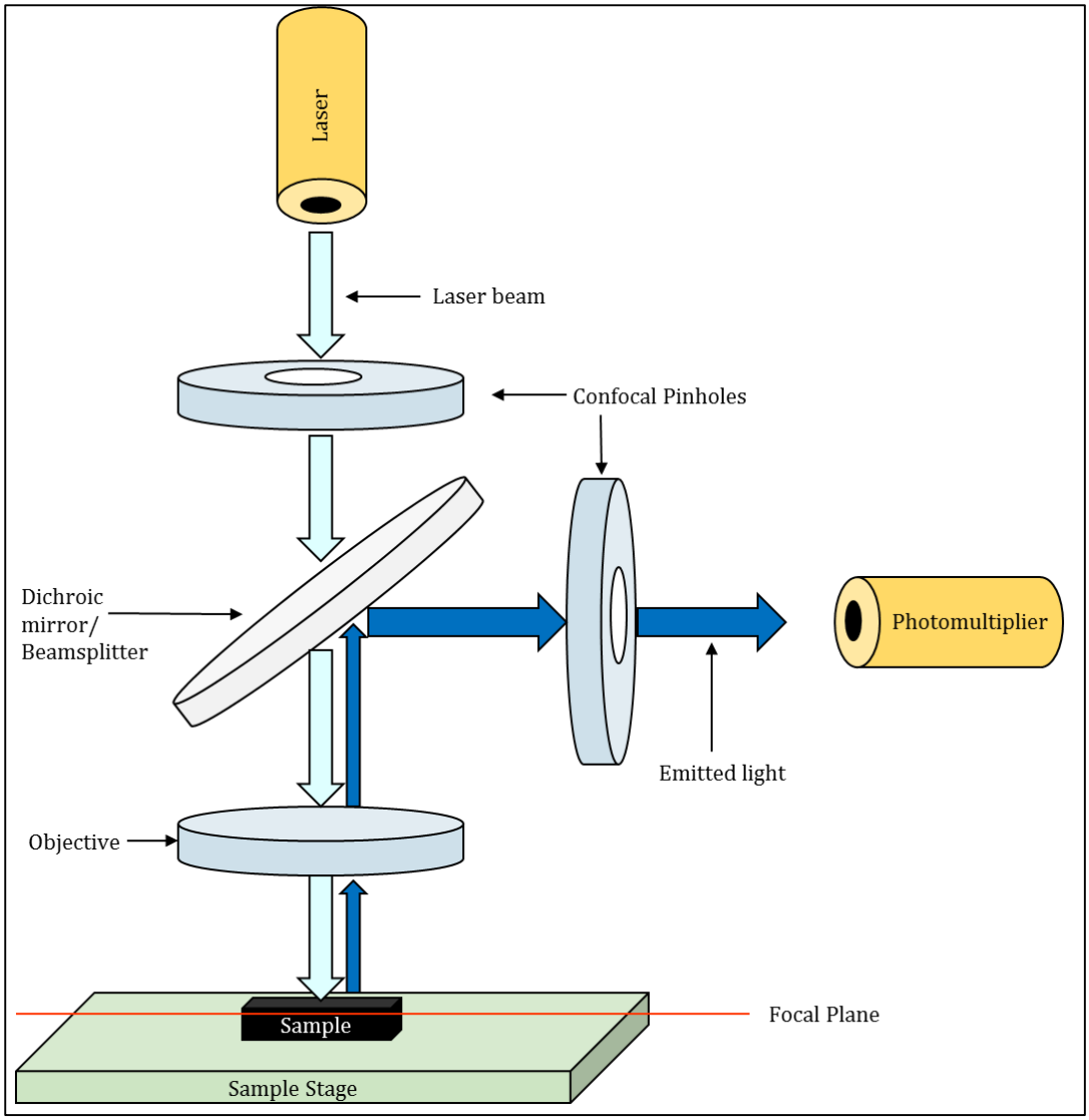

Figure 2.5.4-Simplified image of CLSM setup. *A laser beam of a certain wavelength reaches the sample and excites the fluorophore. Light of a certain wavelength is emitted and reflected by a dichroic mirror through a pinhole only allowing focused light through to the photomultiplier* (Claxton *et al.*, 2006).

The light, emitted from the excited fluorochrome, passes back through the objective lens. As this light is of a longer wavelength in relation to the excitation light, it does not go through the dichroic mirror, but is instead reflected through another pinhole. This pinhole is specifically located to only allow in-focused light through while blocking any out-of-focus light. Beyond the pinhole, there are filters that allow further discrimination of wavelength to pass through to a photomultiplier tube or PMT. The PMT is calibrated to detect the required wavelengths. Within a photomultiplier tube, an

incoming photon hits an electron within the photocathode which initiates a chain reaction of electrons and hence detection on the screen (Claxton *et al.*, 2006).

The fluorescent stain used in this project was SYTO9; a nucleic acid membrane permeable stain and stains all cells whether the bacteria membranes are intact or not (Stocks, 2004). The excitation and emission wavelengths of SYTO9 are shown in **Figure 2.5.5**.

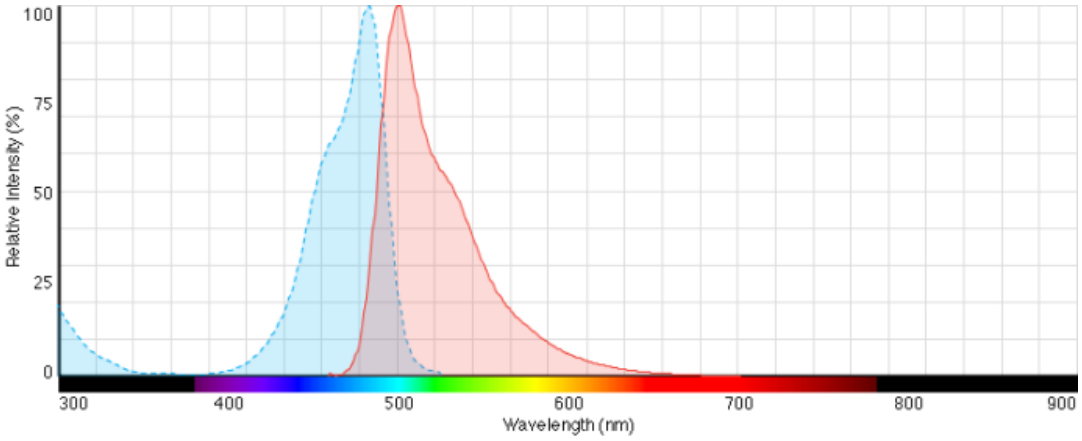

Figure 2.5.5- SYTO9 excitation wavelength in blue and emission wavelength in red. *Peak excitation 485nm and peak emission 498nm (ThermoFisher Scientific, 2015).*

2.5.3.2 Advantages and Limitations

The main advantage of the CLSM is the ability to collect serial optical sections of a sample; made possible by the pin-hole eliminating out-of-focus light before it reaches the photomultiplier and the ability to coordinate the imaging along the Z axis. Compiling these sections into a Z stack, creates a 3D image which can be analysed and quantitative data can be obtained. This is a non-invasive technique allowing the analysis of thick samples without the need to break up the sample. The samples can also be analysed in normal laboratory conditions in contrast to the SEM that requires a vacuum and detailed sample preparation (Claxton *et al.*, 2006).

There are a few limitations of the CLSM. One is the limited number of excitation wavelengths available with the commonly used lasers. Intensive laser irradiation may be harmful to living cells and tissues and the high costs associated with the purchasing and operating of a CLSM (Claxton *et al.*, 2006).

3 Materials and Methods

3.1 Materials

The following section lists all the materials used in the research project including the manufacturing company:

Product	Supplier	Additional Information
¼ strength Ringer's Solution	Oxoid	1 tablet per 500ml of distilled water
25 % Glutaraldehyde Solution	Fisher Scientific	
Absolute Ethanol	Fisher Scientific	
***Acinetobacter baumannii* ATCC 19606**	Thermo Scientific	
API 20NE	BioMérieux Clinical Diagnostics	API 20NE reagents kit. James, NIT 1, NIT 2, Zinc Powder
Bicarinalin	Genscript	Amino acid sequence: KIKIPWGKVKDFLVGGMKAV Molecular weight: 2213.78 C-terminally amidated
BP100	Genscript	Amino acid sequence: KKLFKKILKYL Molecular weight: 1420.88 C-terminally amidated
Chlorine Release Tablets (Haz-tabs)	Appleton Woods	1 tablet per 250ml of water
Colistin Sulphate	Sigma-Aldrich	
Crystal Violet	ProLab	

Gram's Iodine	ProLab	
Baclight Live/dead stain	ThermoFisher Scientific	Contains 3.34mM SYTO9
Methanol	Fisher Scientific	
Mineral Oil	Sigma-Aldrich	
N,N,N',N'-Tetramethyl-p-phenylenediamine dihydrochloride,>=95 %, powder	Sigma-Aldrich	
Safranin	ProLab	
Sigma-Aldrich Sodium cacodylate trihydrate.		
Tryptone Soya Agar (TSA)	Oxoid	An equivalent of 40g of Tryptone soya agar powder was weighed and dissolved in 1 litre of distilled water
Tryptone Soya Broth (TSB)	Oxoid	An equivalent of 30g of Tryptone soya broth powder was weighed and dissolved in 1 litre of distilled water
Virkon S disinfectant	Virkon	

3.2 Equipment

The equipment used in the project, including the manufacturing company, is listed below:

Product	Supplier	Additional Information
0.5" aluminium specimen stubs.	Agar Scientific	
1000 µl, 200 µl, 10 µl pipettes	Bioscope or Sarstedt	
1000 µl, 200 µl, 10 µl tips	Bioscope/Sarstedt	
1ml syringe	Plastipak	Sterile
10ml pipettes	Sarsted	Serological, non-cytotoxic, non pyrogenic
25ml pipette	Fisher Brand	Disposable serological pipettes
211DS Shaking Incubator	Labnet	
96 Well Plates	Sarstedt	Sterile
Atomic Force Microscope Tips-SCANAYST AIR, Silicon top on nitride Lever	Bruker	Cantilever- Tip height-650nm Cantilever length-115µm Cantilever width-25µm Resonance frequency (F_0)-70kHz Spring constant (k)-0.4N/m
Bioscope Catalyst Atomic Force Microscope with Easy align and Scanayst	Bruker	
Nunc-TSP Screening Plate Lids	ThermoScientific	
Chambered #1.0 Borosilicate	Labtek	

Coverglass System-8 chamber		
Colourimeter	Fisher Scientific	
Confocal Laser Scanning Microscope	Leica TCS SP8	
Cuvettes	Sarstedt	1ml polystyrene
Filter	Sartorius Stedium biotech	0.2µm minisart single use filter-sterile, non-pyrogenic
Incubator	Thermo Scientific	37°C
Electronic Pipette	Scientific Laboratory Supplies (SLS) LTD	Integra Pipetboy 2
Light Microscope.	Zeiss Primo Star	
L-shaped Spreaders.	Scientific Laboratory Supplies (SLS) LTD	Sterile
Micro tubes.	Sarstedt	
Mili-Q water dispenser.	Purelab flex	18.2Ω
NanoDrop 2000c Spectrophotometer.	Thermo Scientific	
Inverted Microscope	Nikon Eclipse TE2000-S.	
Parafilm "M" laboratory film.	Parafilm	
Poly-L-lysine coated slides.	Sigma Aldrich	
Scanning Electron Microscope	FEI Quanta FEG 650	
Sterile disposable serological 10ml Pipettes.	Fisherbrand	

3.3 Software Programs

The following programs were used to analyse the results:

- NanoScope Analysis Version 1.50 (Bruker, 2015)
    - Used to create and obtain images of cells from the AFM.

- Gwyddion (Necas and Klaptek, 2012)
    - Used in the analysis and quantification of surface roughness and surface area of cells imaged by AFM.

- Las X (Leica Microsystems, 2015)
    - Used to acquire and analyse CLSM images.

- BITPLANE Imaris x64 Version 8.1.2 (Bitplane, 2015)
    - Used in the quantification of bio-volume of biofilm of CLSM images.

- IBM SPSS Statistics 21 (IBM Corp, 2012)
    - Used in the statistical analysis of results.

3.4 Reoccurring Calculations

3.4.1 Absorbance Calculation

The absorbance calculation was used throughout the project to obtain a standard initial inoculum containing approximately $5x10^5$ viable cells per ml ($2\text{-}7x10^5$ CFU/ml) at the start of each experiment. The British Society for Antimicrobial Chemotherapy (BSAC) recommends this concentration as a standard for susceptibility testing of bacteria (Andrews, 2006).

Tryptone soya broth (TSB) was prepared as described in **Section 3.1**. 10ml of TSB was pipetted into glass universals and autoclaved for 15 minutes at 121°C. A glass universal (labelled #1), containing 10 ml sterile TSB, was inoculated with 2-3 colonies of *A. baumannii* 19606 taken from a Tryptone soya agar (TSA) plate, grown for 24 hours at 37°C. The broth was then incubated overnight at 37°C.

The following day, the absorbance of this overnight broth was measured by pipetting 1 ml into a 1 ml polystyrene cuvette and using a colorimeter (set at a wavelength of 590 nm) calibrated against a 1 ml blank containing sterile TSB.

Applying **Equation 1** below, a calculated volume of overnight broth was pipetted into another universal (labelled #2) containing 9 ml sterile TSB, to give a final volume of 10 ml and a final desired absorbance reading of 0.01. This was confirmed by pipetting 1 ml of this solution into a cuvette and measuring against a sterile TSB blank. The absorbance of 0.01 was chosen as it equated to a cell density of approximately $1x10^7$ CFU/ml based on the results of the growth curve as described in **Section 4.2**.

$$\textbf{Equation 1}: \qquad V1 = \frac{A2\ V2}{A1}$$

Where:

V1=The unknown volume of overnight culture to be added

A1=Initial absorbance reading of the overnight culture at 590 nm

A2=Desired absorbance reading (0.01).

V2=Final volume of TSB within universal (10 ml).

For example:

An overnight broth culture containing *Acinetobacter baumannii* 19606 was removed and an absorbance reading of 0.9 was measured against a 1 ml blank which contained sterile TSB taken from the universal that is going to be inoculated. If an absorbance value of 0.01 is desired, the volume of culture to be added (V1) is:

$$\boldsymbol{V1 = \frac{0.01\ x\ 10\ ml}{0.9}}$$

$$\boldsymbol{V1 = 0.11\ ml}$$

After mixing on a vortex at 500rpm for 10 seconds, 0.11 ml was transferred from the overnight broth to the glass universal currently holding 9 ml (as 1 ml was already used for the blank). From a third universal containing sterile TSB, 0.89 ml is removed and added to the newly inoculated TSB to make a final volume 10ml with a cell density of approximately $1x10^7$ CFU/ml. After vortexing, 1 ml is removed and its absorbance is measured to confirm it is 0.01. 1 ml of this solution was then pipetted into 9ml of sterile TSB broth to give a theoretical cell density of approximately $1x10^6$ CFU/ml.

A final two-fold dilution would then be made to obtain the required concentration of approximately $5x10^5$ CFU/ml (range of $2\text{-}7x10^5$ CFU/ml) (as recommended by BSAC) (Andrews, 2006) which was the concentration used for all experiments. This was confirmed during each experiment by the plate spread method.

3.4.2 Concentration Calculation

The concentration calculation was used to ensure a final desired concentration of a substance, for example, a peptide was present in a certain volume of solution. A standard stock concentration 1024 µg/ml of antimicrobial peptide was prepared for determination of the minimum inhibitory concentration (MIC), minimum bactericidal concentration (MBC) and minimum biofilm inhibitory concentration (MBIC) as discussed in **Sections 3.10, 3.11 and 3.12**. The stock solution was made by firstly weighing 5000µg of peptide within a microtube and dissolving it in 1ml of distilled water to give a peptide concentration of 5000 µg/ml. A stock solution of peptide, for example colistin sulphate, at a concentration of 1024 µl was produced using **Equation 2** below.

$$\textbf{Equation 2:} \qquad V1 = \frac{C2\ V2}{C1}$$

C1= Concentration of dissolved antimicrobial peptide (5000 µg/ml)

V1= Unknown volume of antimicrobial peptide to be added (ml)

C2= Required concentration of antimicrobial stock (1024 µg/ml)

V2=Final volume of stock (1ml)

Using the equation above, V1 was calculated as:

$$V1 = \frac{1024\ x\ 1}{5000}$$

$$V1 = 0.2048ml$$

0.2048ml of 5000 µg/ml was pipetted into 0.7952ml milli-Q water to make a final concentration of 1024 µg/ml. For bicarinalin and BP100, the purity was also

considered. For example, as bicarinalin had a purity of 97.7 % (**Section 2.4.5**), 5000µg of bicarinalin was weighed and dissolved in 1ml distilled water and using the following equation the true amount was calculated.

$$\boldsymbol{True\ mass}\ (\mu\boldsymbol{g}) = \left(\frac{\mathbf{97.7}}{\mathbf{100}}\right) * \mathbf{5000}$$

$$\boldsymbol{True\ mass}\ (\mu\boldsymbol{g}) = \mathbf{4885}\mu\boldsymbol{g}$$

Equation 2 was then used to obtain a stock solution of 1024 µg/ml of bicarinalin.

3.5 Colony Morphology Analysis

3.5.1 Objective

The culturing of bacteria on solid media, such as TSA, allows the bacteria to form visible colonies which can be used to help identify certain bacteria based on distinctive characteristics such as the shape, size (diameter in millimetres), edge/margin, colour, opacity, surface consistency and elevation.

3.5.2 Methodology

A culti-loop of *Acinetobacter baumannii* 19606 was streaked, in aseptic conditions, on a freshly prepared TSA plate. This was incubated for 24 hours at 37°C. After 24 hours, a single colony of *A. baumannii* 19606 was removed with a wire loop under aseptic conditions and streaked onto another TSA plate and incubated for a further 24 hours at 37°C. The colony morphology was analysed by measuring and recording the physical attributes observed (**Section 4.1**).

3.6 Gram Staining and Light Microscope Analysis

3.6.1 Objective

The Gram stain is a technique first developed in 1884 by the Danish scientist Hans Christian Gram and is used to differentiate between two basic groups of bacteria, Gram-positive and Gram-negative. The technique uses three stains and ethanol:

- Crystal Violet, the primary stain,
- Iodine, the mordant,

- Ethanol, the decolourising agent,
- Safranin, the counterstain.

Gram-positive cells stain dark purple from the crystal violet and Gram-negative cells stain pink/red from the safranin (Bauman, 2012).

3.6.2 Methodology

The following procedure, recommended by the University of Lincoln Microbiology Laboratory, was adopted for Gram staining *A. baumannii*. A drop of distilled water was pipetted onto a clean glass slide. A colony of *A. baumannii* was removed with a wire loop from the surface of a streaked TSA plate which had been grown at 37°C for 24 hours. The colony was mixed with the distilled water and spread across the slide. The slide was left to air dry. Once dry, the slide was flooded with crystal violet for 60 seconds. The slide was rinsed with tap water for approximately 5 seconds.

The slide was then flooded with Gram's iodine for 60 seconds and further rinsed with tap water for approximately 5 seconds. The slide was rinsed with 100 % absolute ethanol for approximately 5 seconds and then rinsed with tap water.

The slide was then stained with safranin for 60 seconds. The slide was rinsed with tap water and blotted on absorbent paper. The colour and shape of the bacterial cells were observed under a Zeiss Primo Star Light Microscope with 10x, 20x, 40x and 63x magnifications and the width and length of single cells of *A. baumannii* were measured (**Section 4.1**).

3.7 Analytical Profile Index 20NE Identification Kit

3.7.1 Objective

The bioMérieux Clinical Diagnostics API 20NE identification kit is used to facilitate the identification of non-fastidious, non-Enterobacteriaceae Gram-negative rods. The kit was used to confirm the culti-loops contained *A. baumannii.* The kit consists of twenty cupules each containing different dehydrated substrates.

- Eight of the cupules determine if *A. baumannii* is able to ferment a specific substrate; a colour change within the cupule indicates a positive or negative result.
- Twelve cupules are assimilation tests; they are inoculated with minimal inoculated medium and tests if *A. baumannii* is able to grow by utilising the specific substrate. A clear cupule indicates no growth, a negative result, an opaque cupule indicates growth, a positive result.

The oxidase test (**Section 3.8**) is not included in the API kit but was also used to confirm the identity of *A. baumannii*.

3.7.2 Methodology

Under aseptic conditions, a loop containing *A. baumannii* 19606 was streaked onto a TSA plate and incubated for 24 hours at 37°C. Using a sterile loop, one colony was transferred from the plate into 2ml of saline solution.

5ml of distilled water was distributed throughout the incubation tray to create a humid atmosphere when incubated. Under aseptic conditions, the API strip was removed and placed into the incubation box.

The eight substrate tests were:

- Potassium nitrate ($N0_3$)
- Tryptophane (TRP)
- Glucose (GLU)
- Arginine (ADH)
- Urea (URE)
- Esculin (ESC)
- Gelatine (GEL)
- P-nitrophenyl-β-D-galactopyranoside (PNPG)

The cupules were filled with the inoculated saline until the tubes were full while avoiding the production of air bubbles. Mineral oil was added to the GLU, ADH, URE tubes until a convex meniscus filled the cupules, creating anaerobic conditions.

200 µl of the inoculated saline solution was then transferred into an ampule containing 7ml of API AUX medium and the solution.

The twelve assimilation tests were:

- Glucose (GLU)
- Arabinose (ARA)
- Mannose (MNE)
- Mannitol (MAN)
- N-acetyl-glucosamine (NAG)
- Maltose (MAL)
- Gluconate (GNT)
- Caprate (CAP)
- Adipate (ADI)
- Malate (MLT)

- Citrate (CIT)
- Phenyl-acetate (PAC)

The cupules were filled with the inoculated AUX medium while avoiding the production of air bubbles. The lid was placed onto the strip and incubated at 37°C for 24 hours.

- **GLU, ADH, URE, ESC, GEL, PNPG cupules**: the spontaneous reactions were recorded as positive or negative using the colour results sheet supplied by bioMérieux.
- **NO_3 cupule**: one drop of reagents NIT1 and NIT2 were added to the cupule and after five minutes the result was recorded. As no colour change occurred, 2-3mg of zinc powder was added and left for five minutes and the resulting colour change was recorded. The liquid within the cupule was pipetted out and discarded and the cupule was filled with mineral oil until a convex meniscus was formed.
- **TRP cupule**: a drop of JAMES reagent was added and the resulting colour change was recorded. The liquid within the cupule was pipetted out and discarded and the cupule was filled with mineral oil until a convex meniscus was formed.
- **Assimilation tests**: growth was recorded as negative if the cupule was clear and positive if the cupule was opaque.

5ml of distilled water was replenished in the incubation tray and the strip was re-incubated for a further 24 hours at 37°C. The colours/turbidity of all the cupules were then recorded again except for the first three tests, NO_3, TRP and GLU. A complementary test of growing a streak plate of *A. baumannii* 19606 at 44°C for 24 hours was also carried out.

3.8 Oxidase Test

3.8.1 Objective

The oxidase test is used to test for the presence of cytochrome C oxidase, an enzyme involved in the bacterial electron transport chain. This test distinguishes between the bacterial genera such as *Pseudomonas* and *Neisseria* which are characterised as oxidase positive compared to oxidase negative organisms such as the Enterobacteriaceae family (Bauman, 2011).

A. baumannii is not a member of the Enterobacteriaceae family but does not contain cytochrome c oxidases. The reagent Tetramethyl-p-phenylenediamine dihydrochloride (TMPD) functions as an artificial electron donor and when oxidised by oxidase, a dark blue/purple colour appears. If there is no colour change, the result is recorded as oxidase negative (Bauman, 2011; Jurtshuk and McQuitty, 1976).

The result of this test was used as an additional part of the API identification kit and the results are described in **Section 4.1**.

3.8.2 Methodology

1g of N,N,N,N-tetramethyl-p-phenylenediamine dihydrochloride (TMPD) was dissolved in 100ml of distilled water. 1ml of this solution was impregnated onto filter paper. Using a sterile plastic loop, a sample of *A. baumannii*, grown on TSA for 24 hours at 37°C, was spread across the impregnated filter paper. If a dark purple/blue colour appeared within 10 seconds the result was recorded as oxidase positive and if there was no colour change the result was recorded as oxidase negative. *Pseudomonas aeruginosa* was used as a positive control while *Klebsiella pneumoniae* was used as a negative control.

3.9 30 Hour Growth Curve of *A. baumannii* 19606

3.9.1 Objective

A growth curve for *A. baumannii* 19606 was created to investigate the following:

1. To determine the cell density within a solution of Tryptone soya broth (TSB) at an absorbance of 590nm. The absorbance calculation had to be repeated at the start of each experiment to ensure a standard cell density of $5x10^5$ CFU/ml (**Section 3.4.1**).
2. To find the lag phase, log phase and stationary phase of *A. baumannii* growth (Rolfe *et al.*, 2012; Hall *et al.*, 2014).
    - Lag phase: a delay in time before bacterial exponential growth.
    - Log phase: Bacteria grow exponentially and at a constant rate.
    - Stationary phase: Bacteria cell death and division equal.
    - Death phase: Number of cells dying higher than cells dividing.

3.9.2 Methodology

Acinetobacter baumannii 19606 culti-loop was spread onto a fresh TSA plate and incubated at 37°C for 24 hours. After 24 hours, 2-3 colonies were removed from the plate using a wire loop and two universals containing sterile TSB were inoculated and incubated at 37°C overnight. Four blank controls were also made by removing 1ml sterile TSB from each conical flask and pipetted into 1ml plastic cuvettes.

Using **Equation 1** (**Section 3.4.1**), a calculated volume of inoculated overnight broth was removed and added to three conical flasks containing sterile TSB to give a final absorbance of 0.01 at a wavelength of 590nm in a final volume of 250ml.

The inoculation of each conical flask was staggered by 15 minutes before incubation at 37°C in a shaker incubator set at 140 rotations per minute (rpm). An initial reading was taken at 0 minutes then at every hour for 30 hours.

At each hour, 1ml was pipetted from the conical flask and transferred to a cuvette and the absorbance was measured at 590nm against the blank of TSB made from the corresponding conical flask. Three measurements were taken and an average calculated. If the reading was above 1 the solution was diluted down using sterile TSB and the resulting absorbance value was calculated based on the dilution ratio.

After measuring the absorbance, a further 1ml was removed from the conical flask and pipetted into a glass universal containing 9ml ¼ strength Ringer's solution. A serial 10-fold dilution was completed to a chosen dilution for each hour, as shown in **Section 8.2**. 100 µl was removed from the three highest serial dilutions and pipetted onto TSA and spread using sterile L-shaped spreaders. These plates were incubated at 37°C for 24 hours. For the control, 1ml was removed to measure the absorbance and 100 µl was directly pipetted onto TSA and spread.

After incubation, the colonies on each petri dish (three per hour) were visually counted and the number of viable cells (CFU/ml) were calculated for all thirty hours. A calibration of absorbance against cell number (CFU/ml) was then prepared. Graphs of absorbance and cell number (CFU/ml) against time for the 30 hour growth curve are shown in **Section 4.2**

The spread plating procedure was also repeated at the start of each experiment to ensure the initial bacteria concentration was $5x10^5$ CFU/ml.

3.10 Minimum Inhibitory Concentration (MIC)

3.10.1 Objective

The minimum inhibitory concentration (MIC) experiment was carried out to find the lowest concentration of antibiotic required to inhibit the growth of *A. baumannii* 19606. The MIC was determined for each of the peptides, colistin sulphate, bicarinalin and BP100, using the following method (Wiegand *et al.*, 2008; Eucast, 2003).

3.10.2 Methodology

A glass universal containing 10ml of sterile TSB was inoculated by taking 2-3 colonies of *A. baumannii* from a streaked TSA plate which had been incubated for 24 hours at 37°C. This universal was incubated overnight at 37°C. Using the method described in **Section 3.4.1**, a glass universal containing $1x10^6$ CFU/ml of *A. baumannii* in TSB was prepared.

The peptides were prepared using the method described in **Section 3.4.2**. The solution was sterilised by filtering through a 0.2µm filter into sterile microtubes. Colistin sulphate was stored at 4°C while bicarinalin and BP100 were stored at -18°C.

To produce a 2-fold serial dilution of antimicrobial peptide, 50 µl of sterile TSB was initially added to 12 wells of three rows of a 96 well plate. 50 µl of peptide, at a stock concentration of 1024µg/ml, was added to well 1 and a two-fold dilution was made for each of wells 2 to 12. This was completed by, firstly mixing the TSB and the peptide solution in well 1, then pipetting 50 µl from well 1 into well 2 and mixing again. This was repeated until well 12 where the excess 50µl was removed and discarded.

50 µl of inoculated TSB, containing 1x10^6 CFU/ml of *A. baumannii*, was added to each well resulting in a peptide concentration in each well as shown in **Table 3.10.1** and a cell density of 5x10^5 CFU/ml. This was repeated for two further rows of the same 96 well plate.

Well	Concentration of Antimicrobial Peptide (µg/ml)
1	256
2	128
3	64
4	32
5	16
6	8
7	4
8	2
9	1
10	0.5
11	0.25
12	0.125

Table 3.10.1- Antimicrobial peptide concentration (µg/ml) per well after two fold dilution and addition of bacterial inoculum.

Growth controls were also prepared containing 50µl of TSB and 50 µl of inoculated TSB to make a cell density of 5x10^5 CFU/ml and a sterility control containing 100 µl sterile TSB. The plate was covered in Parafilm to minimise evaporation and incubated at 37°C and 140rpm in a shaking incubator for 24 hours. After 24 hours, the wells were observed and turbid and clear wells were recorded. The lowest concentration of peptide where the well was visibly clear was recorded as the MIC.

This entire experiment was repeated a further two times on two separate 96 well plates to give a total of nine datasets. The results are shown in **Section 4.3**.

3.11 Minimum Bactericidal Concentration (MBC)

3.11.1 Objective

The minimum bactericidal concentration was defined as the lowest concentration of antimicrobial peptide required to kill ≥99.9 % of *A. baumannii* cells (Eucast, 2003; Wiegand *et al.*, 2008). After recording the MIC, the MBC for each peptide was determined by the plate spread method as described below.

3.11.2 Methodology

After recording the MIC, 100 µl was removed from each clear well and pipetted onto TSA and spread using sterile L-shaped spreaders. These plates were incubated at 37°C for 24 hours. After incubation, the number of colonies grown on the plates were counted and the lowest concentration where there was no growth observed on the plate was recorded as the MBC. This was carried out after each MIC test and therefore carried out 3 times. This experiment was repeated two further times to give a total of nine datasets. The results are shown in **Section 4.4**.

3.12 Minimum Biofilm Inhibitory Concentration (MBIC)

3.12.1 Objective

The minimum biofilm inhibitory concentration (MBIC) is defined as the lowest concentration of antimicrobial peptide that caused 90 % inhibition of *A. baumannii* biofilm formation (Gopal *et al.*, 2014). Biofilm formation was quantified using the stain crystal violet method.

Crystal violet or gentian violet stains the bacterial cells by binding to components of the bacterial cell wall such as lipopolysaccharides and peptidoglycan. Crystal violet dissolved in water absorbs light at 590nm (National Centre for biotechnology Information, 2015). A photo spectrometer at this wavelength was used to quantify the amount of crystal violet present.

3.12.2 Methodology

A 96 well plate containing a two-fold dilution of peptide with $5x10^5$ CFU/ml *A. baumannii* was set up as described for the MIC test in **Section 3.10**.

The plate was covered in Parafilm and incubated for 24 hours at 37°C and 140rpm. After 24 hours, under aseptic conditions, the wells were emptied onto absorbent paper. The wells were washed three times with ¼ strength Ringer's solution and air dried for 1 hour in ambient room temperature (22°C).

1 % crystal violet solution was prepared, in distilled water, and added to each well and left at room temperature for 10 minutes. The wells were emptied by pipetting onto absorbent paper, washed three times with distilled water, and air dried for 30 minutes at 37°C.

The stain was solubilised with 100 µl of 96 % ethanol (in distilled water). The plate was covered in Parafilm and shaken at 140rpm for 30 minutes. Using a spectrophotometer, 2 µl was removed from a well and the absorbance of the solution was measured at 590nm compared to a blank of 96 % ethanol. Three samples were taken from each well which were read twice to give six readings for each well. This was completed for all three rows. The experiment was repeated once more to give a dataset of 36 readings for each concentration.

The percentage of biofilm inhibition was calculated using **Equation 3** below:

Equation 3: $\left(1 - \left(\frac{Absorbance\ (@590nm)\ of\ cells\ treated\ with\ test\ agent}{Absorbance\ (@590nm\ of\ untreated\ control}\right)\right)$ x 100

The results are shown in **Section 4.5**.

3.13 Biofilm Removal Assay

3.13.1 Objective

In this experiment, biofilms are grown then the reduction of biofilms (dead or alive) after treatment with increasing concentrations of each peptide is investigated. This contrasts with the preceding MBIC experiment that investigates the inhibition to biofilm growth for each peptide.

24 hour biofilms were grown and then subjected to a range of peptide concentrations for 24 hours. The biofilm present in the well was quantified with crystal violet staining as previously described in **Section 3.12** (Song *et al.*, 2015; Dosler and Karaaslan, 2014).

3.13.2 Methodology

24 hour biofilms of *A. baumannii* were grown in 3 rows of 12 wells of the 96-well plate by adding 50 µl sterile TSB and 50 µl of inoculated TSB with $1x10^6$ CFU/ml. The plate was incubated at 37°C at 140rpm.

On a separate 96 well plate (titration plate) a two-fold serial dilution was prepared with 75 µl of TSB and 75 µl of antimicrobial peptide stock at a concentration of 8192 µg/ml using the same method described in **Section 3.10**.

The wells containing biofilm were washed three times with 150 µl ¼ strength Ringer's solution. 75 µl sterile TSB was then added to each well. 75 µl from the titration plate containing a specific concentration of peptide was added to the corresponding well on the test plate. This resulted in each well containing 150 µl of TSB, which ensured the biofilm was completely submerged, and the test wells containing a two-fold serial dilution of antimicrobial peptide with concentrations shown in **Table 3.13.1** below. 150

µl sterile TSB was added to the negative control wells. The plate was covered in Parafilm and incubated for 24 hours at 37°C and 140rpm in a shaker incubator.

Well	Concentration of Antimicrobial Peptide (µg/ml)
1	2048
2	1024
3	512
4	256
5	128
6	64
7	32
8	16
9	8
10	4
11	2
12	1

Table 3.13.1- Antimicrobial peptide concentration for each well after a twofold-serial dilution.

After 24 hours, the wells were emptied by tipping onto absorbent paper. The wells were washed three times with 200 µl ¼ strength Ringer's solution and air fixed for 1 hour under aseptic conditions.

The percentage of biofilm removal was quantified by measuring the absorbance after applying crystal violet stain as follows. 100 µl of 1 % crystal violet solution in water was added to each well and left at room temperature for 10 minutes. The wells were emptied by tipping and washed three times with 150 µl distilled water and air dried at

37°C for 30 minutes. The stain was solubilised with 100 µl 96 % ethanol in a shaker incubator set at 140rpm for 30 minutes.

The quantification of crystal violet was carried out using the same method as described in **Section 3.12**.

This procedure was repeated for all three rows. The entire experiment was repeated once to give a total of 36 readings for each concentration.

Equation 3 (**Section 3.12**) was used to ascertain the percentage biofilm reduction in the presence of the different antimicrobial peptide concentrations. The results are shown in **Section 4.6**.

3.14 Atomic Force Microscope

3.14.1 Objective

Using previously published methods (Alves *et al.*, 2010; Domingues *et al.*, 2014) the AFM was used to obtain 3D images of *A. baumannii* cells to analyse the surface topography and quantify the cell surface roughness and area when the cells are subjected to concentrations of peptides that equated to ½ MBC, MBC and 2xMBC for each peptide. These concentrations were based on results of the MBC experiment as described in **Section 4.4**.

3.14.2 Methodology

A 150 µl suspension containing inoculated TSB with an *A. baumannii* cell density of $5x10^5$ CFU/ml and peptide concentration as shown in **Table 3.14.1** was prepared using methodology described in **Section 3.10**. A negative control containing 150 µl of *A. baumannii* at $5x10^5$ CFU/ml was also prepared.

The concentrations used for each peptide were based on the results of the MIC and MBC results as shown in **Sections 4.3** and **4.4**. The plate was incubated at 37°C and 140rpm for 2 hours.

Antimicrobial Peptide	Concentration Tested (µg/ml)
Colistin sulphate	0.25
	0.5
	1
Bicarinalin	2
	4
	8
BP100	2
	4
	8

Table 3.14.1- Concentrations of colistin sulphate, bicarinalin and BP100 used for AFM investigation.

After 2 hours the solution was pipetted onto a poly-L-lysine slide and left at ambient room temperature (21±2°C) for 20 minutes. The slide was then rinsed by pipetting distilled water from the top of the slide and letting it run down, washing the surface. The slide was left to air dry for 20 minutes and then analysed using a Bruker Bioscope Catalyst Atomic Force Microscope (AFM) mounted on top of the Nikon Eclipse TE2000-S microscope. Bruker Atomic Force Microscope ScanAsyst-air tips were used with the following characteristics:

- Cantilever tip height-650nm,
- Cantilever length-115µm,
- Cantilever width-25µm,
- Resonance frequency (F0)-70kHz,
- Spring constant (k)-0.4N/m.

Images of the cells were obtained using the software program 'NanoScope 9' with an area of 4μm^2 at a scan rate of 0.5Hz and 256 lines. The surface roughness and surface area of five selected bacterial cells were calculated using the Gwyddion SPM (scanning probe microscopy) software program (Necas and Klaptek, 2012).

The image was firstly height levelled by a setting a plane through three points. A height threshold was produced to form a mask that discriminated the bacterial cell from the rest of the image. This meant that only the bacterial cell was analysed and not the glass slide. The RMS (root-mean-squared) calculation was used to analyse the surface roughness of the bacterial cell. The surface area of each of these cells was also quantified.

The results are shown in **Section 4.7**

3.15 Scanning Electron Microscope

3.15.1 Objective

The SEM was used to visualise the *A. baumannii* biofilm grown on the surface of the polystyrene pegs of the Nunc-TSP Screening Plate Lid.

The biofilm was grown for 24 hours and then subjected to four different concentrations, 1, 10, 100, 1000 µg/ml AMP for 24 hours. These concentrations were chosen based on biofilm removal results (**Section 4.6**).The biofilm was then fixed and prepared for SEM visualisation.

3.15.2 Methodology

Biofilms of *A. baumannii* were grown in 150 µl TSB in four wells of three rows of a 96-well plate as described in **Section 3.13** with the addition of a Nunc-TSP Screening Plate Lids lid containing polystyrene pegs which protruded down into the broth. Two negative controls were produced by pipetting 75 µl inoculated broth and 75 µl sterile TSB into a further two wells. 150 µl of sterile TSB was pipetted into two further wells allocated for sterility controls. The plate was covered in Parafilm and incubated at 37°C and 140rpm for 24 hours.

After 24 hours, the pegs were washed by submerging the plate lid in 200 µl of sterile ¼ strength Ringer's solution and leaving for 2 minutes. This was repeated twice more. Each well was then filled with 100 µl sterile TSB

An antimicrobial challenge plate was prepared in a similar method described for the titration plate in **Section 3.13**. The challenge plate had four wells for each peptide, colistin sulphate, bicarinalin and BP100, containing peptide concentrations as shown in

Table 3.15.1. 200 µl sterile TSB was added to the negative control and sterility control wells. The plate lid was placed onto this challenge plate, covered in Parafilm, and incubated at 37°C and 140rpm for 24 hour.

Well	Concentration of antimicrobial peptide (µg/ml)
1	1
2	10
3	100
4	1000
5	Negative Control
6	Sterility Control

Table 3.15.1- Concentration of antimicrobial peptide used in SEM investigation

After 24 hours the pegs were washed by submerging the plate lid in 250 µl of sterile ¼ strength Ringer's solution and leaving for 2 minutes. This was repeated twice more.

0.1M sodium cacodylate buffer was made up by dissolving 1g in 40ml of distilled water. 1M hydrochloric acid was added to the solution to give a pH reading of 7.2. Distilled water was added to give a final volume of 62.5ml. The plate pegs were then submerged in this solution for 3 minutes.

2.5 % glutaraldehyde was prepared by mixing 5ml 25 % glutaraldehyde solution with 45ml distilled water. The plate lid was placed onto the buffer in a 96 well plate, covered in Parafilm, and left at ambient temperature (21 ±2°C) for 40 minutes. The plate lid was then removed and washed in a 96 well plate containing 275 µl of distilled water in each well for 2 minutes. This was repeated once more. The biofilms were then dehydrated by placing into 2 plates containing 275 µl 50 % methanol, 2 plates containing 70 % methanol and finally 2 plates containing 100 % methanol. The plate lid was left in each solution for 2 minutes. The pegs were then left to dry for 4 days.

The pegs were then removed from the plate lid with flamed pliers and forceps and mounted onto 0.5in aluminium specimen stubs, fixed on carbon tabs. After mounting, the carbon tabs were painted with graphite and the pegs were coated with approximately 15-20nm of platinum. The pegs were visualised using a FEI Quanta FEG 650 Scanning Electron Microscope at the Leeds Electron Microscopy & Spectroscopy Centre, University of Leeds. Images were visualised at 5000x, 10,000x, 20,000x, and 30,000x magnification. Due to a time constraint for 8 hours three concentrations for each peptide, 1, 10, 100 μg/ml were visualised. The results are shown in **Section 4.8**.

3.16 Confocal Laser Scanning Microscope (CLSM)

3.16.1 Objective

The Leica TCS SP8 Confocal Microscope was used to analyse the structure of the biofilm and quantify the biofilm parameter bio-volume (μm^3), defined as the amount of space or biomass occupied by a biofilm in a constant area (Harrison *et al.*, 2006; Yerly *et al.*, 2007).

The analysis was carried out by staining the biofilm with the fluorescent stain, SYTO9, and creating a Z stack of the biofilm by taking optical slices of the biofilm at 0.5µm intervals.

3.16.2 Methodology

A glass universal containing TSB, with a cell density of $1x10^6$ CFU/ml, was prepared as discussed in **Section 3.4.1**. 150 µl of newly inoculated TSB was pipetted into 5 wells of an 8 chambered #1.0 borosilicate coverglass system. A further 150 µl of sterile TSB was added to each of these wells and 300 µl added to well 6 as a sterility control. The chambered coverglass was covered in Parafilm and incubated at 37°C and 140rpm for 24 hours. After 24 hours, the wells were washed by removing the TSB and pipetting 350 µl ¼ strength Ringer's solution into the well and then removing the solution. The Ringer's solution was added and removed a further two times.

Four of the wells were filled with sterile TSB and a calculated concentration of antimicrobial peptide was added, using **Equation 2** (**Section 3.4.2**), to give a final volume of 400 µl. The concentrations of peptide in each well are shown in the **Table 3.16.1** below. 400 µl of sterile TSB was pipetted into well 5, which was allocated for the

negative control, and sterility control. The chambered coverglass was covered with Parafilm and incubated at 37°C and 140rpm for 24 hours.

Well	Concentration of antimicrobial µg/ml
1	1
2	10
3	100
4	1000
5	Negative Control
6	Sterility Control

Table 3.16.1- Concentration of antimicrobial peptide used in CLSM investigation.

The wells were washed 3 times with sterile ¼ strength Ringer's solution. The stain SYTO9 was prepared. 1ml microtubes containing concentrations of 6.7µM SYTO9 were prepared from the stock solutions of 3.34mM from BacLight Live/Dead staining, (Harrison *et al.*, 2006) using **Equation 4** below:

Equation 4: $$Dilution\ Factor = \frac{Orginal\ Concentration}{Final\ Concentrations\ Required}$$

SYTO9 was prepared by adding 3 µl of stain to 997 µl of Mili-Q water (18.2Ω) and stored at 4°C in the dark.

Before use SYTO9 was vortexed at 800rpm for 15 seconds and 250 µl was pipetted into each well. The chamber was covered with silver foil to create dark conditions and incubated at 30°C for 30 minutes. The excess stain was rinsed out of the wells using 250 µl of ¼ strength Ringer's solution twice and a final volume of 200 µl ¼ strength Ringer's solution was added to each well and the chamber was visualised under the CLSM. The biofilm was observed using the 40x using the 488nm PMT2 laser and an emission wavelength range of 490nm-515nm. The results are shown in **Section 4.9**

Biofilm bio-volume was quantified using BITPLANE Imaris x64 Version 8.1.2 (Bitplane, 2015).

3.17 Statistical Methods

The program IBM SPSS Statistics 21 was used for the statistical analysis of MBIC (**Section 3.12**), biofilm removal assay (**Section 3.13**), surface roughness and area of bacteria cell surface visualised on the AFM (**Section 3.14**) and bio-volume quantified by BITPLANE Imaris software using images taken by the CLSM (**Section 3.16**).

The samples t-test was used to find if there was a statistical difference of 95% ($p \leq 0.05$) which was considered as statistically significant or 99% ($p \leq 0.01$) which was considered highly significant between the results from each peptide concentration and the negative controls.

4 Results

4.1 The Identification of *A. baumannii*

4.1.1 Colony Morphology and Gram Stain

A. baumannii 19606 colonies were grown using the methodology described in **Section 3.5**. The colonies are shown in **Figure 4.1.1** after being streaked on TSA. **Figure 4.1.2** illustrates the individual *A. baumannii* cells at a magnification of 40x under a light microscope after Gram staining, as described in **Section 3.5**. The colony morphology and Gram stain results are presented in **Table 4.1.1**.

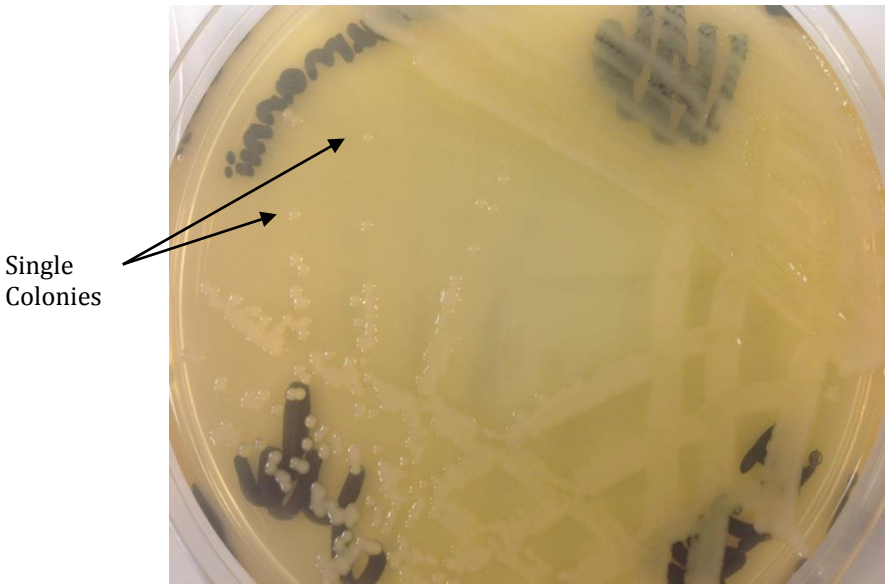

Figure 4.1.1-Streaked A. baumannii 19606 colonies after 24 hour incubation at 37°C.

Description	Observation
Form of colony	Circular
Size of colony (diameter)	Small (~1mm)
Margin of colony	Entire/even
Pigmentation of colony	Pale yellow
Opacity	Opaque
Elevation	Flat
Surface	Smooth, glistening
Consistency/Texture	Moist
Gram stain	Gram-negative (pink-red cells)
Shape of Cell	Cocci-bacilli/short rods
Length of Cell	2-2.5µm
Width of Cell	1-1.5µm

Table 4.1.1-Description of A. baumannii colonies on TSA plate; *after 24 hour incubation at 37°C and light microscope analysis of cells after Gram-staining.*

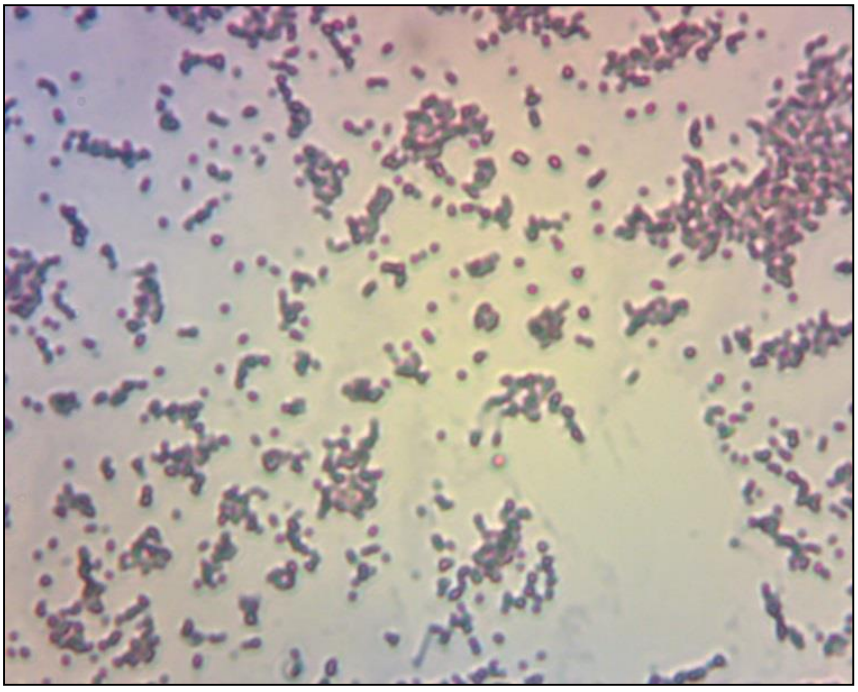

Figure 4.1.2-Gram stain of A. baumannii: coccus-bacillus shaped cells; *stained pink/red indicate Gram negative cell walls (magnification-40x).*

4.1.2 Analytical Profile Index 20NE

The API20NE test was used in the identification of Gram negative non-Enterobacteriaceae (Al Jarousha *et al.*,2009; BioMérieux, 2015). The results of this test are shown in **Sections 4.1.2, 4.1.3 and 4.1.4**.

After 24 hours, the strip was analysed for growth and colour changes in the cupules, using the results table supplied with the API 20NE test (**Section 8.1**). The results of the first eight tests are shown in **Figure 4.1.3** and described below:

- The **potassium nitrate (NO_3)** cupule tested the ability to convert nitrates into nitrites. After the addition of the reagents NIT 1 and NIT 2, the cupule remained colourless indicating *A. baumannii* does not reduce nitrates to nitrites. To investigate if this was a false negative result, due to the formation of nitrogen, zinc powder reagent was added to the cupule and within 5 minutes the cupule turned pink/red. This colour change indicated the presence of nitrates, which had not been converted by *A. baumannii*. The NO_3 cupule test was recorded as a negative result.
- The **L-tryptophan (TRP)** cupule tested the ability to produce indole from the amino acid tryptophan. With the addition of JAMES reagent the cupule remained colourless indicating *A. baumannii* does not produce indole and a negative result was recorded.
- The **glucose (GLU)** cupule contained glucose and tested the ability to ferment glucose in anaerobic conditions. The cupule resulted in a negative colour change of blue indicating the inability of *A. baumannii* to ferment glucose after 24 hours incubation.
- The next three tests assessed the ability of *A. baumannii* to hydrolyse **Arginine (ADH), Urea (URE)** and **Aesculin (ESC)**; all three cupules remained yellow after 24 hours and were recorded as negative results.

- The **Gelatin test (GEL)** assessed the ability to hydrolyse gelatin with the enzyme protease. There was no pigment diffusion seen within the cupule and a negative result was recorded.
- The final and eighth test assessed the ability of *A. baumannii* to hydrolyse **4-nitrophenyl-βD-galactopyranoside (PNPG)**; the cupule remained colourless and was recorded as a negative result.

Figure 4.1.3-First 8 tests of API 20NE; after 24 hour incubation*; NO_3 after the addition of NIT1, NIT2 & Zinc powder and TRP after the addition of JAMES reagent.*

The strip was incubated for a further 24 hours at 37°C and the results are shown in **Figure 4.1.4**. The results are the same as the 24 hour incubation.

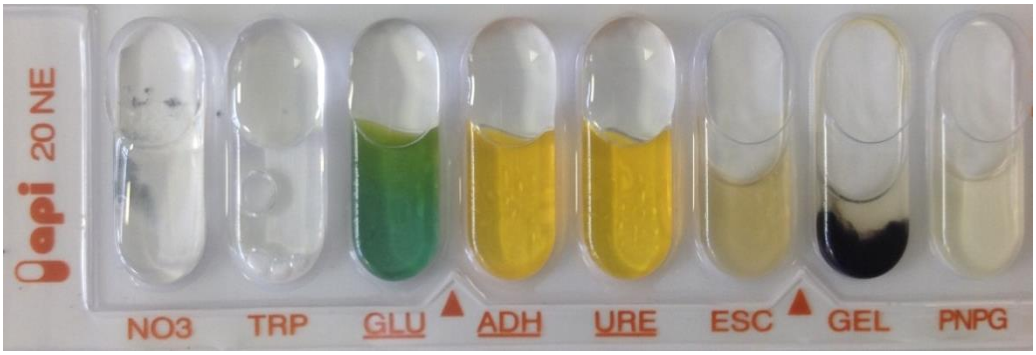

Figure 4.1.4-First 8 tests of API20NE after 48 hour incubation. *Note: Emptying and refilling with mineral oil of cupules NO_3 and TRP. The results are consistent with the 24 hour incubation.*

The assimilation tests assessed the ability of *A. baumannii* to grow in the presence of the substrate in the cupule. The results of the twelve assimilation tests were recorded

after 24 hours and 48 hours; the 48 hour strip is shown as **Figure 4.1.5**, based on whether the cupules were turbid or clear.

After the 24 hour incubation period, the following tests had turbid wells indicating bacterial growth and were recorded as positive results:

- Arabinose (ARA)
- Capric acid(CAP)
- Adipic acid (API)
- Malic acid (MLT)
- Trisodium citrate (CIT)
- Phenylacetic acid (PAC)

The following tests had clear cupules indicating no growth and were recorded as negative results:

- Glucose (GLU)
- Mannose (MNE)
- Mannitol (MAN)
- N-acetyl glucosamine (NAG)
- Maltose (MAL)
- Potassium gluconate (GNT)

The twelve assimilation tests were read again after 48 hours and their results recorded based on turbid or clear cupules. The results at 48 hours were identical as at 24 hours.

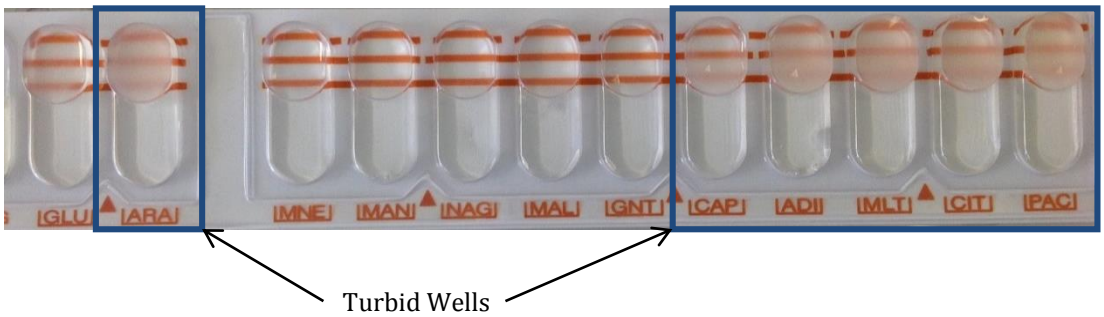

Figure 4.1.5-Assimilation Tests of API 20NE Strip after 48 hours incubation. *Note turbid results for ARA, CAP, ADI, MLT, CIT, PAC cupules; the other cupules remained clear.*

This test confirmed the identification of *A. baumannii/calcoaceticus* with 99.9% confidence (**Section 4.1.4**).

4.1.3 Oxidase Test

The oxidase test was used to test for the presence of cytochrome C oxidase as described in **Section 3.8**. A dark blue/ purple colour change would indicate a positive result.

As shown in **Figure 4.1.6,** *A. baumannii* is oxidase negative as no colour change was observed within 10 seconds. This was compared to the dark blue/purple colour of positive control, *Pseudomonas aeruginosa*, and the colourless sample of the negative control, *Klebsiella pneumoniae*.

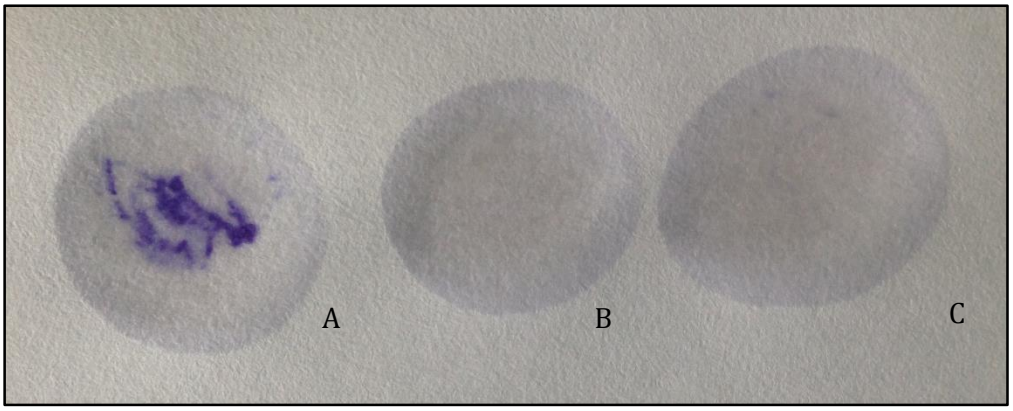

Figure 4.1.6- Oxidase Test Result *showing positive control of Pseudomonas aeruginosa (A), A. baumannii (B) and negative control Klebsiella pneumoniae* (C).

4.1.4 Numerical Profiling of *A. baumannii*

The identification of *A. baumannii* was completed by numerical profiling, by analysing the results with the biomerieux software (Biomerieux, 2015). The twenty tests on the API 20NE strip and oxidase test were split into seven groups of three. Using a results sheet, a 7-digit number was obtained by concatenating the numbered values of 1, 2 and 4 corresponding to positive reactions within the group of three, as shown in the **Figure 4.1.7**.

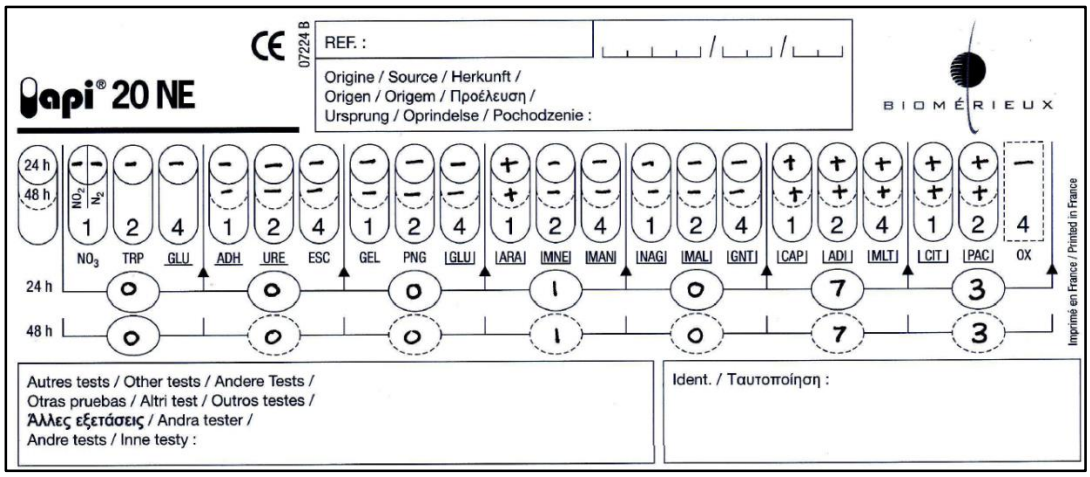

Figure 4.1.7-API20NE Numerical Profiling for the Identification of A. baumannii

The 7-digit number, 0001073, was entered into apiweb which confirmed the identification of the *A. baumannii* group with 99.9% identification confidence as shown in **Figure 4.1.8** (Biomerieux, 2015). The complementary test of growing a spread plate at 44°C was carried out and growth was observed indicating the presence of *A. baumannii* species (Saugar *et al.*, 2006; Vaneechoutte *et al.*, 2011).

EXCELLENT IDENTIFICATION

Strip	API 20 NE V8.0
Profile	0 0 0 1 0 7 3
Note	ID. NOT VALID BEFORE 48 HOURS

Significant taxa	% ID	T	Tests against			
Acinetobacter baumannii/calcoaceticus	99.9	0.95				

Next taxon	% ID	T	Tests against			
Acinetobacter radioresistens	0.1	0.17	ARAa 2%	MLTa 2%	CITa 2%	

Complementary test(s)	44°C			
Acinetobacter baumannii	+			
Acinetobacter calcoaceticus	-			

Figure 4.1.8-apiweb identification of A. baumannii *confirming identification with 99.9% confidence with number 0001073.*

4.2 30 Hour Growth Curve of *A. baumannii* 19606

The objectives and methodology of the 30 hour growth curve are described in **Section 3.9**. **Figure 4.2.1** shows the absorbance at 590nm over 30 hours. The initial absorbance, at hour 0, was 0.01, the lowest reading the photometer was able to read. It shows the lag phase lasted for about 1 hour with an absorbance of 0.034, averaged over the three test samples. At the second hour the absorbance had risen by 400%. The absorbance then increased each hour following an approximately linear relationship for the remainder of the experiment.

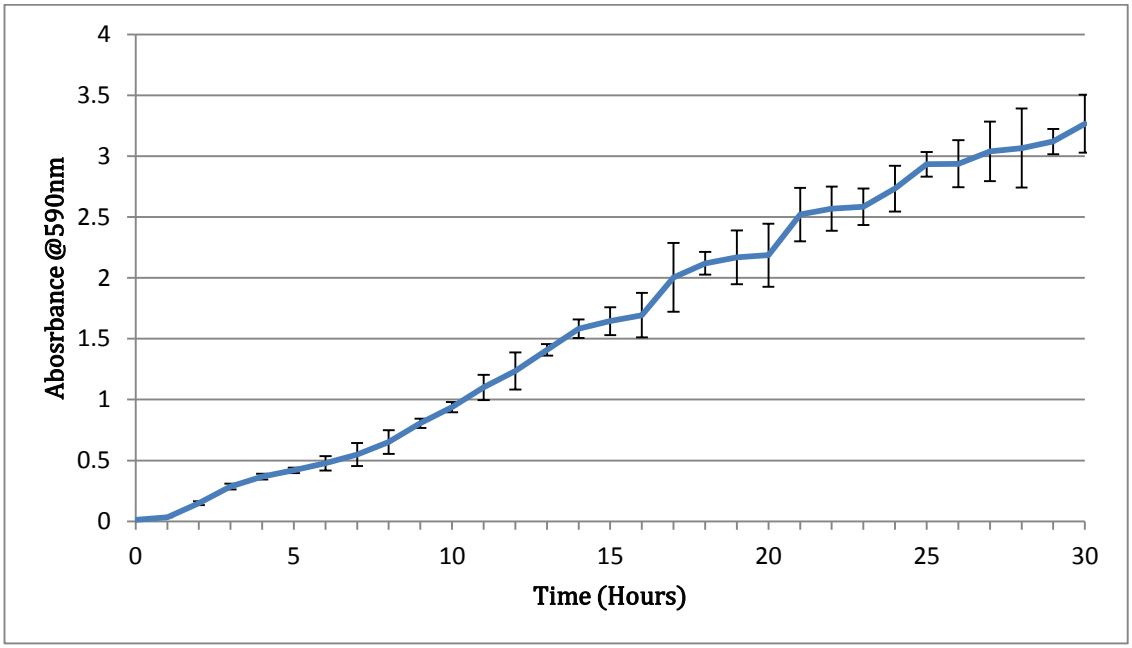

Figure 4.2.1- Graph showing the absorbance of TSB containing A. baumannii over 30 hours. *Results from all three tests samples are used to construct the standard deviation bars at each hour.*

Figure 4.2.2 shows the cell count (CFU/ml) against time. This graph shows the lag phase of *A. baumannii* growth lasting about 1 hour which is consistent with the results shown in **Figure 4.2.1**. The growth is approximately exponential to 26 hours indicating the log phase (**Section 3.9.1**). The experiment was not extended sufficiently to confirm

the stationary phase but it may starts at about 26 hours as indicated by the CFU/ml plateau.

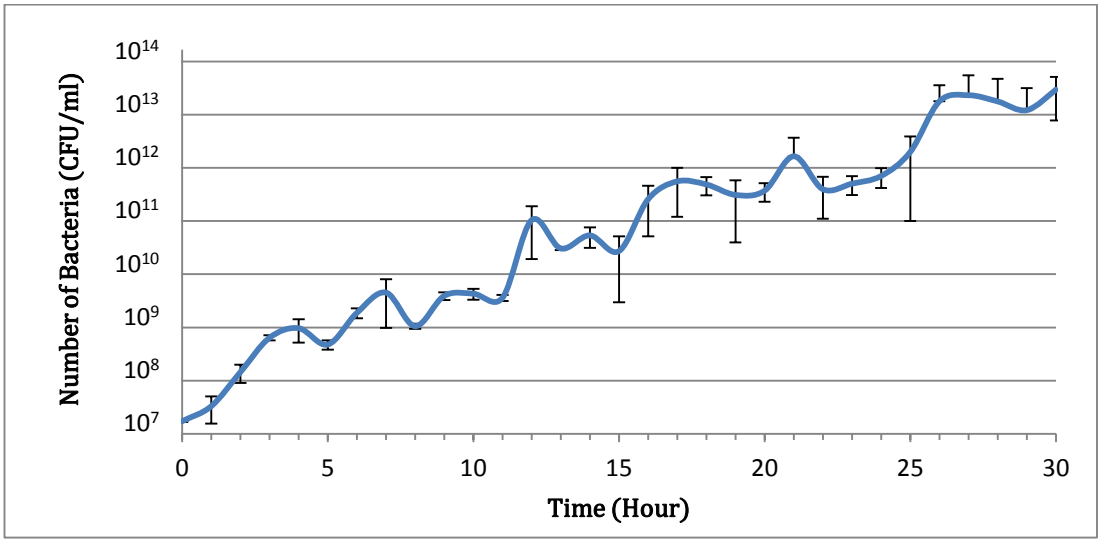

Figure 4.2.2-CFU/ml per hour on a logarithmic scale. *Results from all three tests samples are used to construct the standard deviation bars at each hour.*

The absorbance for a specific viable cell count (CFU/ml) was found by plotting the absorbance against the CFU/ml. The absorbance at the start was 0.01 and the average CFU/ml at this absorbance was $1x10^7$ CFU/ml. This absorbance value was used in **Equation 1** in the absorbance calculation described in **Section 3.4.1**.

4.3 Minimum Inhibitory Concentration (MIC)

The MIC experiment was carried out to find the lowest concentration of antibiotic required to inhibit the growth of *A. baumannii* following the methodology described in **Section 3.10** (Eucast, 2003; Wiegand *et al.*, 2008). The clear wells indicate no growth and the turbid wells indicate growth. The lowest concentration of peptide in a well which was clear was recorded as the MIC. The MIC for colistin sulphate was 0.5 µg/ml, 4 µg/ml for bicarinalin and 4 µg/ml for BP100 as shown in **Figures 4.3.1, 4.3.2 and 4.3.3**.

In **Figures 4.3.1-4.3.3**, rows A, B and C are identical test rows. Negative controls are in wells D1-3 and sterility controls in wells D10-12**.** All of the growth controls were turbid indicating growth and the sterility controls remained clear indicating no contamination to the assay.

Figure 4.3.1 displays the MIC results for colistin sulphate. Turbid wells were observed for wells 11 and 12 from all test rows. The MIC was determined to be the colistin sulphate concentration in Column 10 which was 0.5µg/ml.

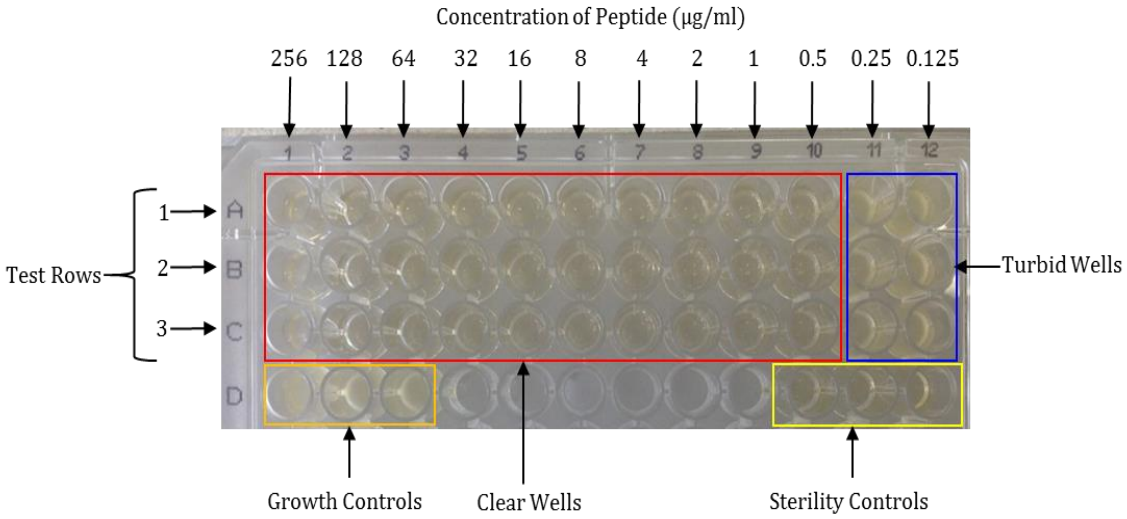

Figure 4.3.1-96 well plate showing minimum inhibitory concentration of colistin sulphate; *MIC is 0.5 µg/ml as shown with clear broth in well 10 in all three test rows. Note: Concentration range: Well 1: 256 µg/ml -Well 12:0.125 µg/ml.*

Figure 4.3.2 displays the MIC results for bicarinalin. Turbid wells were observed for wells 8 to 12 from all test rows. The MIC was determined to be the bicarinalin concentration in Column 7 which was 4 µg/ml.

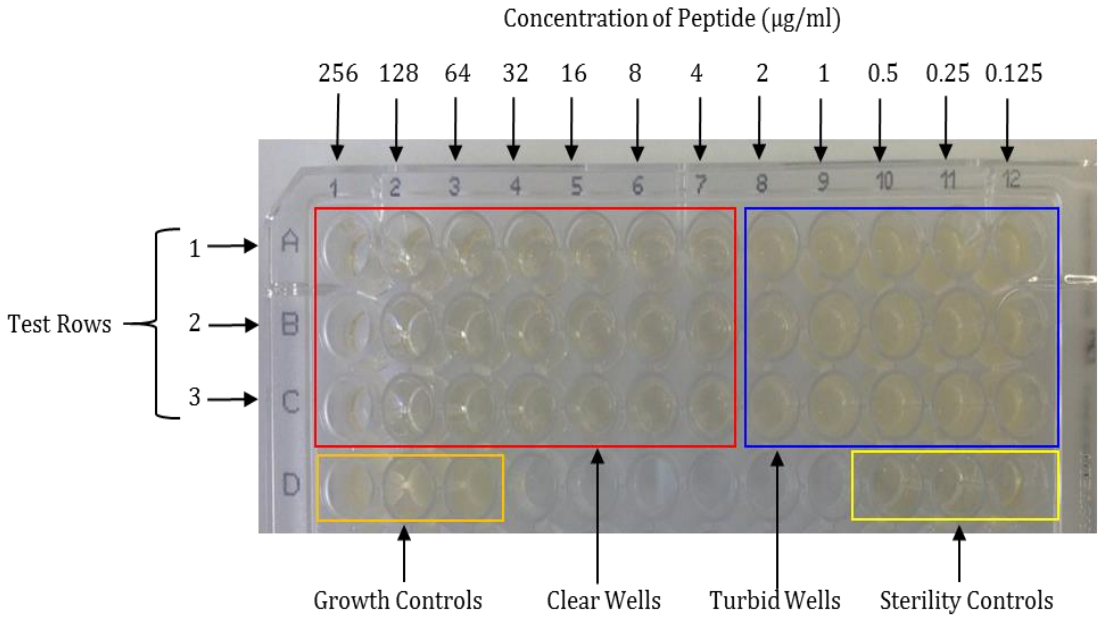

Figure 4.3.2-96 well plate showing minimum inhibitory concentration of bicarinalin; *MIC is 4 µg/ml as shown with clear broth in well 7 in all three rows. Note: Concentration range: well 1: 256 µg/ml to well 12: 0.125 µg/ml.*

Figure 4.3.3 displays the MIC results for BP100. Turbid wells were observed for wells 8 to 12 from all test rows. The MIC was determined to be the BP100 concentration in Column 7 which was 4 µg/ml.

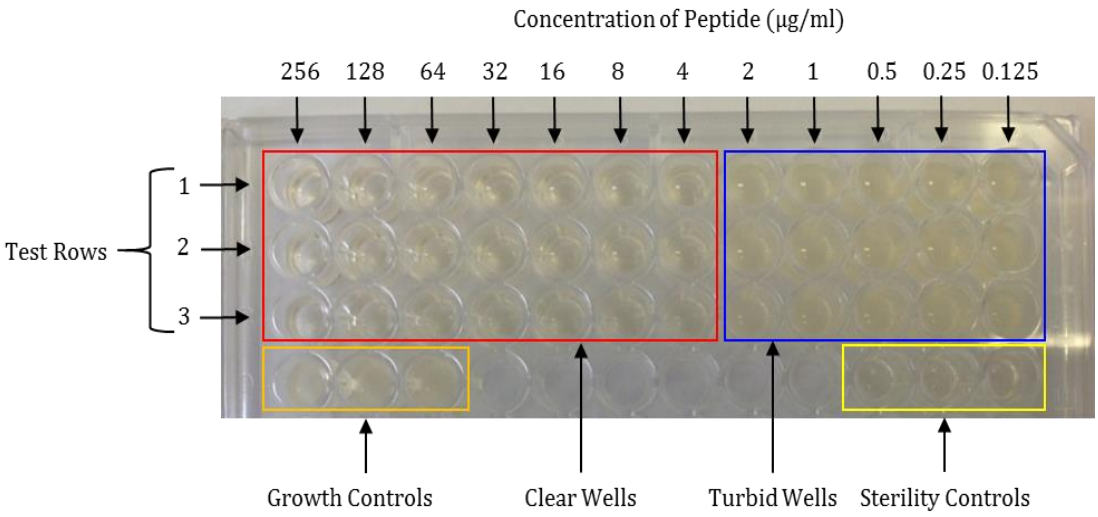

Figure 4.3.3-96 well plate showing minimum inhibitory concentration of BP100; *MIC is 4 µg/ml as shown with clear broth in well 7 in all three rows. Note: Concentration range: Well 1: 256 µg/ml -Well 12: 0.125 µg/ml.*

The recorded MIC is a maximum as, due to the two-fold dilution technique, the inhibition of growth would be between the last turbid well and the first clear well. For example, colistin sulphate had a MIC of 0.5 µg/ml, recorded for the first clear well. The MIC lies between 0.25 µg/ml (turbid well) and 0.5 µg/ml (clear well). The MICs for bicarinalin and BP100 both are between 2 µg/ml and 4 µg/ml. A more accurate MIC could be derived by a further detailed analysis of peptide concentrations within the range (**Section 5.2**).

Peptide	Minimum Inhibitory Concentration (µg/ml)	Minimum Inhibitory Concentration (µmol/l)
Colistin sulphate	0.5	0.43
Bicarinalin	4	1.8
BP100	4	2.8

Table 4.3.1- MIC for colistin sulphate, bicarinalin and BP100.

In **Table 4.3.1** the MIC according to molar concentration is also tabulated. The molar concentration has been calculated from the molecular weights of each peptide. Bicarinalin has the highest molecular weight at 2213.78 g/mol of the peptides tested with colistin sulphate weighing 1155.4 g/mol and BP100 weighing 1420 g/mol (Rifflet *et al.*, 2012; Alves *et al.*, 2010; Velkov *et al.*, 2010).

4.4 Minimum Bactericidal Concentration (MBC)

The minimum bactericidal concentration was defined as the lowest concentration of antimicrobial peptide required to kill ≥99.9 % of *A. baumannii* cells (Eucast, 2003; Wiegand *et al.*, 2008). The clear wells from the MIC experiment were spread onto TSA plates. The methodology is described in **Section 3.11**. The lowest concentration of peptide where there was no growth observed on the plate was recorded as the MBC. In **Table 4.4.1**, the MBC for each peptide is shown.

Similar to the MIC experiment results as described in **Section 4.3**, the MBC recorded is a maximum and could be between the peptide concentrations tested. For colistin sulphate, the solution from wells 1-10, where well 10 had 0.5 µg/ml of peptide, were spread as they were clear. No growth was observed on the plate for 0.5 µg/ml so this was recorded as the MBC; the true MBC would be between 0.5 µg/ml and 0.25 µg/ml where there was growth observed in the well.

Peptide	*Minimum Bactericidal Concentration (µg/ml)*	*Minimum Bactericidal Concentration (µmol/l)*
Colistin sulphate	0.5	0.43
Bicarinalin	4	1.8
BP100	4	2.8

Table 4.4.1- MBC for colistin sulphate, bicarinalin and BP100.

4.5 Minimum Biofilm Inhibitory Concentration (MBIC)

The minimum biofilm inhibitory concentration (MBIC) was defined as the lowest concentration of antimicrobial peptide that caused 90 % inhibition of *A. baumannii* biofilm formation (Gopal *et al.*, 2014). Biofilm formation was quantified using the stain crystal violet method as described in **Section 3.11.**

Figure 4.5.1 shows 90 % of biofilm formation was inhibited when *A. baumannii* cells were subjected to concentrations of 0.5 µg/ml colistin sulphate and 4 µg/ml of bicarinalin and BP100.

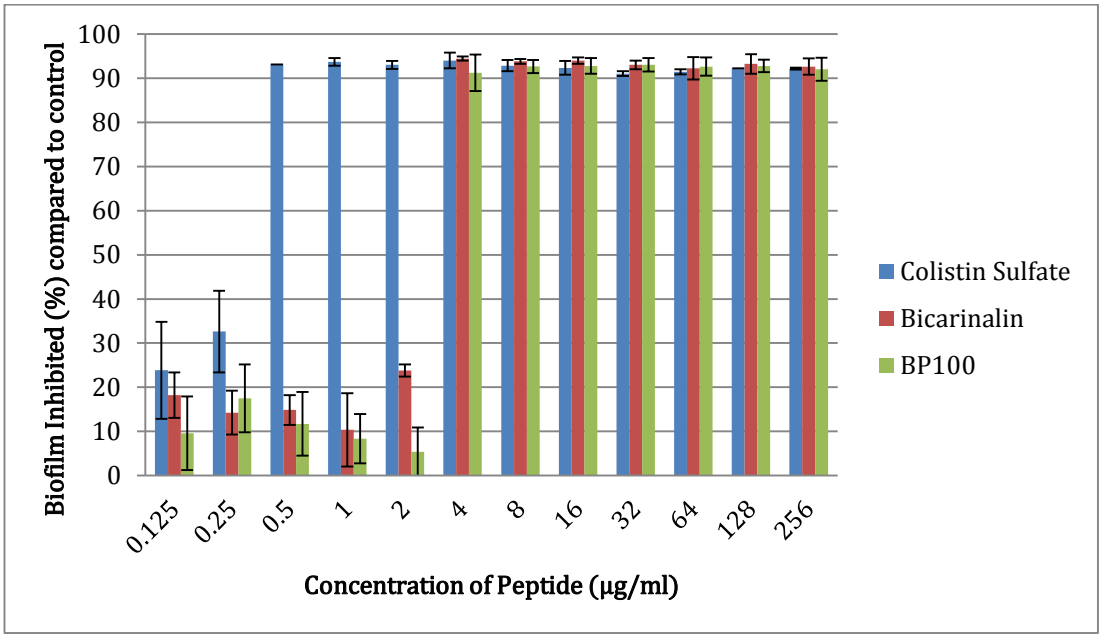

Figure 4.5.1-MBIC for colistin sulphate, bicarinalin and BP100. *Estimated MBIC values are Colistin sulphate 0.5µg/ml, bicarinalin 4µg/ml and BP100 4µg/m. All results were p<0.01 apart from BP100 at 2 µg/ml.*

A sample T test (**Section 3.17**) was carried out to test the statistical significance between each concentration of peptide and the negative control. All the results for colistin sulphate, bicarinalin and BP100 were found to be highly significant at $p<0.01$ apart from the result for BP100 at 2 µg/ml which was not statistically significant.

The data shows that for all peptides, biofilm formation was inhibited by more than 90 % for concentrations at and above the peptide's respective MBC (**Section 4.4**).

4.6 Biofilm Removal Assay

The amount of the biofilm was quantified by crystal violet staining. The percentage of biofilm removed by the peptide was calculated by comparing the biofilm grown (as the negative control, containing a theorised 100% of biofilm) with the amount of biofilm remaining after 24 hours after being subjected to a concentration of peptide in the range of 1 to 2048 µg/ml. Biofilms of *A. baumannii* were grown for 24 hours in separate wells of 96 well plates and then subjected to a concentration range of each of the antimicrobial peptides. The methodology is described in detail in **Section 3.13** and the results are shown below.

One set of representative plates for each of the three peptides are shown in **Figures 4.6.1, 4.6.2 and 4.6.3**. There is a noticeable lighter shade of purple from the crystal violet staining in the BP100 plate (**Figure 4.6.3**) from concentrations 256 µg/ml to 2048 µg/ml compared to bicarinalin (**Figure 4.6.2**) and colistin sulphate (**Figure 4.6.1**) suggesting more biofilm has been removed.

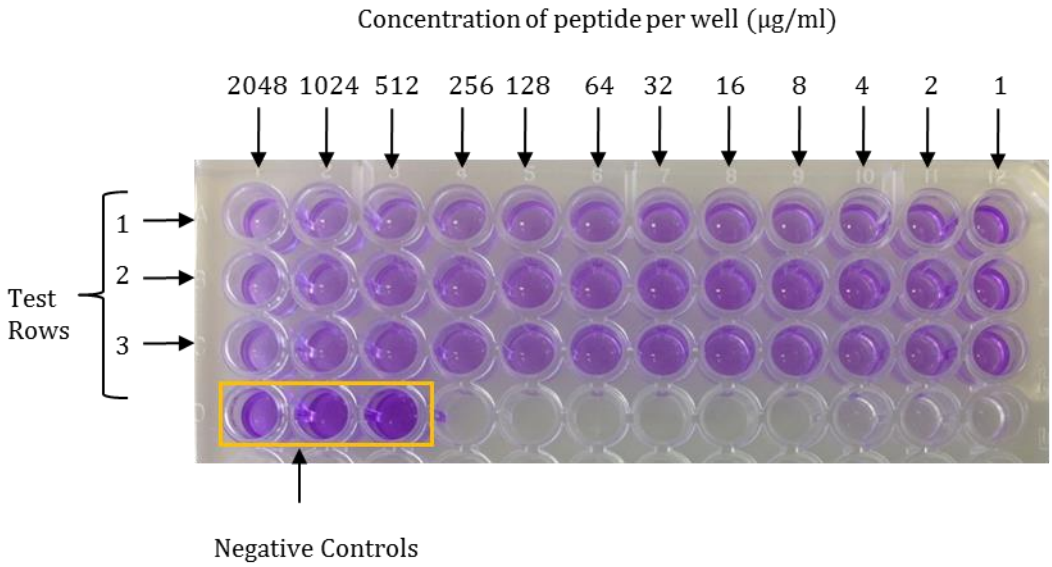

Figure 4.6.1- Well plate showing biofilm removal by colistin sulphate; *peptide concentration from 2048µg/ml to 1µg/ml.*

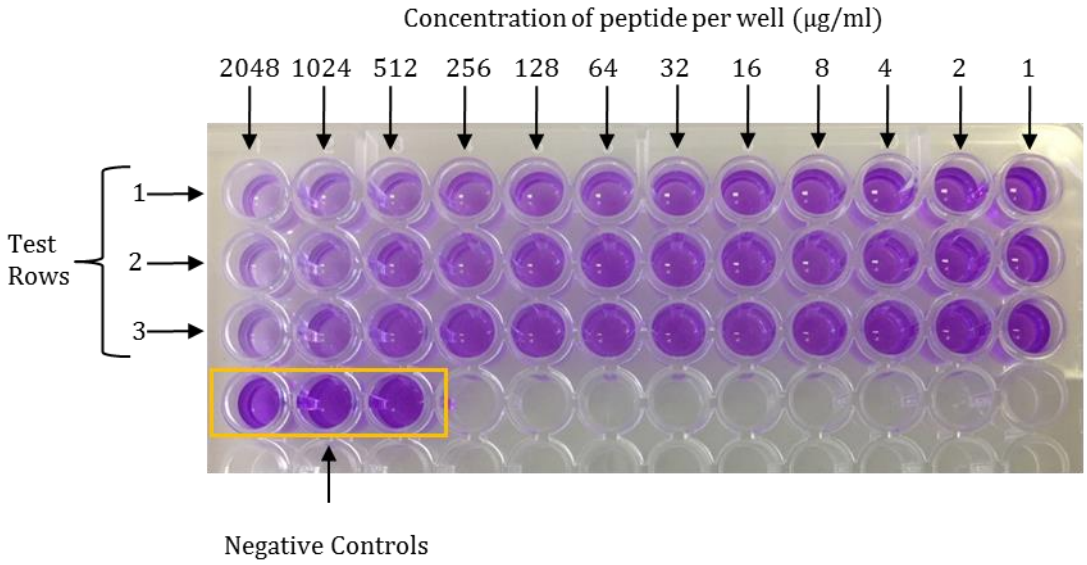

Figure 4.6.2- Well plate showing biofilm removal by bicarinalin; *peptide concentration from 2048µg/ml to 1µg/ml.*

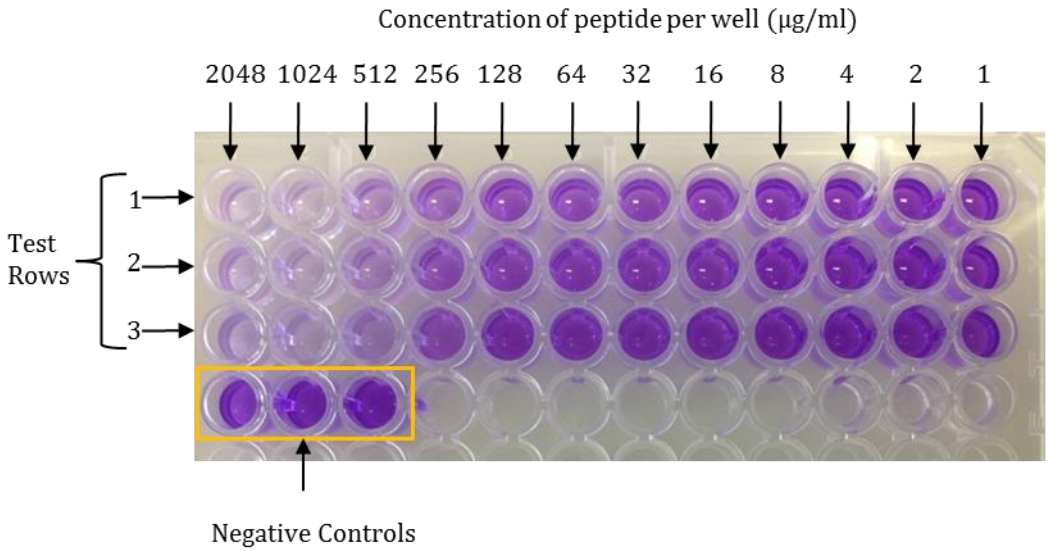

Figure 4.6.3-Well plate showing biofilm removal by BP100; *peptide concentration from 2048µg/ml to 1µg/ml.*

The crystal violet stain was quantified using a spectrophotometer at 590nm. The results were then compared to an average of the negative control wells which contained a theoretical 100% biofilm. The lowest concentration of antimicrobial peptide tested was 1 µg/ml and the maximum was 2048 µg/ml. The results are shown in **Figure 4.6.4**.

The results indicate that bicarinalin and BP100 exhibited anti-biofilm activity which was optimal for bicarinalin at 128 µg/ml and BP100 at 2048 µg/ml. Statistical analysis of all the concentrations for all three peptides, compared against the negative control, was carried out using IBM SPSS 21 by the samples T-test.

- **Colistin sulphate** at a concentration of 1 µg/ml removed 27 % of the biofilm. The eradication increased as the concentration increased until at 512 µg/ml colistin sulphate removed 52 % of the biofilm, the maximum eradication for all the concentrations tested. The eradication decreased marginally to 44% at the highest concentration tested of 2048 µg/ml compared to 512 µg/ml but this decrease was not statistically significant.

- **Bicarinalin** at 1 µg/ml removed 19% of biofilm and at 128 µg/ml, removed 70% of the biofilm. This concentration appeared optimal as there was no further increase above 128 µg/ml.
- **BP100** at 1 µg/ml concentration removed 15% of biofilm and at 128 µg/ml, the elimination was 54%. BP100 was better at eradicating more biofilm than colistin sulphate at concentrations at and above 128 µg/ml and better than bicarinalin from 256 µg/ml. While colistin and bicarinalin percentage removal plateaued, the percentage of biofilm reduced by BP100 continued to increase to the highest concentration tested of 2048 µg/ml where it had removed 95 % of the biofilm. This was nearly double that of colistin sulphate with 52%.

.

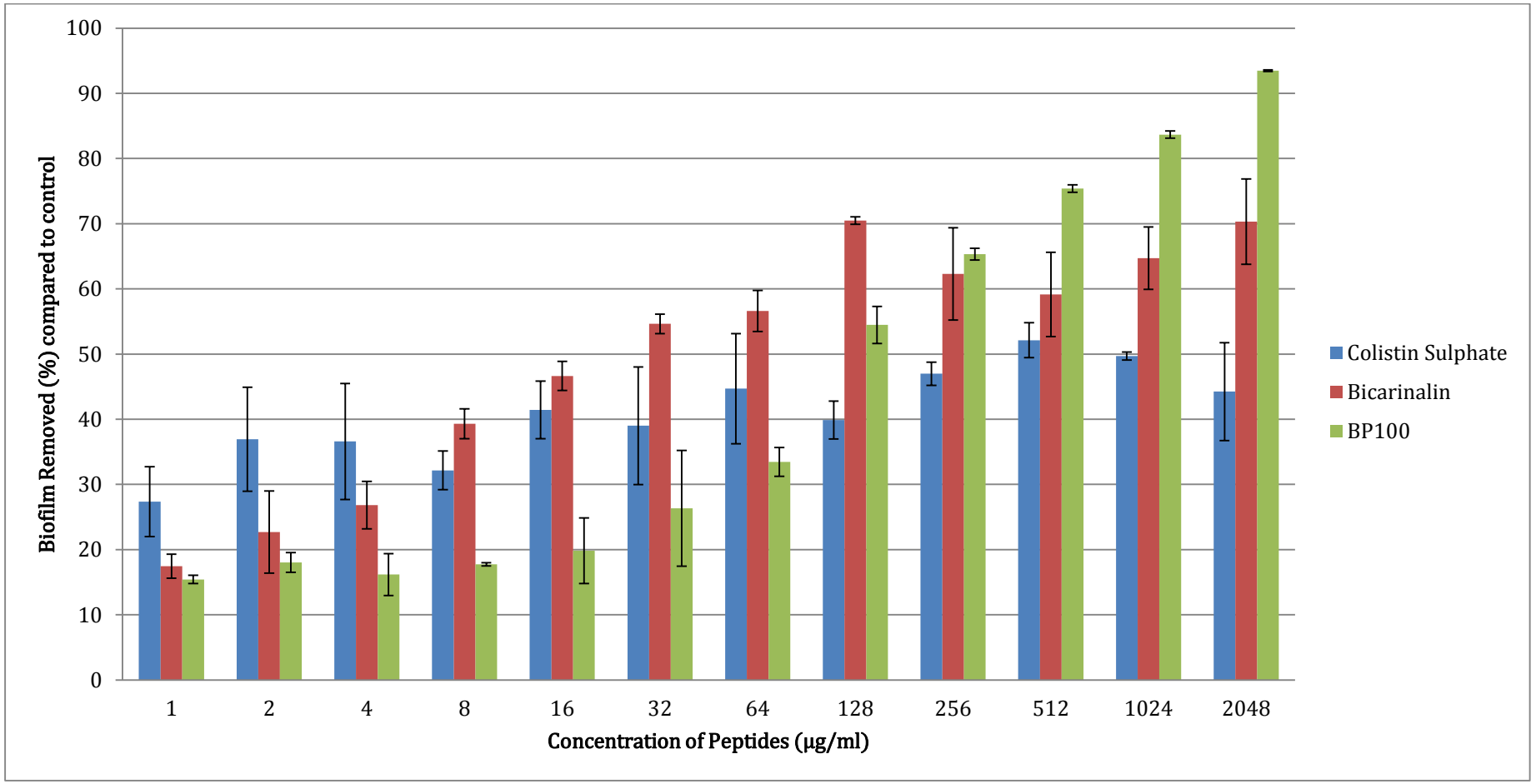

Figure 4.6.4-Percentage biofilm removed after being exposed to increasing concentrations of colistin sulphate, bicarinalin and BP100

4.7 Atomic Force Microscope

The AFM was used to visualise single cells after being subjected to the three peptides. The data obtained from the MIC and MBC experiments (**Sections 4.3 and 4.4**) were used to establish the peptide concentrations which were determined to be ½ MBC, MBC and 2x MBC for each peptide.

4.7.1 Colistin sulphate

Images obtained with the AFM show *A. baumannii* cells when they had been subjected to 0 µg/ml, 0.25 µg/ml (½ MBC), 0.5 µg/ml (1xMBC), 1 µg/ml (2xMBC) of colistin sulphate for 2 hours (**Figure 4.7.1)**.

Image A is a control and shows an *A. baumannii* cell with no addition of colistin sulphate. This cell exhibits the uniform coccus-bacillus shape and a smooth cell surface with no visible pili or surface appendages.

Image B shows a cell that has been subjected to 0.25 µg/ml (½ MBC) of colistin sulphate. The cell still has a recognisable coccus-bacillus shape as in the control but the surface shows evidence of morphological changes which may be pores or indents due to peptide activity. This specific image shows the cell starting to undergo binary fission indicating cells are still metabolically active and undergo cell division below the MBC concentration of peptide.

Image C shows a cell which has been subjected to 0.5 µg/ml (MBC) of colistin sulphate. The cell shape has been severely disrupted by antimicrobial activity to the extent that the cocci-bacilli shape is no longer recognisable. There is also evidence of surface distortion.

Image D shows an *A. baumannii* cell after being subjected to 1 μg/ml (2xMBC) of colistin sulphate. The AFM images clearly show that the cell surface has become extensively disrupted at concentrations equal or above the MBC of colistin sulphate.

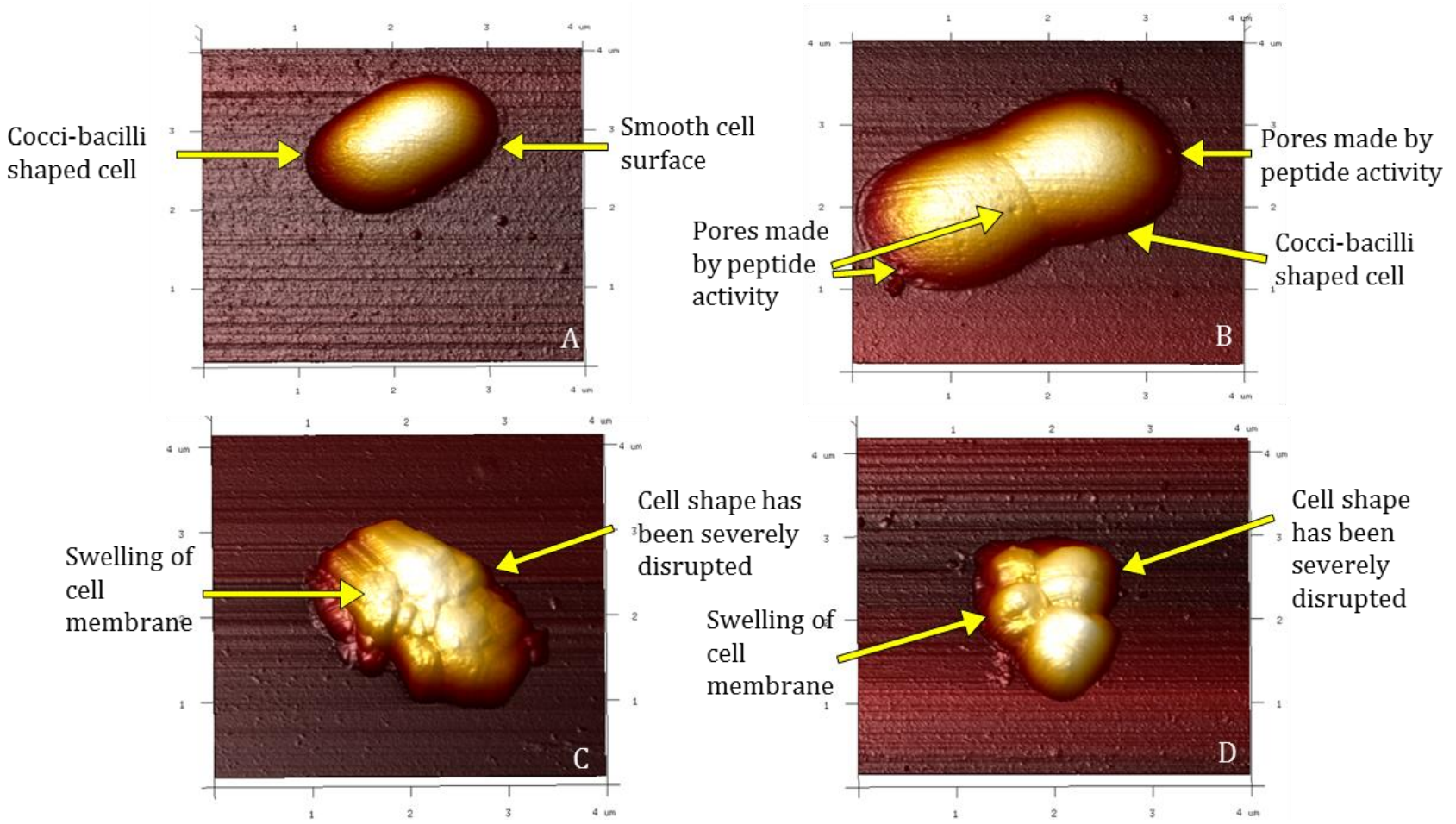

Figure 4.7.1- AFM Images: A. baumannii cells after being subjected to colistin sulphate*; treatment for 2 hours with variable concentrations of colistin sulphate and fixed onto a glass slide coated with poly-L-lysine. Image A) Control no peptide, B) 0.25 µg/ml, C) 0.5 µg/ml, D) 1µg/ml. Images were 4µm² and 256 lines at 0.5Hz*

The surface roughness was quantified by taking the root mean square (RMS) of the measurements from five cells. The mean was determined at colistin sulphate concentrations of 0.25 µg/ml (½ MBC), 0.5 µg/ml (1xMBC) and 1 µg/ml (2xMBC). A statistical analysis, using IBM SPSS 21 independent-samples T test, was carried out by comparing each peptide concentration against the control. The results are shown in **Figure 4.7.2**.

The degree of statistical significance is indicated by the * symbols where * indicates high significance ($p<0.05$) and ** indicates very high significance ($p<0.01$).

The negative control cells had an average cell roughness of 65nm with a value deviation of 8.9 nm. When the cells were subjected to 0.25 µg/ml colistin sulphate there was no significant change in the cell roughness. When the cells were subjected to a concentration of 0.5 µg/ml, the surface roughness increased to 136 nm ($p \leq 0.05$). After the cells were exposed to 1 µg/ml concentration the surface roughness decreased to 103nm ($p \leq 0.05$) suggesting the destruction of the membrane.

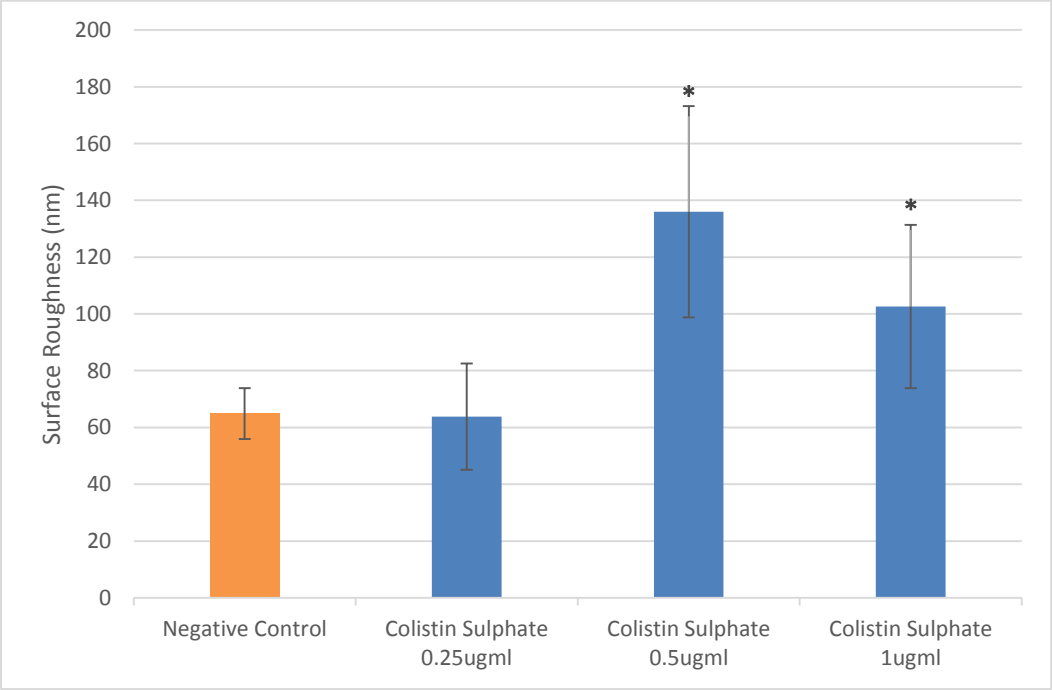

Figure 4.7.2- Surface roughness of cells after colistin sulphate treatment. *Concentrations at 0.5 x, 1 and 2 x MBC, compared to the control, treatment for 2 hours. * statistical significance ($p< 0.05$), error bar indicates range of measurements from the 5 cell samples.*

These results show that, at the MBC and above, the surface roughness of the cell significantly increases suggesting membrane disruption caused by the peptide.

The cell surface area was also quantified in addition to surface roughness. Five cells were selected from each group subjected to 0.25 µg/ml, 0.5 µg/ml and 1 µg/ml colistin sulphate concentrations. The surface area was calculated and values averaged; the results are shown in **Figure 4.7.3**. The control had an average surface area of 2.6 μm^2. At 0.25 µg/ml this increased to 4.12 μm^2 ($p<0.05$). This decreased to 3.43 μm^2 at 0.5 µg/ml and 2.24 μm^2 at 1 µg/ml, which is below the control average.

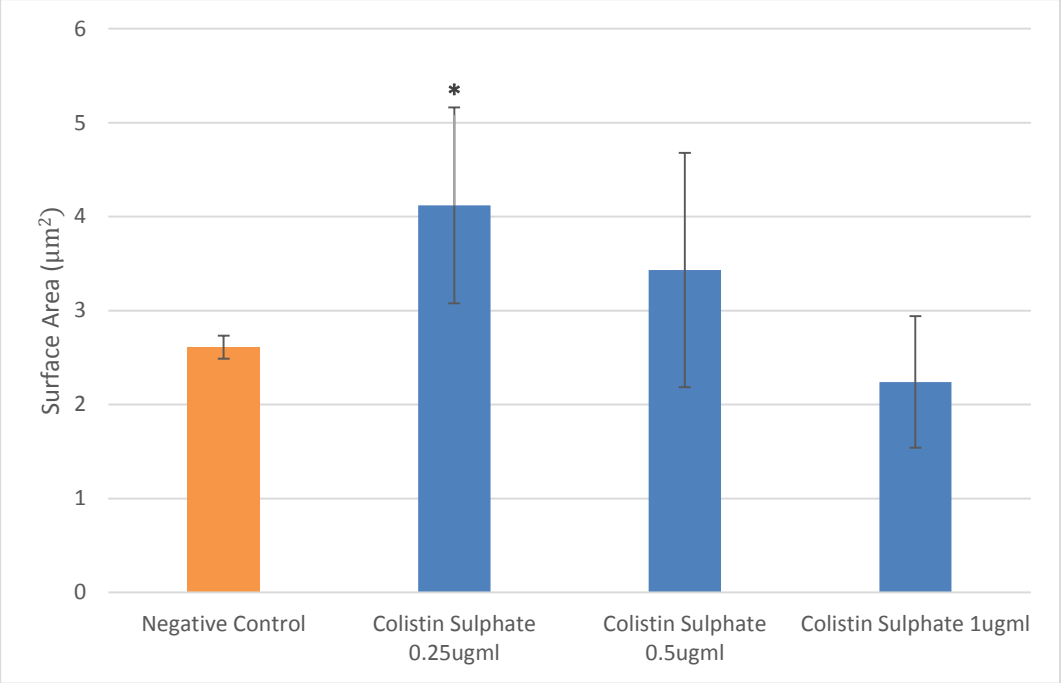

Figure 4.7.3-Surface area of cells after colistin sulphate treatment. *Concentrations at 0.5, 1 and 2 x MBC, compared to the control, treatment for 2 hours. * Statistical significance ($p< 0.05$)*

4.7.2 Bicarinalin

In **Figure 4.7.4,** the images show *A. baumannii* cells when they had been subjected to concentrations 2 µg/ml (½ MBC), 4 µg/ml (1xMBC), 8 µg/ml (2xMBC) of bicarinalin for 2 hours.

Image A is a control and shows an *A. baumannii* cell with the uniform coccus-bacillus shape and a smooth cell surface.

Image B shows a cell that has been subjected to 2 µg/ml of bicarinalin. It still has a recognisable coccus-bacillus shape and smooth cell surface as seen in the control**.**

Image C shows a cell which has been subjected to 4 µg/ml of bicarinalin. The cell shape is unrecognisable and shows some membrane swelling and the overall cell has shrunk.

Image D shows a cell after being subjected to 8 µg/ml, similar to image C, the membrane has been severely disrupted and the cell has shrunk with membrane swelling.

.

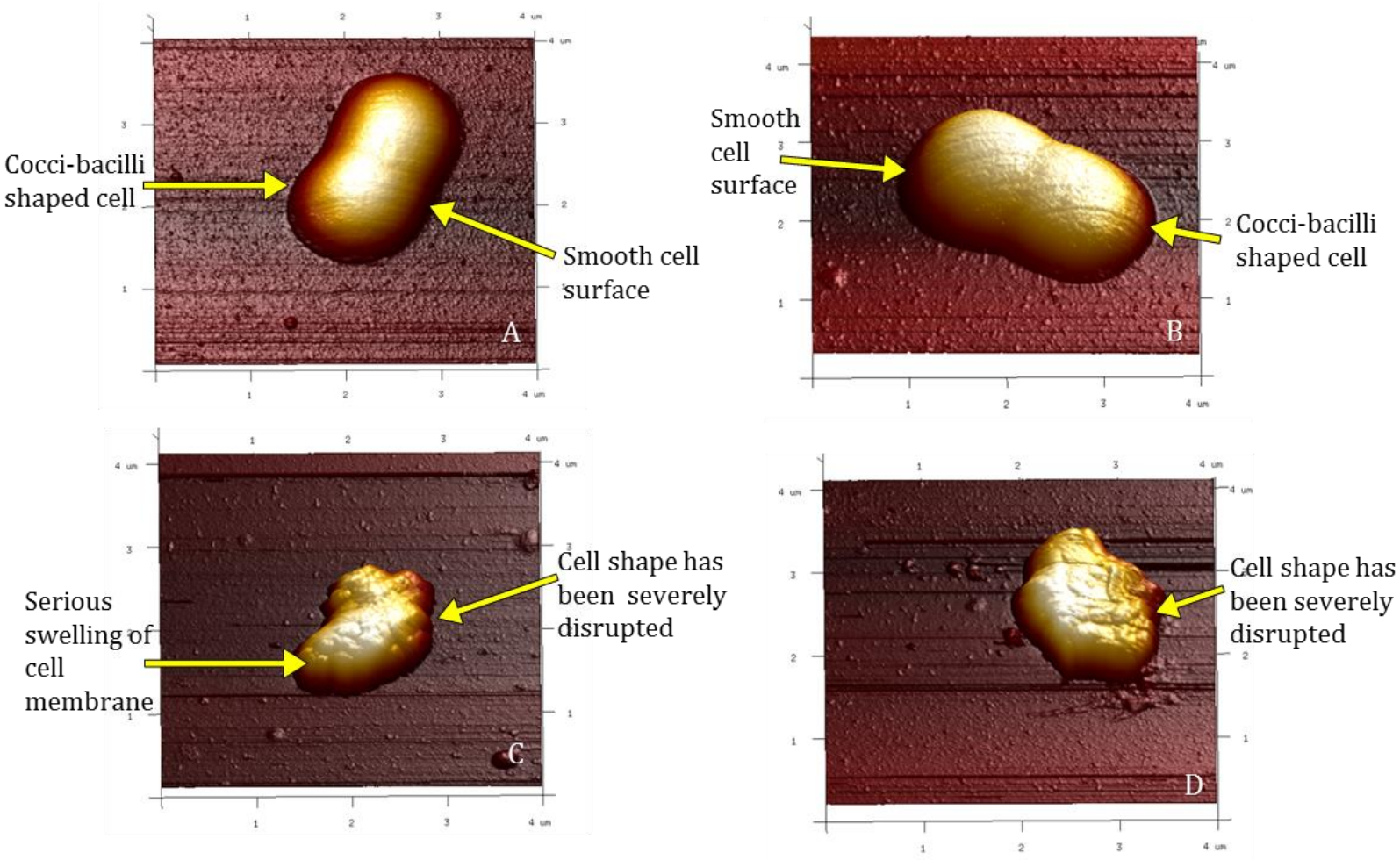

Figure 4.7.4- AFM Images: A. baumannii cells after being subjected to bicarinalin*; treatment for 2 hours with variable concentrations of bicarinalin and fixed onto a glass slide coated with poly-L-lysine. Image A) Control (no peptide), B) 2 µg/ml, C) 4 µg/ml, D) 8 µg/ml. Images were 4µm² and 256 lines at 0.5Hz.*

The surface roughness of each cell was quantified using Gwyddion as explained in **Section 3.14.1**. The results are shown in **Figure 4.7.5**.

The negative control cells had an average cell roughness of 64.9 nm with a value deviation of 8.9 nm. When the cells were subjected to 2 µg/ml of bicarinalin there was no significant change in the cell roughness. When the cells were subjected to 4 µg/ml the surface roughness increased to 139.9 nm ($p \leq 0.05$). There was a decrease to 71.4 nm in surface roughness as the cells were exposed to 8 µg/ml.

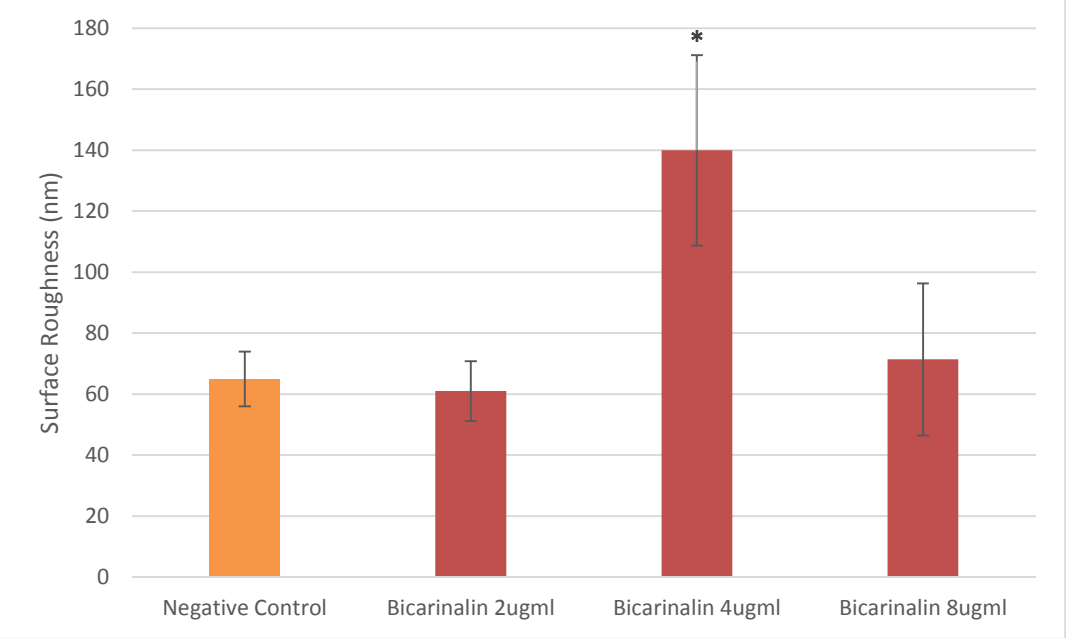

Figure 4.7.5- Surface roughness of cells after bicarinalin treatment. *Concentrations at 0.5 x, 1 and 2 x MBC, compared to the control, treatment for 2 hours. * statistical significance ($p < 0.05$), error bar indicates range of measurements from the 5 cell samples.*

The surface roughness significantly increased when subjected to a peptide concentration equivalent to the MBC similar to the results for colistin sulphate.

The cell surface area was quantified using five cells subjected to 2 µg/ml, 4 µg/ml and 8 µg/ml and the results are shown in **Figure 4.7.6**. The control had a mean surface area of 2.6 μm^2. At 2 µg/ml this increased to 3.1 μm^2 ($p \leq 0.01$). The surface area decreased to

2.67 µm² at 4 µg/ml and further to 1.91 µm² at 8 µg/ml ($p \leq 0.05$), which was less than the control area.

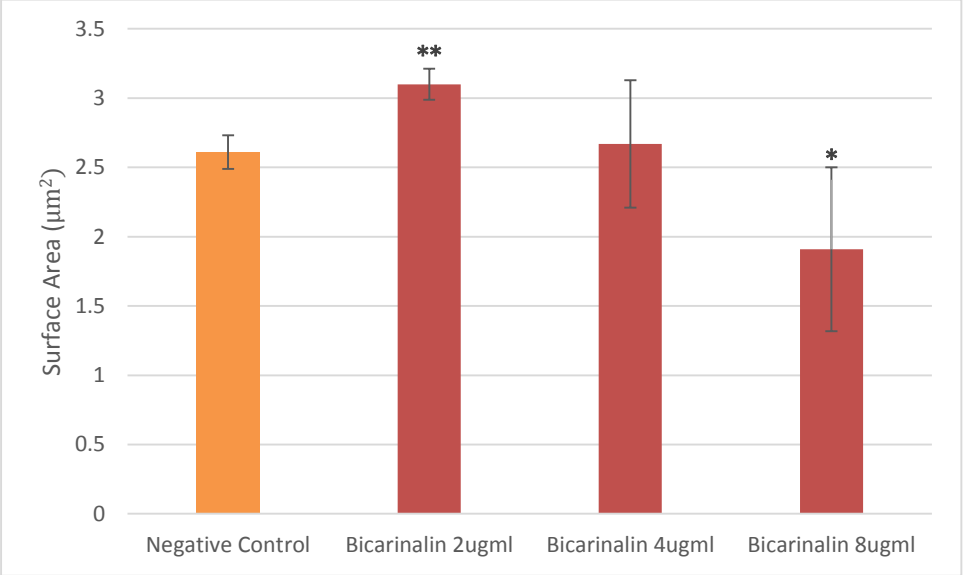

Figure 4.7.6- Surface area of cells after bicarinalin treatment. *Concentrations at 0.5, 1 and 2 x MBC, compared to the control, treatment for 2 hours. * Statistical significance ($p < 0.05$) ** ($p \leq 0.001$)*

4.7.3 BP100

In **Figure 4.7.7,** the images show *A. baumannii* cells when they had been subjected to concentrations 2 µg/ml (½ MBC), 4 µg/ml (1xMBC), 8 µg/ml (2xMBC) of BP100 for 2 hours.

Image A is a control and shows a cell exhibiting the uniform cocci-bacilli shape and a smooth cell surface.

Image B shows a cell that has been subjected to 2 µg/ml BP100. This image shows the cell undergoing cell division but still has a smooth cell membrane and is cocci-bacilli shaped.

Image C shows a cell which has been subjected to 4 μg/ml of BP100. The cell shape has been severely disrupted by antimicrobial activity to the extent that the cocci-bacilli shape is no longer recognisable along with membrane swelling and blebbing.

Image D shows a cell after being subjected to 8 μg/ml; the surface has been severely disrupted and the cell has shrunk.

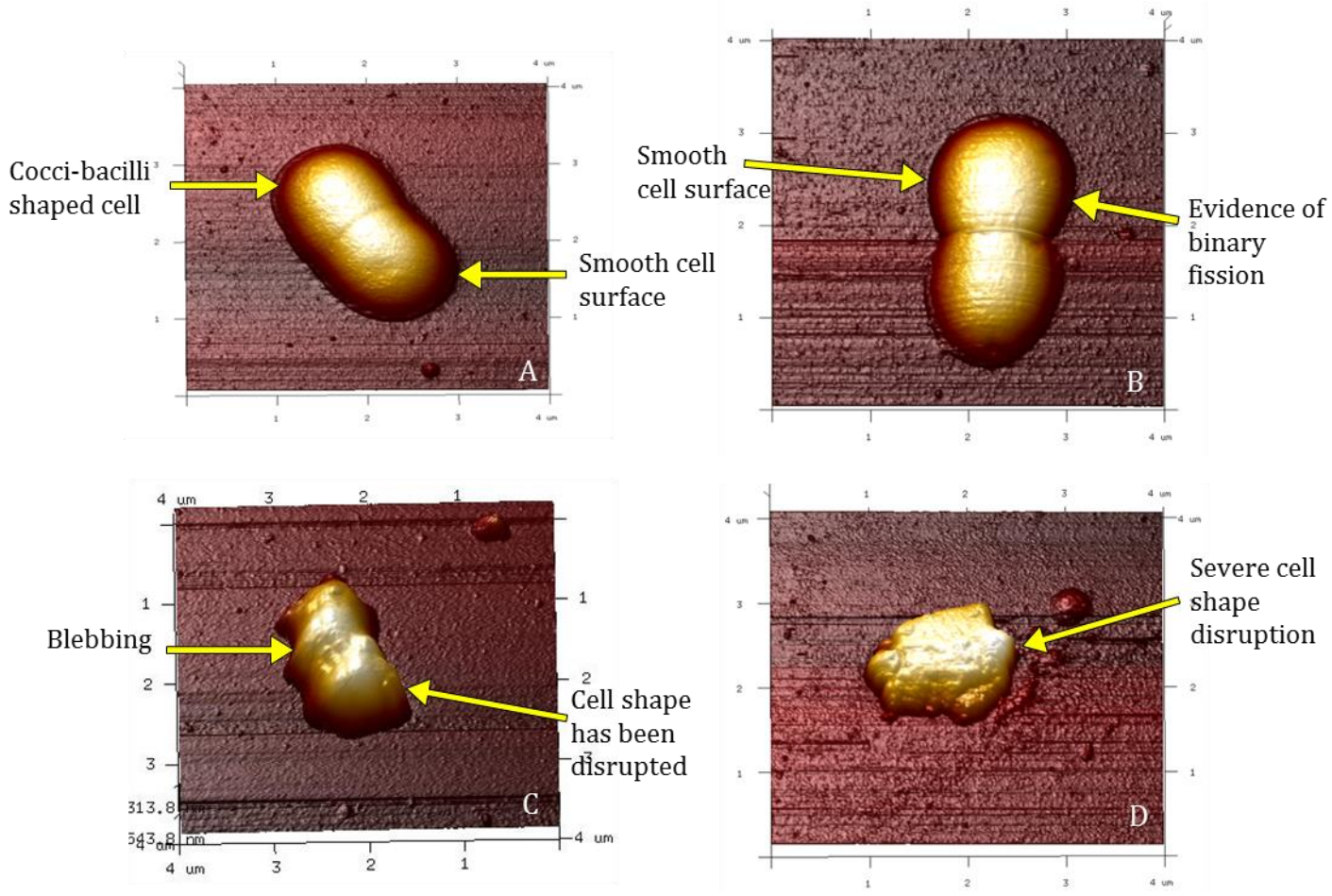

Figure 4.7.7- AFM images of *A. baumannii* cells after being subjected to BP100 treatment for 2 hours and fixed onto a glass slide coated with poly-L-lysine. Image A) Control, B) 2 µg/ml, C) 4 µg/ml, D) 8 µg/ml. Images were 4µm² and 256 lines at 0.5htz

The surface roughness of each cell was quantified using Gwyddion as explained in **Section 3.14.1**. The RMS average of five cells at 2 µg/ml, 4 µg/ml and 8 µg/ml of BP100 were quantified. A statistical analysis using IBM SPSS 21 independent-samples T test was completed by comparing each peptide concentration against the control. The results are shown in **Figure 4.7.8**.

The negative control cells had an average cell roughness of 64.9 nm with a value deviation of 8.9 nm. At each of the concentrations tested, 2 µg/ml, 4 µg/ml and 8 µg/ml, there was no significant change ($p > 0.05$) in the surface roughness when compared with the negative control. There was however a greater range of surface roughness as the peptide concentration increased with a value deviation of 11.1 nm at 2 µg/ml, 20.5 nm at 4 µg/ml and 30.3 at 8 µg/ml. This suggests that there was a membrane disruption but for only some of the cells.

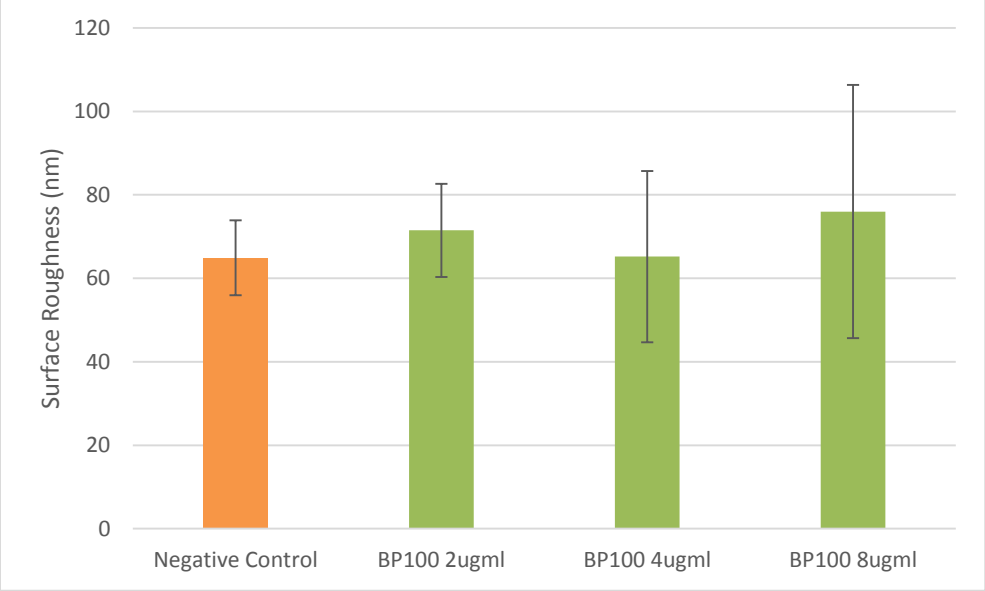

Figure 4.7.8- Surface roughness of cells after BP100 treatment. *Concentrations at 0.5 x, 1 and 2 x MBC, compared to the control, treatment for 2 hours. * statistical significance ($p < 0.05$), error bar indicates range of measurements from the 5 cell samples.*

The cell surface area was also quantified using five cells subjected to 2 µg/ml, 4 µg/ml and 8 µg/ml; the results are shown in **Figure 4.7.9**. The control had a mean surface area of 2.6 µm^2. At 2 µg/ml this increased to 3.1 µm^2 ($p \leq 0.05$). This remained at 3.1 µm^2 at 4 µg/ml and then decreased to 2.2 µm^2 at 8 µg/ml.

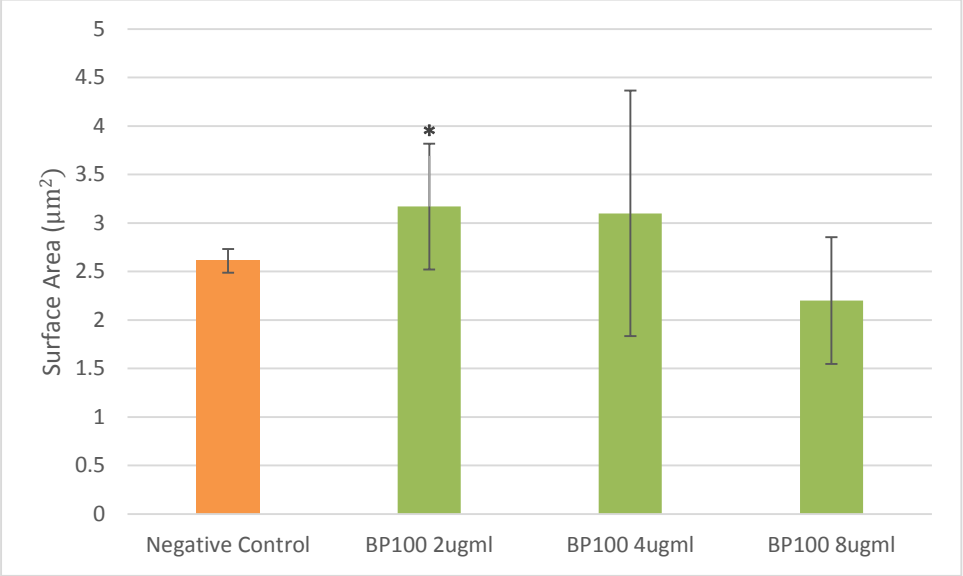

Figure 4.7.9- Surface area of cells after BP100 treatment. *Concentrations at 0.5, 1 and 2MBC, compared to the control, treatment for 2 hours. * Statistical significance ($p < 0.05$)*

4.8 Scanning Electron Microscope

The SEM was used to visualize pre-formed 24 hour *A. baumannii* biofilms after being subjected to one of the three peptides for 24 hours at concentrations 1, 10, 100, 1000µg/ml. These concentrations were selected based on the results from the biofilm removal assay (**Section 4.6**).

4.8.1 Colistin sulphate

A. baumannii biofilms were grown on polystyrene pegs for 24 hours and then subjected to a specific concentration of colistin sulphate (1, 10, 100, 1000µg/ml) for 24 hours and prepared for SEM visualisation as explained in **Section 3.15**. The biofilms were visualised at the magnifications 5,000x, 10,000x, 20,000x and 30,000x. The 5,000x and 30,000x for the concentrations 1, 10, 100 µg/ml are shown in **Figure 4.8.1**. Due to the time available the samples subjected to 1000 µg/ml were not visualised.

Image A shows a control sample; the biofilm was grown for 48 hours without the addition of any peptide. The image at 30,000x magnification shows the cells are normal in size and shape and there is evidence of some pili between cells. The 5,000x magnification insert shows the cells carpet the whole of the peg surface.

Image B shows the biofilm which had been subjected to 1 µg/ml colistin sulphate, (2x MBC). At 30,000x magnification the cells have a smooth cell surface and uniform coccus-bacillus shape and multiple pili are seen between cells. At 5,000x, there are a few gaps in the biofilm.

Image C shows the biofilm which has been subjected to 10 µg/ml of colistin sulphate, (20x MBC). At 30,000x magnification, a large proportion of the cells have shrunk and the shape disrupted. At 5,000x magnification there are significant gaps in the biofilm.

Image D shows the biofilm which has been subjected to 100 μg/ml of colistin sulphate (200x the MBC). Severe membrane disruption has caused nearly all the cells to shrink. In the image, there is also evidence of completely lysed cells or cytoplasmic remnants leaked from the cells. At 5,000x magnification there are significant gaps in the biofilm.

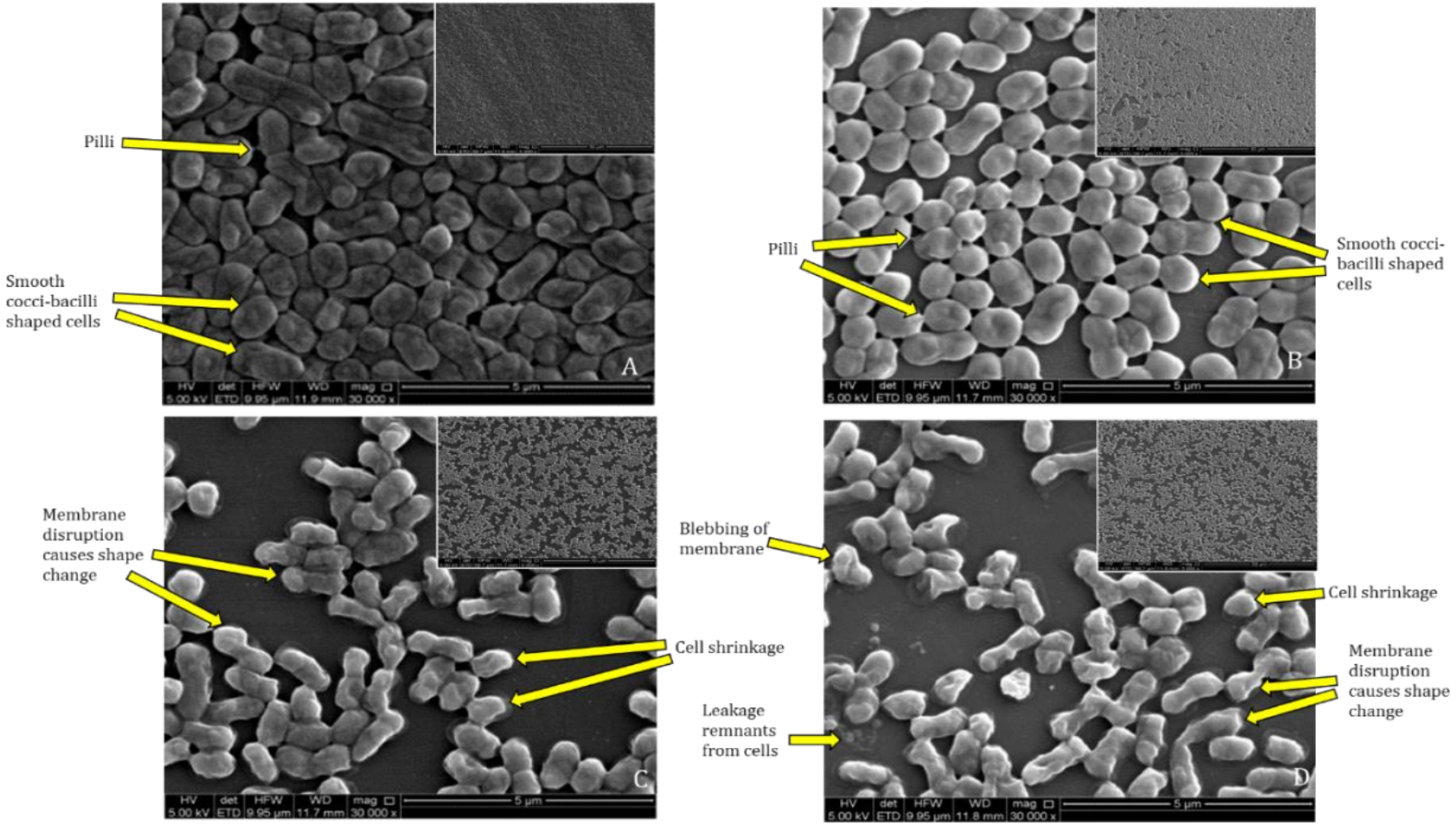

Figure 4.8.1- SEM images: A baumannii biofilms after being subjected to colistin sulphate, *biofilms grown for 24 hours then treatment for 24 hours with variable concentrations of colistin sulphate. Image A) Control no peptide, B) 1 µg/ml, C) 10 µg/ml, D) 100 µg/ml. Large image at 30,000x magnification and insert at 5,000x magnification.*

4.8.2 Bicarinalin

A. baumannii biofilms were grown on polystyrene pegs for 24 hours and then subjected to a specific concentration of bicarinalin (1, 10, 100 or 1000µg/ml) for 24 hours and prepared for SEM visualisation as explained in **Section 3.15**. The biofilms were visualised at the magnifications 5000x, 10000x, 20000x and 30000x. The images with 5000x and 30000x magnification, for the concentrations 1, 10, 100 µg/ml are shown in **Figure 4.8.2**.

Image A shows the control sample used and analysed in **Section 4.8.1**.

Image B shows the biofilm which had been subjected to 1 µg/ml bicarinalin, (0.25x MBC). At 30,000x the cells have a smooth surface and uniform cocci-bacilli shape and multiple pili are seen between cells. At 5,000x, there are very small gaps in the biofilm but otherwise the cells carpet the peg.

Image C shows the biofilm which has been subjected to 10 µg/ml of bicarinalin (2.5x MBC). At 30,000x magnification there is evidence of blebbing and minor membrane disruption.

Image D shows the biofilm which has been subjected to 100 µg/ml of bicarinalin (25x MBC). Severe membrane disruption in all the cells can be seen and evidence of widespread cell lysis. At 5,000x magnification large and numerous gaps in the biofilm are seen.

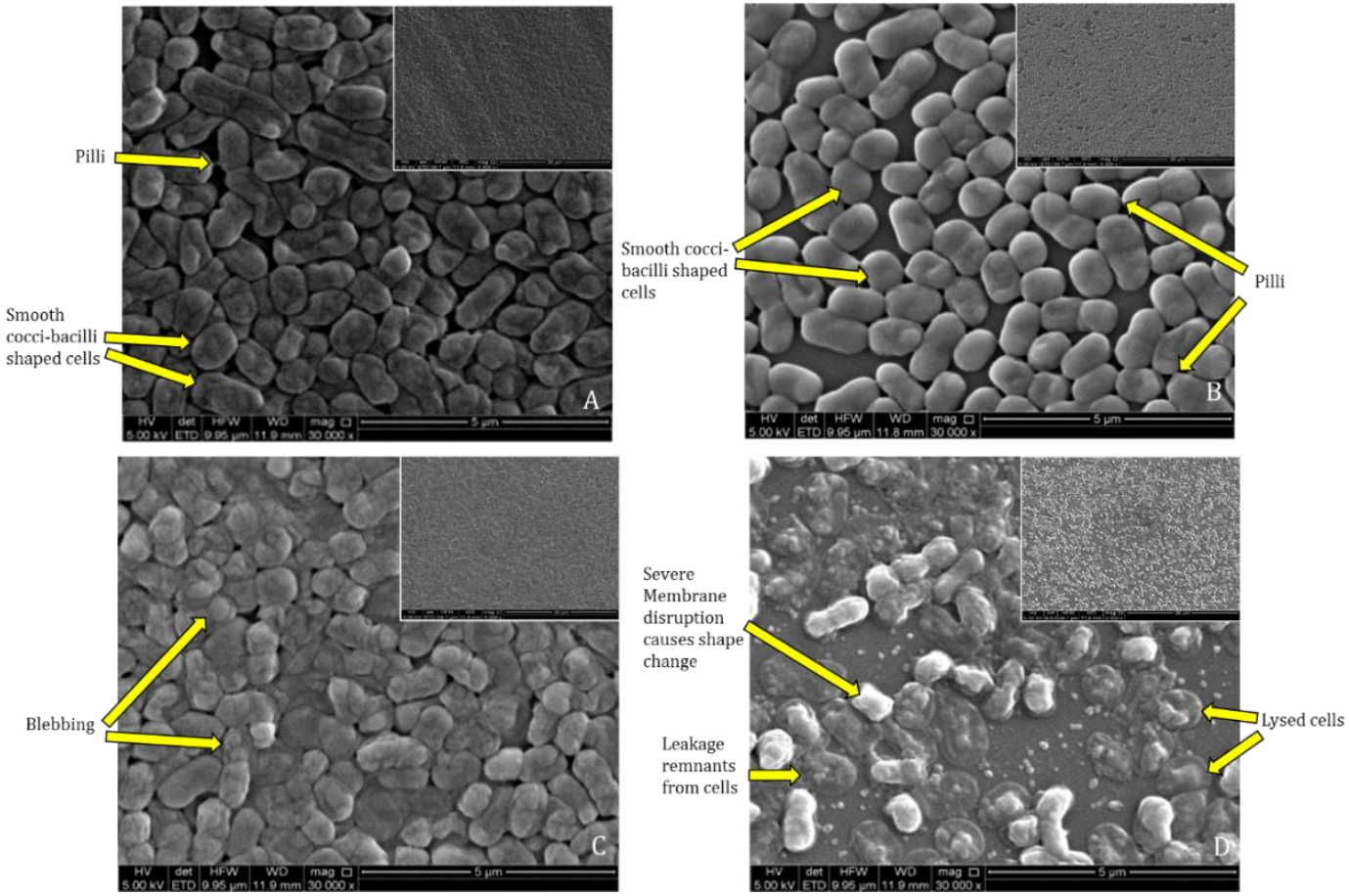

Figure 4.8.2-SEM images: A baumannii biofilms after being subjected to bicarinalin*, biofilms grown for 24 hours then treatment for 24 hours with variable concentrations of bicarinalin. Image A) Control no peptide, B) 1 µg/ml, C) 10 µg/ml, D) 100 µg/ml. Large image at 30,000x magnification and insert at 5,000x magnification*

4.8.3 BP100

A. baumannii biofilms were grown on polystyrene pegs for 24 hours and then subjected to a specific concentration of BP100 (1, 10, 100, 1000µg/ml) for 24 hours and prepared for SEM visualisation as explained in **Section 3.15**. The biofilms were visualised at the magnifications 5000x, 10000x, 20000x and 30000x. The 5000x and 30000x for the concentrations 1, 10, 100 µg/ml are shown in **Figure 4.8.3**.

Image A shows the control sample used and analysed in **Section 4.8.1**.

Image B shows the biofilm which had been subjected to 1 µg/ml BP100 (0.25x MBC). At 30000x the cells have a smooth cell surface and uniform cocci-bacilli shape and multiple pili are seen between cells. At 5000x, there are very small gaps in the biofilm but otherwise the cells carpet the peg.

Image C shows the biofilm which has been subjected to 10 µg/ml of BP100 (2.5x MBC). At 30000x magnification there is evidence of blebbing and minor membrane disruption with a few cells showing severe membrane disruption.

Image D shows the biofilm which has been subjected to 100 µg/ml of BP100 (25x MBC). Severe membrane disruption in all the cells can be seen and evidence of pores through the membrane. At 5000x magnification there are large and numerous gaps in the biofilm.

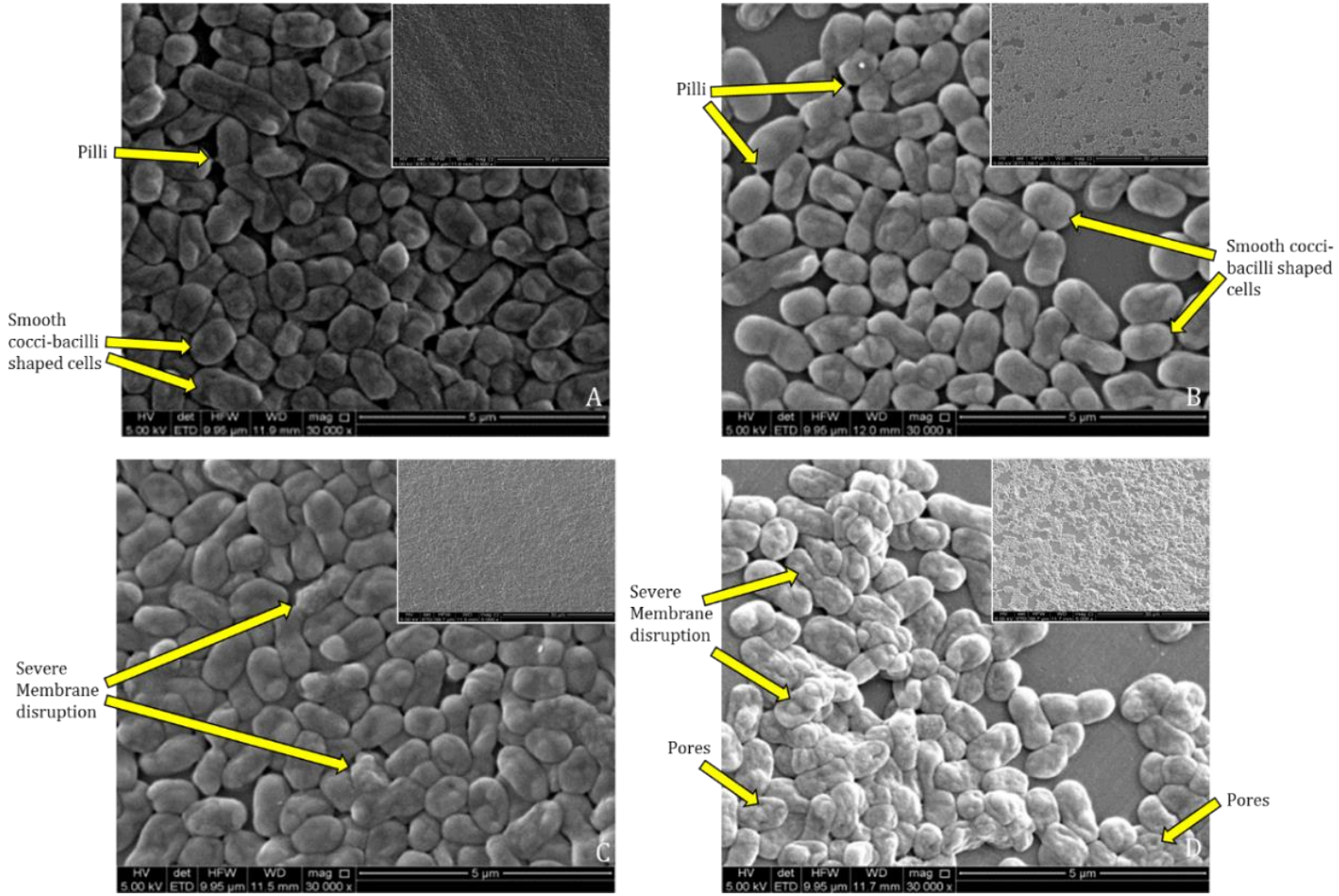

Figure 4.8.3- SEM images: A baumannii biofilms after being subjected to BP100, *biofilms grown for 24 hours then treatment for 24 hours with variable concentrations of BP100. Image A) Control no peptide, B) 1 µg/ml, C) 10 µg/ml, D) 100 µg/ml. Large image at 30,000x magnification, insert at 5,000x magnification.*

4.9 Confocal Laser Scanning Microscope (CLSM)

CLSM was used to visualise 48 hour *A. baumannii* biofilms after being subjected to one of the three peptides for 24 hours at concentrations 1, 10, 100, 1000µg/ml. These concentrations were selected based on the results from the biofilm removal assay (**Section 4.6**). The 40x magnification was used to visualise an area of 290µm^2. Five samples were taken of each biofilm. A biofilm at each of the peptide concentrations and a control are shown where the SYTO9 stain has been fluoresced.

4.9.1 Colistin sulphate

SYTO 9 stains all cells whether they are living or dead. **Image A** shows the control sample used. From **image B to E**, the peptide concentration increased by 10-fold in each figure. The images show a reduction in the area of the biofilm as the peptide concentration increases.

To quantify the decrease in biofilm as the colistin sulphate concentration increases, the bio-volume of the biofilm at each peptide concentration was calculated using BITPLANE Imaris software. The results are shown in **Figure 4.9.2**. The control had a bio-volume of 227,067 µm^3 with a standard deviation of 8,668 µm^3. At 1µg/ml and 10µg/ml peptide concentrations, there was no significant difference compared to the control ($p \leq 0.05$). At 100µg/ml, the bio-volume was 163,427 µm^3 ($p \leq 0.01$). The biofilm volume increased slightly to 171,070 µm^3 at 1000 µg/ml ($p \leq 0.05$) but with no statistical difference ($p > 0.05$). This represented a bio-volume reduction of approximately 25%.

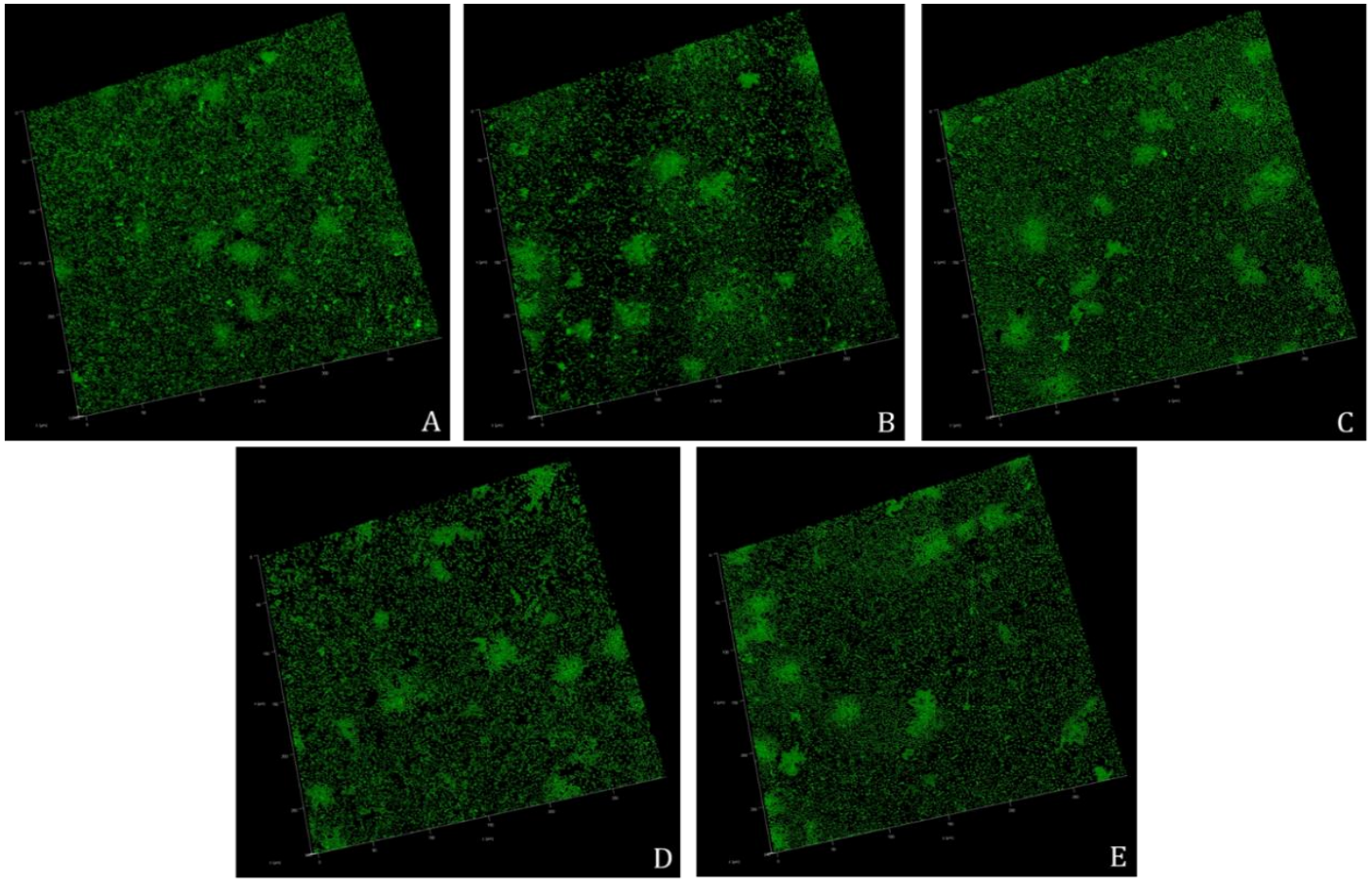

Figure 4.9.1- CLSM images: A. baumannii biofilms after being subjected to colistin sulphate; *grown for 24 hour in a chambered cover glass then subjected to a specific concentration of colistin sulphate for 24 hours. Biofilms were stained with SYTO 9 for visualisation. Colistin sulphate concentration in image A) Control (no peptide) B) 1 µg/ml, C) 10 µg/ml, D) 100 µg/ml, E) 1000 µg/ml*

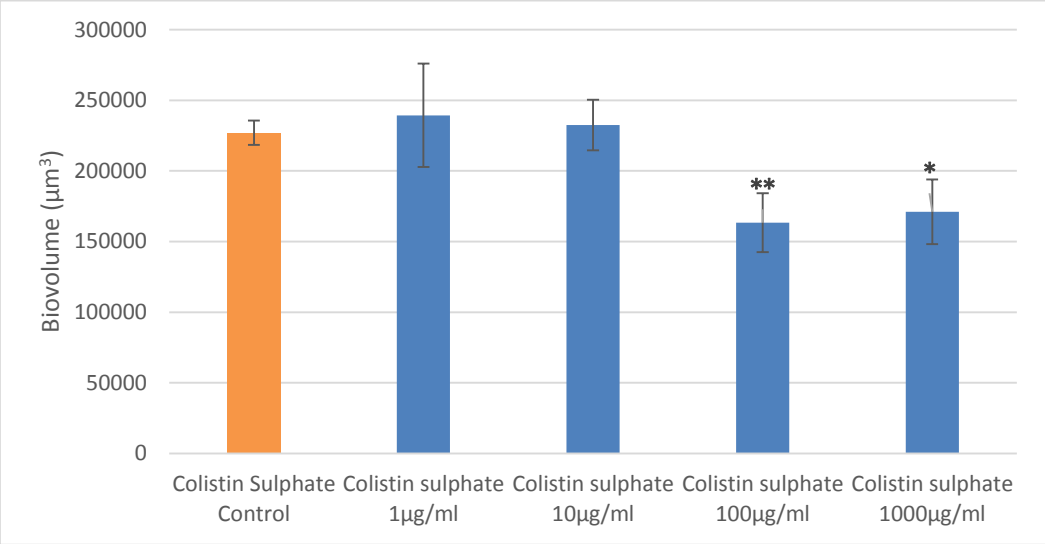

*Figure 4.9.2- Bio-volume (µm³) of biofilm at different concentrations of colistin sulphate. * p≤0.05, ** p≤0.01*

4.9.2 Bicarinalin

Image A shows the control sample used. From **image B to E** the peptide concentration increases by 10 fold and the images indicate a significant decrease in biofilm especially in image E.

Using the BITPLANE Imaris software the biofilm bio-volume was quantified at four concentrations of Bicarinalin, 1, 10, 100, 1000 µg/ml; the results are shown in **Figure 4.9.4**. The control had a bio-volume of 227,067 μm^3 with a deviation of 8,668 μm^3. At 1µg/ml and 10µg/ml there was no significant difference from the control ($p>0.05$). At 100µg/ml the bio-volume was 184,097 μm^3 ($p\leq0.05$). This decreased to 119,947 μm^3 at 1000 µg/ml ($p\leq0.01$). This represented a bio-volume reduction of nearly 50%.

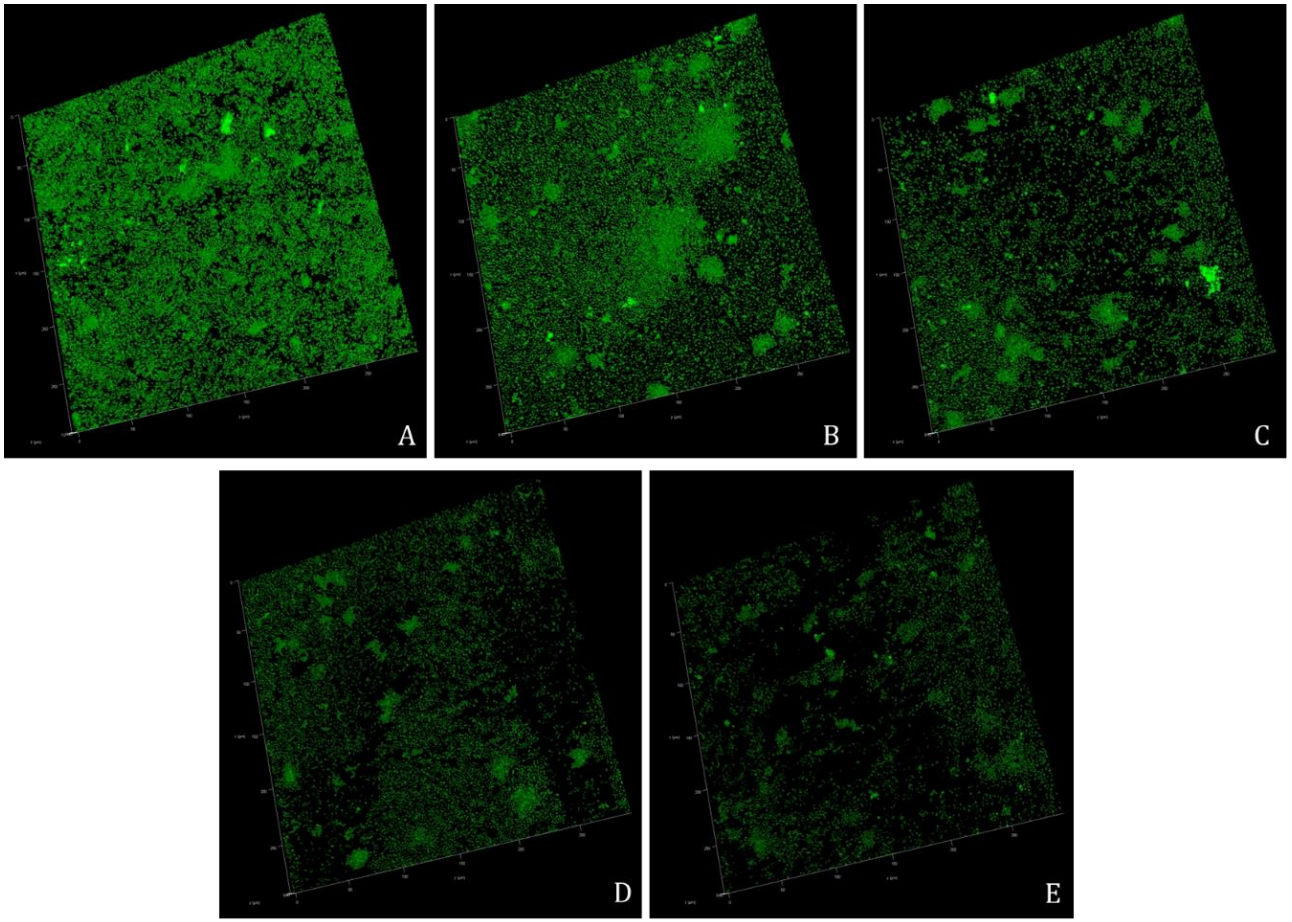

Figure 4.9.3- CLSM images: A. baumannii biofilms after being subjected to bicarinalin; *grown for 24 hour in a chambered cover glass then subjected to a specific concentration of bicarinalin for 24 hours. Biofilms were stained with SYTO 9 for visualisation. Bicarinalin concentration in image A) Control (no peptide) B) 1 µg/ml, C) 10 µg/ml, D) 100 µg/ml, E) 1000 µg/ml.*

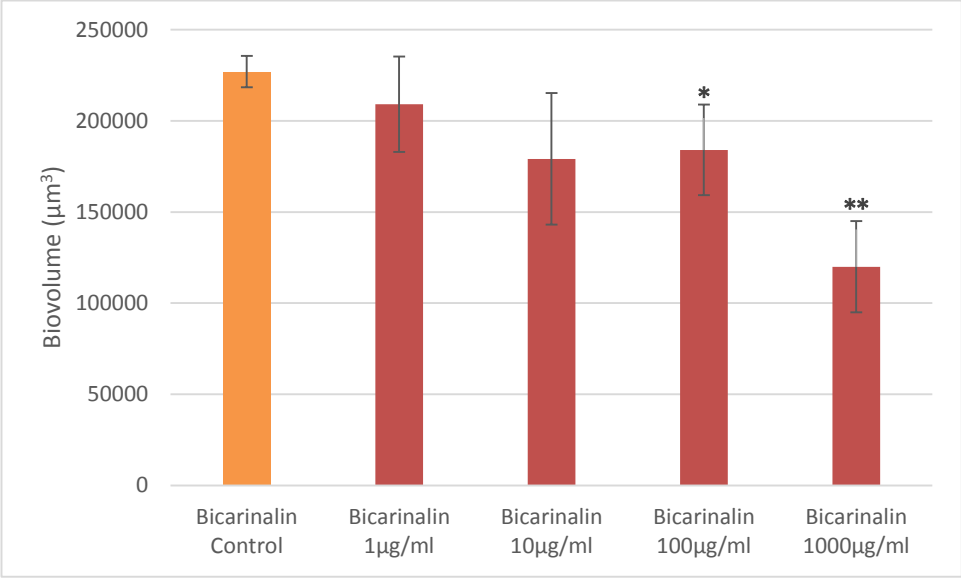

Figure 4.9.4-Bio-volume (µm³) of biofilm at different concentrations of bicarinalin. ** p≤0.05, ** p≤0.01*

4.9.3 BP100

Image A shows the control sample used. From **image B to E** the peptide concentration increases by 10 fold in each picture and the images indicate a very significant decrease in biofilm especially in images D and E.

Using the BITPLANE Imaris software the biofilm bio-volume was quantified at four concentrations of BP100, 1, 10, 100, 1000 µg/ml; the results are shown in **Figure 4.9.6**. The control had a bio-volume of 227,067 μm^3.with a deviation of 8,668 μm^3. At 1µg/ml and 10µg/ml there was no significant difference from the control ($p>0.05$). At 100µg/ml the bio-volume was 129,225 μm^3 ($p\leq0.05$). This decreased to 104,257 μm^3 at 1000 µg/ml ($p\leq0.01$). This represented a bio-volume reduction of nearly 55%.

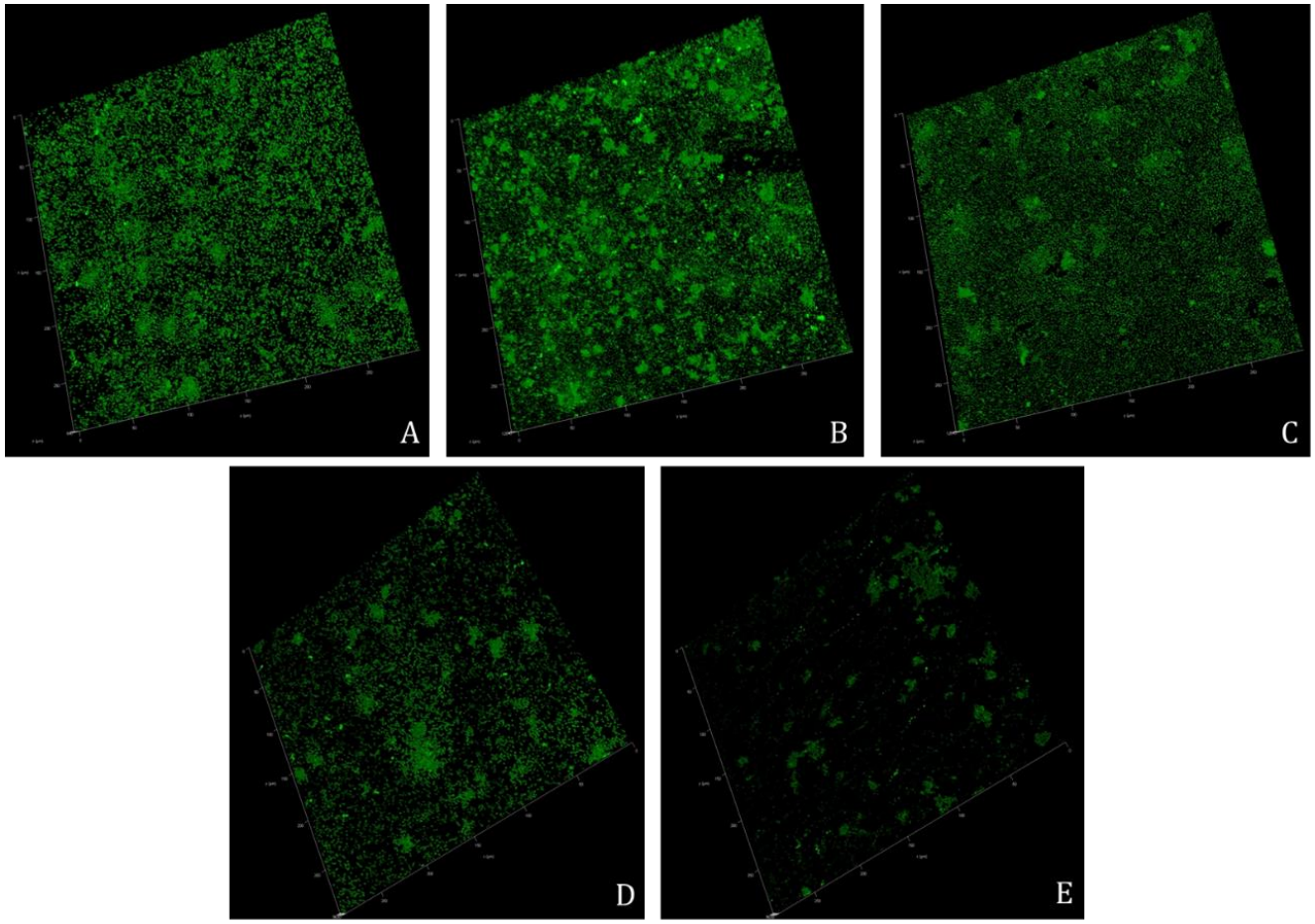

Figure 4.9.5- CLSM images: A. baumannii biofilms after being subjected to BP100; *grown for 24 hour in a chambered cover glass then subjected to a specific concentration of BP100 for 24 hours. Biofilms were stained with SYTO 9 for visualisation. BP100 concentration in image A) Control (no peptide) B) 1 µg/ml, C) 10 µg/ml, D) 100 µg/ml, E) 1000 µg/ml.*

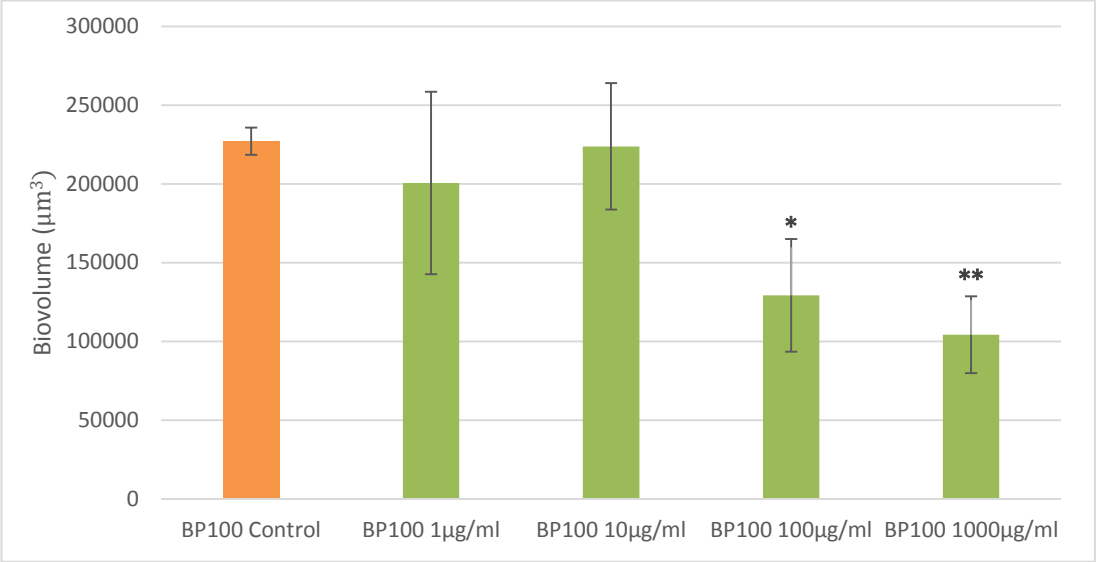

Figure 4.9.6- Bio-volume (µm³) of biofilm at different concentrations of BP100. ** p≤0.05, ** p≤0.01*

5 Discussion of Results and Recommendations

The primary objective of this research was to visualise the action of two potentially therapeutic antimicrobial peptides, bicarinalin and BP100, against *A. baumannii* cells and biofilms and compare their activity with the current treatment of last resort, colistin sulphate, using microbiological assays and microscopes.

The MIC and MBC for the three peptides against planktonic *A. baumannii* cells were determined. The data were used in AFM analysis to visualise and quantify transformations in cell surface and shape, exerted by increasing peptide concentrations.

The MBIC and biofilm removal assays quantified the effects of peptides on the formation of *A. baumannii* biofilms and the removal of pre-formed biofilms. The consequence of peptide action on the biofilm was imaged with SEM and CLSM. The CLSM was also used to quantify the changes in bio-volume of the biofilm with increasing peptide concentration.

5.1 The Identification and Growth of *A. baumannii* 19606

5.1.1 Identification

Gram-staining, the API 20NE test and the oxidase test were carried out to confirm the identity of *A. baumannii*. The results of these tests are described in **Section 4.1**. The colony morphologies, as described in **Table 4.1.1,** are similar to those described in Peleg (2008). The results of the API20NE and oxidase tests (**Section 4.1.4**) identified, with 99.9% certainty, the presence of the *A. baumannii*/*calcoaceticus* complex (**Figure**

4.1.8); the complementary 44°C test indicated the presence of *A. baumannii* species (Saugar *et al.*, 2006; Vaneechoutte *et al.*, 2011).

The *A. baumannii* complex members are indistinguishable from each other using phenotypic methods such as those used in this project: Gram-staining, API 20NE test and colony morphology. Molecular and genotypic methods, such as 16S rRNA, *rpoB* gene sequencing and MALDI-TOF MS (matrix assisted laser desorption ionisation-time of flight mass spectrometry), can be used if required to differentiate between the species of this complex. (Toh *et al.*, 2015; Dortet,*et al.*, 2006; Schumann and Pukall, 2013).

The API 20E test may also be used in the identification of *A. baumannii* complex as, although it is not a member of the Enterobacteriaceae family, it is a non-fastidious Gram negative bacterium (Djeribi, *et al.*, 2012; The Global Health Network, 2013).

The results of the three phenotypic tests strongly suggest that the *A. baumannii* complex was identified including the presence of *A. baumannii* species. The specific strain *A. baumannii* 19606 could not be confirmed from these diagnostic tests. The scope of this project required confirmation of genus and species but not of the strain.

5.1.2 Growth Curves

It was essential that each experiment was performed at the same stage in the bacterial growth curve to establish effective quantitative comparisons between different peptides at varying concentrations. A growth curve for *A. baumannii* 19606 was created to investigate the viable cell count (CFU/ml) within a solution of TSB by measuring the absorbance of the solution at 590nm. The number of CFUs and absorbance at 590nm was also measured at each time interval to ensure a reliable calibration between CFU/ml and absorbance. For each experiment, the initial CFU/ml

was confirmed by the spread plate method. This information was used at the start of every experiment to ensure an initial standard CFU/ml. The results are shown in **Section 4.2.** An absorbance of 0.01 was determined to be equal to approximately $1x10^7$ CFU/ml; the solution was then diluted to ensure the standard cell density of $5x10^5$ CFU/ml.

It was intended that the growth curve would determine the lag phase, log phase and stationary phase of *A. baumannii* growth (**Figure 5.1.2**). The lag and log phases were established but the experiment was not conducted for long enough to conclusively determine the stationary phase. **Figure 4.4.2** shows the plateauing of CFU/ml after 26 hours but no plateauing was seen in **Figure 5.1.1**.

For this project, it was important to identify the start and duration of the log phase. The results obtained (**Figure 5.1.1**) indicated that an overnight incubation of 10-15 hours ensured the bacteria were in the log phase of growth.

Subsequent experiments were commenced when the bacteria were in log phase to be at their optimum rate of growth. Determining the stationary phase was not essential for the scope of this project as the length of time *A. baumannii* spent in log phase was in excess of 30 hours which meant that overnight incubation was acceptable for the experiments (Fernando and Kumar, 2012).

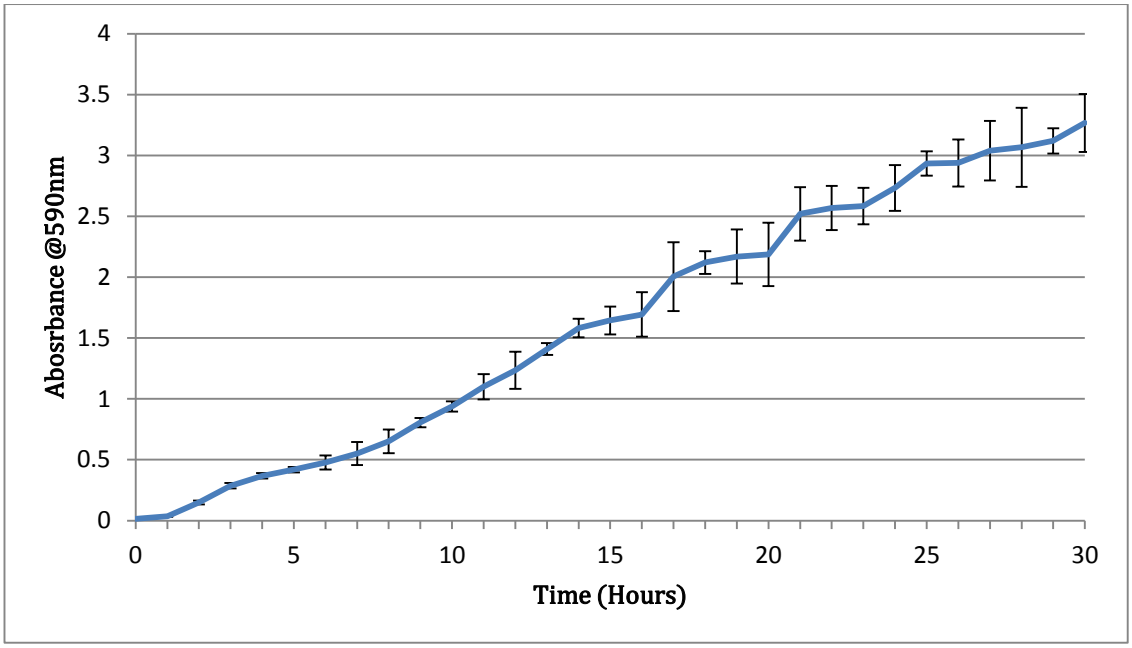

Figure 5.1.1 Graph showing the absorbance of A. baumannii* culture in *TSB cover 30 hours. *Results from all three test samples are used to construct the standard deviation bars at each hour. Figure as shown in Section 4.2.*

The Time-Absorbance curve constructed in this project (**Figure 5.1.1**) is similar to that of Fernando (2012) which was undertaken for 16 hours. In Fernando (2012) the lag phase lasted for about 1.5 hours and no stationary phase was found within 16 hours.

Further repeats could be performed to obtain a smoother curve and the experiment could be carried out for longer to determine the stationary phase. At the start of all subsequent experiments, the absorbance at 590nm was verified to be 0.01 and spread plate confirmed the inoculum of approximately $1x10^7$CFU/ml. There was therefore a high degree of confidence that the initial inoculum used was approximately $1x10^7$ CFU/ml for each experiment.

5.2 Comparison of Peptide Treatment on Planktonic Cells of *A. baumannii*

5.2.1 Microbiological Assays

The MIC and MBC were determined to compare the bacteriostatic and bactericidal activity of three antimicrobial peptides: colistin sulphate, bicarinalin and BP100. The methodology used was adapted from that described by Eucast (2003) and Wiegand (2008). These results were used in the AFM analysis to produce images and determine the surface roughness and surface area of single *A. baumannii* cells at different peptide concentrations in relation to the MBC. The methodology is described in **Sections 3.9**, **3.10** and **3.14** and the results in **Sections 4.3**, **4.4** and **4.7**.

Against planktonic *A. baumannii* cells, colistin sulphate had the lowest MIC and MBC concentration of 0.5µg/ml; this was less than bicarinalin and BP100 which both had MIC and MBC concentrations of 4µg/ml.

Due to the two-fold serial dilution method applied, the recorded MIC and MBC concentrations are considered as a maximum since the true values could be between the recorded MIC/MBC concentration value and the next lowest concentration. For example, colistin sulphate had a MIC of 0.5 µg/ml, recorded for the first clear well. The MIC therefore lies between 0.25 µg/ml (turbid well) and 0.5 µg/ml (clear well). The MIC and MBC for bicarinalin and BP100 were identical and between 2 µg/ml and 4 µg/ml using this methodology. The maximum value of the MIC and MBC is therefore reported in this thesis.

It is likely that that the MBC would be greater than the MIC with more detailed analysis. A more accurate MIC and MBC could be determined by testing the concentration of peptide, within the two-fold dilution range to investigate any differences between the

MIC and MBC, and between bicarinalin and BP100. For this project, the recorded MIC and MBC values were considered sufficiently accurate for atomic force microscope analysis.

The *A. baumannii* 19606 susceptibility to colistin sulphate obtained in this project was similar to those in Li (2006) who showed *A. baumannii* 19606 had a MIC range of 0.25-2 μg/ml. This value of the MIC also confirms that the *A. baumannii* 19606 strain is colistin sulphate susceptible as defined by The Clinical and Laboratory Standards Institute (Li *et al*., 2006). Saugar (2006) also confirmed *A. baumannii* 19606 strain is colistin sulphate susceptible.

The results for the MIC and MBC for bicarinalin against *A. baumannii* 19606 were compared with those of Rifflet (2012) and Téné (2014) who investigated other bacterial species of *Cronobacter*, *Enterobacter* and *Staphylococcus*. The results suggest that *A. baumannii* is more susceptible to bicarinalin compared with *Cronobacter sakazakii* (MIC: 12.8 μg/ml, MBC: 13.5 μg/ml), *Enterobacter cloacae* (MIC: 22.8 μg/ml, MBC: 45.1 μg/ml), *Enterobacter aerogenes* (MIC: 20.4 μg/ml, MBC: 40.7 μg/ml) and *Staphylococcus aureus* (MIC: 6-6.5 μg/ml). However, *A. baumannii* is not as sensitive as *Staphylococcus xylosus (*MIC: 1 μg/ml) to bicarinalin.

The results for the MIC and MBC for BP100 against *A. baumannii* 19606 were similar to the activity of BP100 against other bacteria when compared with previous studies: *Escherichia coli* (MIC:2.84 μg/ml, MBC:4.26±0.852 μg/ml), *Klebsiella pneumonia* (MIC:1.42 μg/ml, MBC-4.97±0.71 μg/ml), *Pseudomonas aeruginosa* (MIC: 11.36 μg/ml, MBC:11.36 μg/ml), *Pseudomonas syringae* (MIC:3.55±7.1 μg/ml), *Xanthomonas axonopodis* (MIC:7.1-10.65 μg/ml) and *Erwina amylovora* (MIC:3.55-7.1 μg/ml) (Torcato *et al*., 2013; Badosa *et al*., 2007; Alves *et al*., 2010).

The MIC and MBC experiments showed that against *A. baumannii* 19606, colistin sulphate had bacteriostatic and bactericidal activity at a lower concentration compared to bicarinalin and BP100.

5.2.1.1 Efficacy of Peptides with Regard to Structure

All three peptides tested exhibit amphipathicity within their structure as shown in **Sections 2.4.4, 2.4.5 and 2.4.6**. Amphipathicity is a characteristic of antimicrobial peptides and enable their interaction with the phospholipid bilayer of the bacterial membranes (Laverty *et al.*, 2011; Wadhwani *et al.*, 2014; Rifflet *et al.*, 2012; Velkoy *et al.*, 2010). Colistin sulphate has the lowest MIC in terms of weight at 0.5 µg/ml and moles of peptide required at 0.43 µmol/l. Cyclic peptides have been found to generally have higher efficacy than linear peptides such as bicarinalin and BP100 (Hoo, 2012).

Bicarinalin has the highest molecular weight at 2213.78 g/mol of the peptides tested with colistin sulphate weighing 1155.4 g/mol and BP100 weighing 1420 g/mol. Compared to BP100, bicarinalin has a lower MIC value in terms of its mole concentration at 1.8 µmol/l than BP100 at 2.8 µmol/l to inhibit bacterial growth. This indicates less moles of bicarinalin are required to exert the same inhibitory effect on *A. baumannii* than BP100. A factor could be the length of bicarinalin with 20 amino acids compared to 11 amino acids in BP100 potentially enabling it to traverse the phospholipid bilayer which BP100 is unable to do. BP100 thus may require a higher threshold concentration to permeabilise the membrane assuming the carpet model mechanism (Wadhwani *et al.*, 2014; Tene *et al.*, 2014; Rifflet *et al.*, 2012).

5.2.2 Visualisation and Quantification of Peptide Treatment using the Atomic Force Microscope

The effect of peptide activity on *A. baumannii* was visualised by AFM using previously described methods (Alves *et al.*, 2010; Domingues *et al.*, 2014). The images for each of the three peptides clearly show that, below the peptide MBC, the coccus-bacillus cell shape is conserved; at concentrations at and above the MBC, the cell surface, shape conformity and size are drastically affected (**Section 4.7**).

Membrane disruption caused by peptide activity is noted from various studies (Li *et al.*, 2007; Braga and Ricci, 1998; Stukalov *et al.*, 2008; Alves *et al.*, 2010; Soon *et al.*, 2009, & 2011; *Domingues et al.*, 2014). In this research project, indentations and pores are seen in the bacterial surface with resulting cytoplasmic leakage and debris. Some cells show a decrease in height and deflation, possibly due to a loss of turgor pressure (Dickson *et al.*, 2015). As the peptide concentration increased, more intense membrane perturbation and cytoplasmic leakage were visualised. Similar observations were described by Li *et al.*(2007).

The membrane disruption was confirmed by the quantification of the surface roughness and surface area. The surface roughness data from all three peptides (**Figure 5.2.1**) showed that there was no statistical difference between the control and at ½ MBC. For colistin sulphate and bicarinalin, there was a significant increase in roughness at the MBC. This increase in surface roughness has been previously recorded when bacterial cells are subjected to antibacterial peptide activity (Sharma *et al.*, 2003; Domingues *et al.*, 2014; Alves *et al.*, 2010). Alves (2010) found a significant increase in bacterial roughness at the MIC concentration of BP100 against *Escherichia coli*, consistent with the results of this project.

For colistin sulphate and bicarinalin, the roughness decreased at 2x MBC. This decrease is likely to be due to the membrane collapsing (Dickson *et al.*, 2015).

The results are less clear for BP100 as the error bars show a big variance in the data set. Further repeats would be recommended to obtain a more statistically valid data set to determine if the trend follows that of colistin sulphate and bicarinalin.

The surface area data (**Figure 5.2.2**) also supported the observation that the cells shrunk as peptide concentration increased above the MBC and these results were consistent for all three peptides. At ½ MBC, the cell surface area increased compared to the control. This is believed to be because, at this concentration, normal cellular functions and mechanisms were still able to function, including binary fission (Reeks *et al.*, 2005) . Most of the images analysed at this concentration showed elongated cells during the process of cell division resulting in an increased surface area (Robert, 2015).

Due to the size of the data set, most of the cells at this concentration were in the process of division. The control sample data set was larger as it was carried out twice so selected images showing single cells could be chosen. At all other concentrations, data collection was carried out once so a smaller data set was obtained.

At the MBC, although there was greater data variance, the average cell area was significantly less than at ½ MBC, although broadly similar to the control. Doubling the MBC showed a significant decrease in surface area evident in the images obtained for all peptides. The results indicated that it required a concentration above the MBC for the cells to shrink.

Five cells at each concentration for each peptide were quantified for the surface roughness and surface area. Further repeats should be carried out to image more cells and increase the statistical accuracy of the data set. Further samples would also reduce the skew in the surface area data at ½ MBC as more single cells could be found, imaged and measured.

Although imaging bacterial cells in air is a widely used technique (Alves *et al.*, 2010; Domingues *et al.*, 2014; Webb *et al.*, 2011), it can lead to dehydration of the cell and changes in the cell surface that were not directly caused by peptide activity. The AFM does allow the imaging of cells in their natural physiological conditions such as in broth. This is discussed in **Section 2.5.1** and further in **5.6.2.**

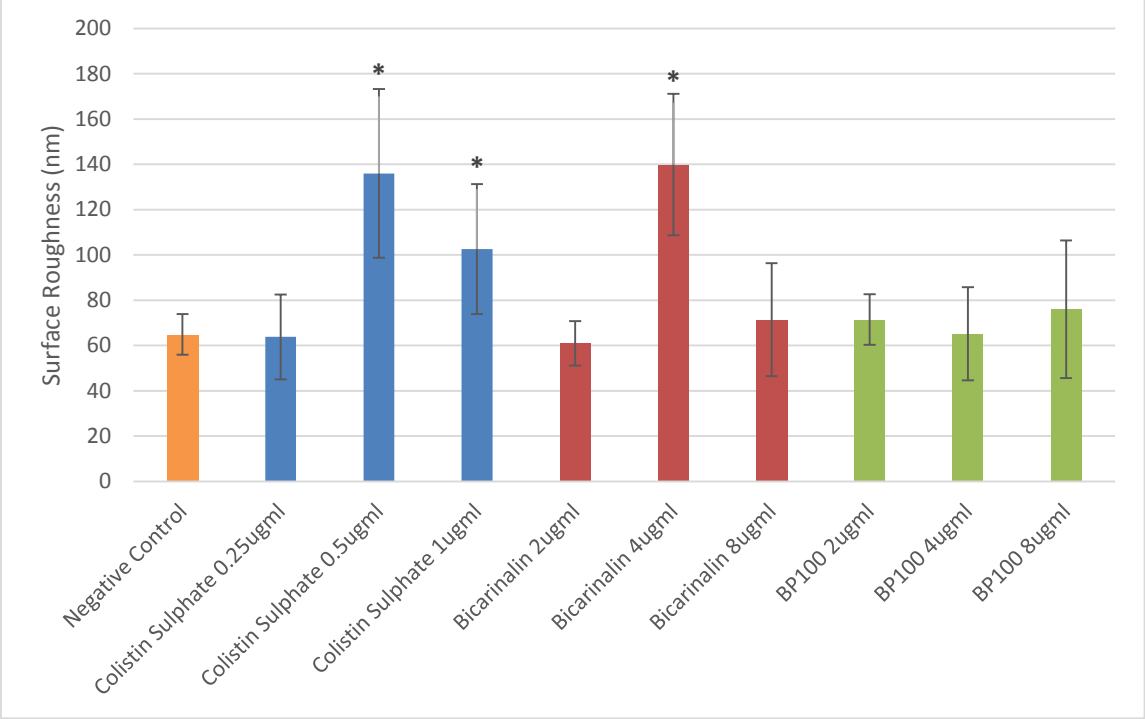

Figure 5.2.1- Surface roughness with increasing peptide concentrations. *Tests subjected for 2 hrs compared to the control. * denotes p ≤0.05; ** p≤0.001. Results from sections 4.7.1, 4.7.2, 4.7.3.*

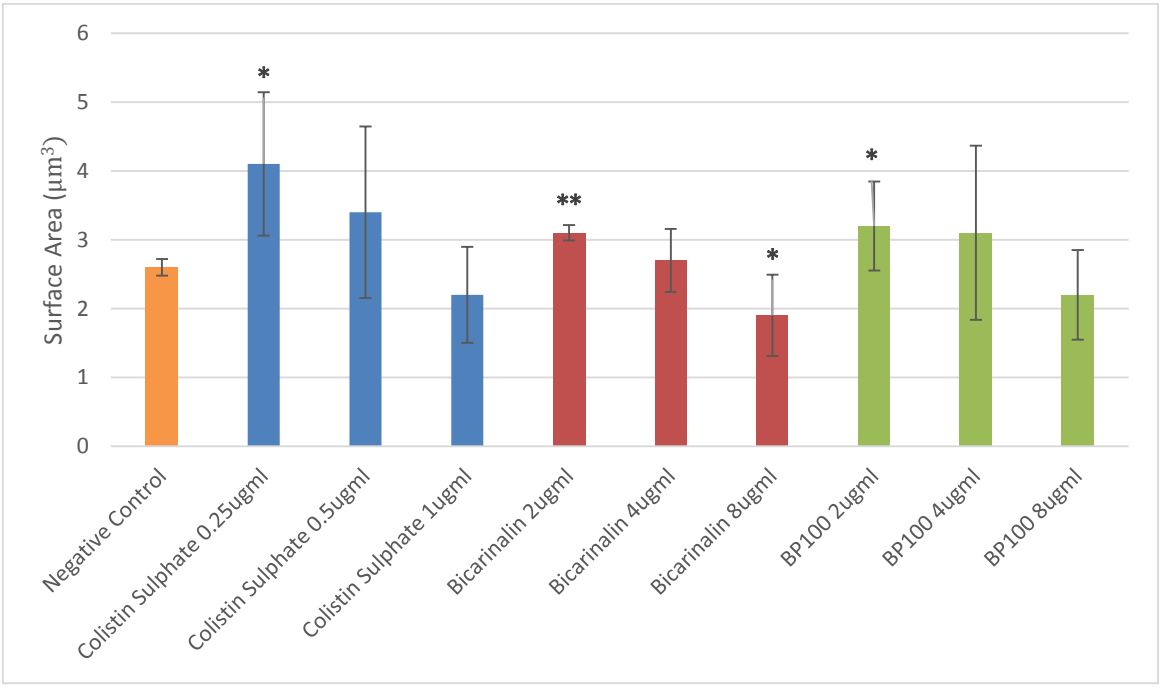

Figure 5.2.2- Surface area with increasing peptide concentrations. *Tests subjected for 2 hrs compared to the control. * denotes p ≤0.05; ** p≤0.001. Results from sections 4.7.1, 4.7.2, 4.7.3.*

5.3 Comparison of Peptide Treatment on *A. baumannii* Biofilms

5.3.1 Minimum Biofilm Inhibitory Concentration (MBIC)

The minimum biofilm inhibitory concentration (MBIC) is defined as the lowest concentration of antimicrobial peptide that caused 90 % inhibition of *A. baumannii* biofilm formation. Using methods similar to those described by Gopal *et al* (2014), as shown in **Section 3.12,** biofilm formation was quantified using the crystal violet stain method; the results are shown in **Section 4.5**.

A twofold dilution method was used to estimate the MBIC as for the MIC and MBC. The results showed that, at the MBC for all three peptides, there was no formation of biofilm. This is consistent with the MIC and MBC results as, if the cells are dead at the MBC concentration, they would be unable to adhere, divide and produce the exopolysaccharide matrix leading to biofilm formation (Wiegand *et al*., 2008).

The recorded MBIC for colistin sulphate was 0.5 µg/ml; the actual MBIC value will be between 0.25 µg/ml and 0.5 µg/ml as biofilm formation may still occur at a lower concentration than the recorded MBIC. A more accurate MBIC could be determined by testing the concentration of peptide, within the two-fold dilution range.

5.3.2 Biofilm Removal Assay

The methodology is described in **Section 3.12** and is similar to those described by Dosler (2014) and Song (2015). The results are shown in **Section 4.6** and shown below in **Figure 5.3.1**. The results indicate that bicarinalin is superior at eradicating *A. baumannii* biofilms than colistin sulphate above its MBC and both bicarinalin and BP100 were better at concentrations above 128 µg/ml.

Colistin sulphate removal activity was better at low concentrations; this was as expected due to its lower MBC which is nearly an order of magnitude less than bicarinalin and BP100. However, the maximum biofilm removed was only 52% at 512 μg/ml.

Bicarinalin was the most effective between 8 μg/ml, where it removed 39%, to 128 μg/ml, where it eradicated 70% of the biofilm. A further concentration increase had no additional apparent effect on the biofilm.

The removal activity of BP100 started slowly and at 16 μg/ml it had removed 20% of the biofilm, half that of colistin sulphate. Above 16 μg/ml BP100 increased linearly to exceed bicarinalin activity above 512 μg/ml. At 2048 μg/ml, the highest concentration tested, BP100 had eradicated 94% of the biofilm.

It is not known whether the cells within the biofilm are living or dead as the analysis is testing simply the presence of the total biofilm. Further research, involving the minimum biofilm eradication concentration (MBEC) method, is recommended (**Section 5.6.1**).

Colistin sulphate had the most biofilm removal activity, as expected, at low concentrations of 1-4 μg/ml, below the bicarinalin and BP100 MBC. Bicarinalin was the best between 8 to 128 μg/ml and BP100 was the most effective from 256 to 2084 μg/ml. The superior performance of bicarinalin, and particularly that of BP100, was not anticipated especially considering the MBC is nearly ten times that of colistin.

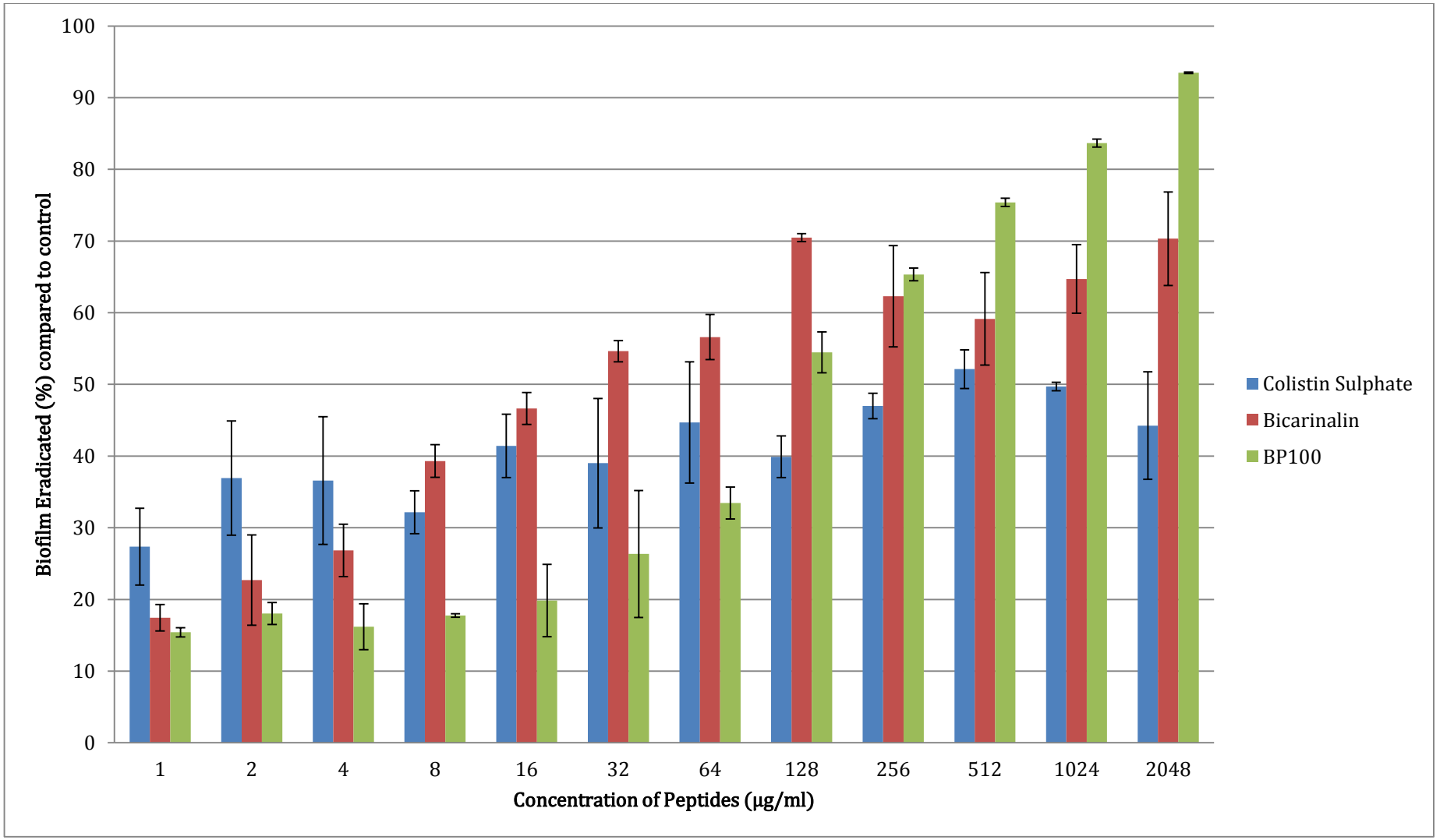

Figure 5.3.1- Biofilm removed (%) after being exposed to the three peptides: colistin sulphate, bicarinalin and BP100. *Figure reproduced from section 4.6.*

5.3.3 Visualisation and Quantification of Peptide Treatment using the Scanning Electron Microscope

The SEM has been widely used to image bacterial biofilms (Alhede *et al.*, 2012; Djeribi *et al.*, 2012;). The images revealed, with increasing concentrations of peptide, progressive changes in cellular shape and structure of the biofilm (**Section 4.8**).

The images only showed the surface layer of the biofilm and not the formation of protruding micro-colonies (Gaddy *et al.*, 2009). 24 hours were allowed for the formation of a biofilm, which may not be sufficient for the extensive formation of micro-colonies (Gaddy *et al.*, 2009; McConnell *et al.*, 2013).

Time-growth studies, further described in **Section 5.6.1**, would add to the understanding of the growth of *A. baumannii* biofilms. Another factor impacting biofilm growth could be due to the rotating conditions of 140rpm that were used. This rotation may have inhibited the formation of thick biofilms (Merritt *et al.*, 2011). Further experiments could include a comparison of biofilm growth in static conditions and rotating conditions. SEM images could be made of biofilms during the time studies as described in **Section 5.6.1**.

Membrane protrusions between bacterial cells were seen in the control sample and at 1µg/ml concentrations for each peptide. Pili or cellular filaments between cells have been previously documented within biofilms (Gaddy *et al.*, 2009; Eaktasang *et al.*, 2013). At the higher concentrations of 10 µg/ml and 100 µg/ml, these protrusions were not visible suggesting the inability of the cells to form pili at these peptide concentrations (Longo *et al.*, 2014; Gaddy *et al.*, 2009).

The effect of the peptides on the cells within the biofilm caused cell shrinkage, severe disruption to membrane and cellular conformity along with cytoplasmic leakage and debris. These changes were also visualised in the AFM images.

The 1000 µg/ml sample for each of the peptides were not visualised due to the time constraint of viewing all samples within the 8 hour period at the Electron Microscopy & Spectroscopy Centre at the University of Leeds. At this concentration, there is likely to be extensive or complete cell lysis. **Figure 5.3.2** illustrates the effect of bicarinalin at 100 µg/ml and at this concentration most of the cells are lysed. The higher magnification images only show a small sector of the biofilm and the inset image, at 5,000x magnification displays a larger area of the biofilm.

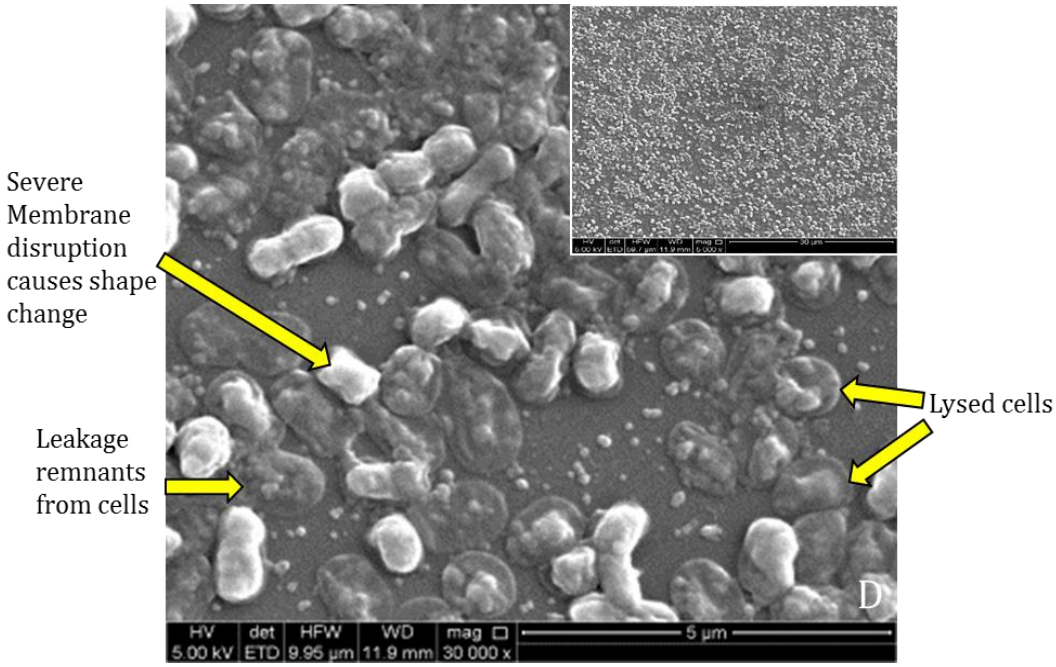

Figure 5.3.2- SEM images of A. baumannii biofilms subjected to 100 µg/ml Bicarinalin for 24 hours. *Biofilms grown on polystyrene pegs for 24 hours. 30000x magnification. Insert magnification 5000x. Figure reproduced from section 4.8.2.*

5.3.4 Visualisation and Quantification of Peptide Treatment using the Confocal Laser Scanning Microscope

The method and preparation for CLSM visualisation is described in **Section 3.16** and is similar to methodologies previously used (Innovotech Inc., 1996; Yerly *et al.*, 2007; Harrison *et al.*, 2006). In this project, BacLight stain containing SYTO9, was applied to the *A. baumannii* biofilms to visualise and quantify the biofilm bio-volume with

increasing concentrations of peptide. The method was similar to that described by Harrison (2006).

The CLSM images (**Section 4.9**), showed a decrease in biofilm as the peptide concentration increased. This was quantified by calculating the bio-volume using BITPLANE Imaris software.

Bio-volume was chosen to be quantified as it best represented the change in biofilm as the peptide concentration increased. Other biofilm characteristics may also be quantified such as biofilm roughness, by a root-mean-squared calculation, as described in the quantification of surface roughness in the AFM images (**Section 4.7**). Average biofilm thickness could be assessed by measuring the depth of the biofilm from the surface at multiple points on the biofilm and averaging the values. The maximum thickness could also be determined by measuring the depth of the biofilm from the surface level to the highest point. All these measurements would quantify the effect of peptide activity on the biofilm.

Biofilms at each of the four peptide concentrations were visualised and quantified (**Section 4.9**). The error bars for some of the results were wide especially for BP100. Five different areas of the biofilm were analysed for each peptide at each concentration. The results are very dependent on the samples analysed, are semi quantitative and measure dead as well as living biofilms. The experiment was only carried out once so has a high variance in the results. It is recommended that further repeats are carried out to obtain a larger set of statistically robust data and to validate the accuracy of the results obtained in this project. However, with the results discussed in **Section 4.9**, the following conclusions may be drawn. The trends are consistent to those obtained by the biofilm removal assay described in **Section 4.6** (and summarised in **Figure 5.3.1**) which is encouraging and indicates a confidence in the methodologies and results.

With increasing concentration of colistin sulphate from 10 and 100 μg/ml, there was a progressive reduction in bio-volume. There was no noticeable reduction above 100 μg/ml consistent with the results in **Figure 5.3.1**. The maximum bio-volume reduction compared with the control was approximately 25%.

With bicarinalin, the biofilm reduction was immediate from 1 μg/ml and increased to the maximum concentration tested of 1000 μg/ml. At concentrations higher than 1000 μg/ml, the peptide performed better than colistin sulphate with a 50% biofilm reduction compared to 25%.

The results for BP100 showed at high concentrations (>100 μg/ml) the peptide was more effective than bicarinalin and colistin. At 1000 μg/ml the biofilm reduction was 55% compared with only 25% for colistin.

The results were very encouraging and showed a similar trend to those obtained from the biofilm removal assay described in **Section 5.2.1**. They indicate that both bicarinalin and BP100 are more effective than colistin sulphate against *A. baumannii* biofilms especially at high concentrations.

5.4 Significance of the Results

The results indicate that bicarinalin and BP100 both have similar bactericidal and generally better biofilm activity against *A. baumannii* than colistin sulphate, an antibiotic currently used as a 'last resort' treatment (Karageorgopoulos and Falagas, 2008). At all concentrations (>MBC) bicarinalin is more effective at removing *A. baumannii* biofilms than colistin sulphate. At concentrations at and above 128 µg/ml, BP100 is more effective against *A. baumannii* biofilms than colistin sulphate. At the highest concentrations tested (2048 µg/ml), BP100 is even more effective than bicarinalin and is twice as effective as colistin sulphate. Cytotoxic studies, as described in **Section 5.6.1,** will determine whether, at these concentrations, bicarinalin and BP100 can be used in clinical treatment.

The results support the hypothesis that AMPs, like bicarinalin and BP100, could be used in the treatment of biofilms (Dawgul *et al.*, 2014). Colistin sulphate performs well against single cells but significantly less well against the biofilms. Colistin sulphate against *P. aeruginosa* has been shown to have a MIC concentration of 0.25-2 µg/ml and a MBC concentration of 0.5-2 µg/ml. This increased to 160-2560 µg/ml when tested against biofilms, a 320-1280% increase (Dosler and Karaaslan, 2014). *A baumannii* is able to form biofilms so it is essential that future tests to investigate peptide efficiency are performed on bacterial biofilms. The results of both bicarinalin and BP100 against biofilms are therefore extremely significant and encouraging.

5.5 Additional research

Additional research should be carried out to verify the accuracy and reliability of the results obtained in this project.

The biofilm removal assay (**Sections 3.13 and 4.6**) was carried out twice in triplicate. This should be repeated at least once more to obtain more statistically robust results.

Five cells were imaged and measured for each peptide and concentration using AFM (**Sections 3.14 and 4.7**). Further repeats to obtain a larger data set for each concentration and peptide should be made.

For the SEM analysis (**Sections 3.15 and 4.8**), the 1000 µg/ml for each peptide was not imaged due to the time constraint at the University of Leeds. This concentration should be visualised.

The CLSM investigation was carried out once (**Sections 3.16 and 4.9**). This should be repeated at least a further two times until statistically robust results are obtained.

5.6 Further Research

Further research, using microbiological assays and AFM, SEM and CLSM, can be carried out to gain a comprehensive understanding of *A. baumannii* biofilm growth and peptide activity on single cells and biofilms.

5.6.1 Microbiology Assays

Further research should be carried out to understand more about ***A. baumannii* biofilm growth in different conditions and timescales**. Biofilms grown in static conditions and a range of rotating frequencies will help determine the optimum conditions in which they form.

A recommended timescale experiment is to investigate how **quickly a peptide exerts its activity on planktonic cells and preformed biofilms** (Vila-Farres *et al.*, 2011). The following techniques are recommended:

1. **Planktonic Cells**- Concentrations of peptides at 1xMIC, 2xMIC, 4xMIC and 8xMIC could be added to 10ml aliquots of *A. baumannii* at $5x10^5$ CFU/ml and incubated. Samples would then be taken at time intervals such as 0, 4, 7, 24, 48 hours, the peptide neutralised and the solution spread onto an agar plate and colonies counted after incubation. A reduction of 3 log10 CFU/ml compared to the initial inoculum would be considered bactericidal.
2. **Biofilm**-A preformed biofilm, grown for a defined length of time, using data from the biofilm growth curve, is formed in the 96 well plates. A specified concentration of peptide, possibly derived from the MBEC experiment (as the concentration is known) will kill all the cells in the biofilm. The peptide would be incubated with the biofilm for periods such as 0.5, 1, 2, 4, 12, 24, 24 hours. At the specified time, the biofilms would be washed with a neutraliser to inhibit any further peptide activity. Crystal violet stain will quantify the remaining biofilm using CLSM.

The construction of accurate **biofilm growth curves** could be made. The quantity of biofilm presence can be measured by crystal violet, similarly to the MBIC method and quantification of biofilm removal experiments. Time intervals such as at 0.5, 1, 6, 12, 24, 48 hours can be investigated. This would help understand if biofilm constantly increases, if there is a plateau or if it starts to reduce after a certain length of time. For example, if the biofilm starts to break down after 12 hours during a 24 hours experiment then the decrease in biofilm would not be completely due to peptide activity (Vila-Farres *et al.*, 2011). This will help to decide the optimum time to add a peptide, before a potential decrease in biofilm.

The **minimum biofilm eradication concentration (MBEC)** is a widely used technique to determine the concentration of peptide required to kill all bacterial cells within a biofilm (Olson *et al.*, 2002; Ceri *et al.*, 1999; Feng *et al.*, 2013; Dosler and Karaaslan, 2014; Marumo *et al.*, 2013). This experiment is a refinement of the MBIC experiment as it measures the eradication or death of cells within the biofilm. Biofilms are grown on the polystyrene pegs, such as the plate pegs used in this project for SEM visualisation. The biofilms are then subjected to a twofold dilution of peptide. The pegs are then ultra-sonicated and incubated. The lowest concentration, where no regrowth was observed, is recorded as the MBEC. This investigation could follow the biofilm removal experiment (**Section 3.13**).

Using the methods described in this project, **other antimicrobial peptides** could be tested against *A. baumannii* cells and biofilms. Additional peptides that may be considered for a project include haloganan *(Shin et al.*, 2014), pleurocidin (Souza *et al.*, 2013), and alyteserin 1c (Subasinghage, *et al.*, 2011).

In this project, the colistin sulphate susceptible *A. baumannii* strain 19606 was used. AMPs should be tested against **multi-drug resistant *A. baumannii* strains**. Strains such as *A. baumannii* 208628 and 201630, are known to be colistin sulphate resistant and should be investigated (Saugar *et al.*, 2006).

Bicarinalin and BP100 could be tested against **other clinically relevant bacteria** such as the Gram negative *Klebsiella pneumonia* and *Pseudomonas aeuroginosa* and the Gram positive bacteria *Staphylococcus aureus, Enterococcus faecalis* and *Streptococcus gordonii* (Rice, 2008; Boucher *et al.*, 2009).

After determining the MBEC and MBC for each peptide, **cytotoxic studies** should be carried out. Human erythrocytes or keratinocytes could be used (Feng *et al.*, 2013; Rifflet *et al.*, 2012). This will highlight the potential of these two AMPs for use in systemic medical treatment by their ability not to kill eukaryotic cells at bactericidal concentrations.

5.6.2 Atomic Force Microscope

One to five cells were imaged during one session of about 2-3 hours. This meant that cells imaged at the end of the session may have evolved a slightly different topographically compared to the cells imaged at the start. One way to counter this would be to analyse the cells under their natural physiological conditions such as liquid broth and a controlled temperature and potentially to visualise the morphological alterations on the bacterial cell surface exposed to the peptides as they occur (Braga and Ricci, 1998; Doktycz *et al.*, 2003).

The mechanical and adhesive properties of bacterial cells can be investigated by measuring force-distance curves. This measures the interaction of forces between the AFM tip and bacterial cells and its cell wall components with a high resolution of tens of pico-newtons. This, in principle, would allow the determination of the turgor pressure within the bacterial cell (Stukalov *et al.*, 2008).

5.6.3 Scanning Electron Microscope

The SEM could be used to visualise biofilms grown for different timescales or subjected to AMPs for different timescales as proposed in **Section 5.6.1**.

5.6.4 Confocal Laser Scanning Microscope

The CLSM can be used with the SEM to visualise and quantify biofilm growth, by bio-volume and other parameters such as roughness and thickness, during the time studies of *A. baumannii* biofilm growth, as suggested in **Section 5.6.1**.

SYTO9 is often used in tandem with another nucleic stain propidium iodide (PI). PI is a nucleic acid membrane impermeable stain and only stains cells with a disrupted membrane. As it has a higher affinity for nucleic acid it will displace the SYTO9 stain and these cells would fluoresce red. In theory, cells that fluoresce green with SYTO9 are alive and cells that fluoresce red with PI are dead. Using different excitation and emission ranges for each of the stains it is possible to different between the two. This would enable the quantification of live and dead cells within a population or biofilm (Stocks, 2004; Harrison *et al.*, 2006).

6 Conclusions

6.1 Project Objectives

This project investigated the opportunistic pathogen *A. baumannii,* responsible for various infections such as pneumonia, septicaemia, wound infections and meningitis. It is clinically important due to its ability to become rapidly resistant to a wide range of antimicrobials and also to persist on clinical surfaces by forming biofilms.

Acinetobacter baumannii is the most clinically relevant species of the Acinetobacter genus and, due to the emergence of MDR strains; it is recognised as a major opportunistic pathogen by its inclusion as a member of the 'ESKAPE' group.

Recent novel antibiotic classes have been limited to the treatment of Gram-positive infections while it is the Gram-negative infections, caused by pathogens such as *Pseudomonas aeruginosa*, *Enterobacteriaceae*, and *A. baumannii*, that are in most urgent need of new therapies.

The objective of this research was to compare and visualise the activity of two potentially therapeutic antimicrobial peptides, bicarinalin and BP100, with the currently used colistin sulphate, against *A. baumannii.* The activity of the peptides against planktonic cells and biofilms of *A. baumannii* were investigated both quantitatively and qualitatively using microbiological assays and microscopes.

6.2 Project Results

The *A. baumannii* genus and species was verified (**Section 4.1**). However, the specific strain *A. baumannii* 19606 could not be confirmed from these diagnostic tests which

were outside scope of the current project. Ribotyping and MALDI-TOF MS could be carried out to identify a specific strain (**Section 5.1**).

The MIC and MBC experiments showed that, for planktonic cells of *A. baumannii*, colistin sulphate had bacteriostatic and bactericidal activity at a lower concentration compared to bicarinalin and BP100 (**Sections 4.3 and 4.4**). The effect of peptide activity on individual cells of *A. baumannii* was visualised by the AFM. The images for each of the three peptides clearly showed that, below the MBC, the coccus-bacillus cell shape is conserved; at concentrations at and above the MBC, the cell surface, conformation and size are drastically affected (**Section 4.7**).

The surface area and roughness data, measured by the AFM, also supported the observation that the cells shrunk as peptide concentration increased above the MBC and these results were consistent for all three peptides (**Section 4.7**).

However, the analysis of the peptides against biofilms of *A. baumannii* gives significantly different results. The biofilm removal assay (**Section 4.6**) and the CLSM investigation (**Section 4.9**) show that both bicarinalin and BP100 have considerably better biofilm removal activity against *A. baumannii* biofilms than colistin sulphate at high concentrations above 1000μg/ml. (**Section 5.3**).

In terms of biofilm removal, colistin sulphate was relatively the most effective at low concentrations, from 1 to 4 μg/ml, but the most it removed was approximately **50%** of the biofilm at 512 μg/ml. Bicarinalin was relatively the most effective from 8 μg/ml to 128 μg/ml, where it eradicated **70%** of the biofilm. The biofilm removal by BP100 started more slowly but at higher concentrations, above 128 μg/ml, it exceeded colistin sulphate activity and, above 512 μg/ml, it exceeded bicarinalin activity. At 2048 μg/ml, the highest concentration tested, BP100 eradicated nearly **95%** of the biofilm (**Section 4.6**).

The semi-quantitative biofilm removal tests using the CLSM also showed that bicarinalin and BP100 were more effective than colistin sulphate, especially at high concentrations (**Section 4.9**). At 1000 µg/ml, bicarinalin and BP100 removed approximately 50-55% of biofilm, twice as much as colistin.

The effect of the peptides on the cells within the biofilm involved cell shrinking and severe disruption in membrane and cellular conformity. Shrinkage of the cells was also observed together with cytoplasmic leakage and debris with the SEM (**Section 4.8**).

6.3 Comments on the Results

The results support the hypothesis that potential alternative AMPs, as bicarinalin and BP100, could be used in the treatment of infections caused by biofilm-producing prokaryotes. Colistin sulphate performs well against planktonic cells but significantly less well against biofilms. As *A. baumannii* is able to form biofilms, it is essential that future tests investigating peptide efficiency are performed on bacterial biofilms. Colistin sulphate is traditionally used as an antibiotic of the last resort and has several adverse side effects (**Section 2.4.4**). The results for both bicarinalin and BP100 against *A. baumannii* biofilms are therefore considered as extremely significant and encouraging.

7 References

Abbott, I., Cerqueira, G., Bhuiyan, S. and Peleg, A. (2013) Carbapenem resistance in *Acinetobacter baumannii*: laboratory challenges, mechanistic insights and therapeutic strategies. *Expert review of anti-infective therapy* 11(4) 395–409. Available from http://www.tandfonline.com/doi/full/10.1586/eri.13.21 [Accessed 21st November 2015].

Adams, M., Nickel, G., Bajaksouzian, S., Lavender, H., Murthy, R., Jacobs, M. and Bonomo, R. (2009) Resistance to colistin in *Acinetobacter baumannii* associated with mutations in the PmrAB two-component system. *Antimicrobial Agents and Chemotherapy* 53(9) 3628–3634. Available from http://www.ncbi.nlm.nih.gov/pmc/articles/PMC2737849/ [Accessed 28th November 2015].

Al Jarousha, A., El Jadba, A, Al Afifi, A., and El Qouqa, I., (2009) Nosocomial multidrug-resistant *Acinetobacter baumannii* in the neonatal intensive care unit in Gaza City, Palestine. *International journal of infectious diseases,* 13(5) 623–8. Available from http://www.sciencedirect.com/science/article/pii/S1201971208016901 [Accessed 15th November 2015].

Alhede, M., Qvortrup, K., Liebrechts, R., Høiby, N., Givskov, M. and Bjarnsholt, T. (2012) Combination of microscopic techniques reveals a comprehensive visual impression of biofilm structure and composition. *FEMS Immunology and Medical Microbiology*, 65(2) 335–342. Available from http://femsim.oxfordjournals.org/content/65/2/335 [Accessed 1st December 2015].

Alves, C., Melo, M., Franquelim, H., Ferre, R., Planas, M., Feliu, L., Bardají, E., Kowalczyk, W., Andreu, D., Santos, N., Fernandes, M. and Castanho, M. (2010) *Escherichia coli* cell surface perturbation and disruption induced by antimicrobial peptides BP100 and pepR. *Journal of Biological Chemistry*, 285(36) 27536–27544. Available from http://www.ncbi.nlm.nih.gov/pubmed/20566635 [Accessed 21st November 2015].

Andrews, J. (2006) BSAC standardized disc susceptibility testing method (version 5). *Journal of Antimicrobial Chemotherapy*, 58 511-529. Available from: http://jac.oxfordjournals.org/content/58/3/511.full.pdf [Accessed 1st December 2015].

Badosa, E., Ferre, R., Planas, M., Feliu, L., Besalú, E., Cabrefiga, J., Bardají, E. and Montesinos, E. (2007) A library of linear undecapeptides with bactericidal activity

against phytopathogenic bacteria. *Peptides,* 28(12) 2276–2285. Available from http://www.sciencedirect.com/science/article/pii/S0196978107003890 [Accessed 23rd November 2015].

Bauman ,R., (2011) Microbiology with Diseases by Body System. International edition, 3rd edition. San Francisco, CA: Pearson Education.

Berney, M., Hammes, F., Bosshard, F., Weilenmann, H-U. and Egli, T. (2007) Assessment and Interpretation of Bacterial Viability by Using the LIVE/DEAD BacLight Kit in Combination with Flow Cytometry. Applied and Environmental Microbiology, 73(10) 3283-3290. Available from: http://www.ncbi.nlm.nih.gov/pmc/articles/PMC1907116/ [Accessed 24th November 2015].

Biomerieux. (2015) Apiweb. Available from: apiweb.biomerieux.com [Accessed 26th November 2015].

Bitplane. (2015) Imaris x64 [software] version 8.1.2, Imaris XT, Bitplane. Available from: http://www.bitplane.com/ [Accessed 19th November 2015].

Bjarnsholt, T. (2013) The role of bacterial biofilms in chronic infections. *APMIS* 2013; 121 (Suppl. 136): 1–54. Available from http://onlinelibrary.wiley.com/doi/10.1111/apm.12099/epdf [Accessed 26th November 2015].

Bonomo, R.A. and Szabo, D. (2006) Mechanisms of Multidrug Resistance in *Acinetobacter* Species and *Pseudomonas aeruginosa*. *Clincial Infectious Diseases,* 43(S2) S49-S56. Available from http://cid.oxfordjournals.org/content/43/Supplement_2/S49.long [Accessed 31st October 2015].

Boucher, H., Talbot, G., Bradley, J., Edwards, J., Gilbert, D., Rice, L., Scheld, M., Spellberg, B. and Bartlett, J. (2009) Bad bugs, no drugs: no ESKAPE! An update from the Infectious Diseases Society of America. *Clinical infectious diseases : an official publication of the Infectious Diseases Society of America,* 48(1) 1–12. Available from http://cid.oxfordjournals.org/content/48/1/1.long [Accessed 19th November 2015].

Braga, P. and Ricci, D. (1998). Atomic force microscopy: application to investigation of *Escherichia coli* morphology before and after exposure to cefodizime. *Antimicrobial Agents and Chemotherapy*, 42(1) 18–22. Available from: http://www.ncbi.nlm.nih.gov/pmc/articles/PMC105449/ [Accessed 19th November 2015].

Brogden, K. (2005) Antimicrobial peptides: pore formers or metabolic inhibitors in bacteria? *Nature reviews. Microbiology,* 3(3) 238–250. Available from http://www.nature.com/nrmicro/journal/v3/n3/full/nrmicro1098.html [Accessed 23rd November 2015].

Brossard, K. and Campagnari, A. (2012) The *Acinetobacter baumannii* Biofilm-Associated Protein Plays a Role in Adherence to Human Epithelial Cells. Infection and Immunity, 80(1) 228-233. Available from: http://www.ncbi.nlm.nih.gov/pmc/articles/PMC3255684/ [Accessed 18th November 2015].

Bruker. (2011) Application Note #133 Introduction to Bruker's ScanAsyst and PeakForce Tapping AFM Technology. Bruker. Available from: https://www.bruker.com/fileadmin/user_upload/8-PDF-Docs/SurfaceAnalysis/AFM/ApplicationNotes/Introduction_to_Brukers_ScanAsyst_and_PeakForce_Tapping_Atomic_Force_Microscopy_Technology_AFM_AN133.pdf [Accessed 16th November 2015].

Bruker. (2015) NanoScope Analysis [software] version 1.50. Bruker. Available from http://www.brukerafmprobes.com/a-3831-nanoscope-analysis-version-150.aspx [Accessed 24th November 2015].

Bruker. (2015) Scanasyst-air. [online]; Bruker. Available from: http://www.brukerafmprobes.com/Product.aspx?ProductID=3726 [Accessed 23rd November 2015].

Butler, M., Blaskovich, M. and Cooper, M. (2013) Antibiotics in the clinical pipeline in 2013. *The Journal of Antibiotics*, 66(10) 571–591. Available from http://www.nature.com/ja/journal/v66/n10/full/ja201386a.html [Accessed 16th November 2015].

Cabeen, M. and Jacobs-Wagner, C. (2005) Bacterial cell shape. *Nautre Reviews Microbiology*, 3 601-610. Available from: http://www.nature.com/nrmicro/journal/v3/n8/full/nrmicro1205.html [Accessed 30th November 2015].

Camp, C. and Tatum, O. (2010) A Review of *Acinetobacter baumannii* as a Highly Successful Pathogen in Times of War. *Laboratory Medicine*, 41(11) 649–657. Available from http://labmed.ascpjournals.org/content/41/11/649.short [Accessed 19th November 2015].

Ceri, H., Olson, M., Stremick, C., Read, R., Morck, D. and Buret, A. (1999) The Calgary Biofilm Device : New Technology for Rapid Determination of Antibiotic Susceptibilities of Bacterial Biofilms The Calgary Biofilm Device : New Technology for Rapid Determination of Antibiotic Susceptibilities of Bacterial Biofilms. *Journal of Clinical Microbiology* 37(6) 1771-1776. Available from: http://www.ncbi.nlm.nih.gov/pmc/articles/PMC84946/ [Accessed 30th November 2015].

Chang, K., Chiang, Y., Yang, C. and Liou, J. (2012) Atomic force microscopy in biology and biomedicine. *Tzu Chi Medical Journal*, 24(4) 162–169. Available from http://www.sciencedirect.com/science/article/pii/S1016319012000845 [Accessed 29th November 2015].

Chembase. cn. (2014) Colistin Sulphate. Available from: CBID:682 http://www.chembase.cn/molecule-682.html [Acessed 5th April 2016).

Claxton, N., Fellers, T. and Davidson, M. (2006) Laser Scanning Confocal Microscopy. *Encyclopedia of Medical Devices and Instrumentation*, 1979(21) 1–37. Available from http://onlinelibrary.wiley.com/doi/10.1002/0471732877.emd291/full [Accessed 13th November 2015].

Dawgul, M., Maciejewska, M., Jaskiewicz, M., Karafova, A., and Kamysz, W. (2014) Antimicrobial peptides as potential tool to fight bacterial biofilm. *Acta poloniae pharmaceutica*, 71(1) 39–47. Available from: http://www.ncbi.nlm.nih.gov/pubmed/24779193 [Accessed 10th November 2015].

Dickson, M., Liang, E., Rodriguez, L., Vollereaux, N. and Yee, A. (2015) Nanopatterned polymer surfaces with bactericidal properties. *Biointerphases*, 10(2) 021010-1-021010-8. Available from: http://scitation.aip.org/content/avs/journal/bip/10/2/10.1116/1.4922157 [Accessed 12th November 2015].

Djeribi, R., Bouchloukh, W., Jouenne, T. and Menaa, B. (2012) Characterisation of bacterial biofilms formed on urinary catheters. *American Journal of Infection Control*, 40(9) 854-859. Available from: http://www.sciencedirect.com/science/article/pii/S0196655311012636 [Accessed 13th November 2015].

Doktycz, M., Sullivan, C., Hoyt, P., Pelletier, D., Wu, S. and Allison, D. (2003) AFM imaging of bacteria in liquid media immobilized on gelatin coated mica surfaces. *Ultramicroscopy*, 97(1-4) 209-216. Available from:

http://www.sciencedirect.com/science/article/pii/S0304399103000457 [Accessed 21st November 2015].

Domingues, M., Silva, P., Franquelim, H., Carvalho, F., Castanho, M. and Santos, N. (2014) Antimicrobial protein rBPI21-induced surface changes on Gram-negative and Gram-positive bacteria. *Nanomedicine: Nanotechnology, Biology, and Medicine*, 10(3) 543–551. Available from: http://www.sciencedirect.com/science/article/pii/S1549963413005911 [Accessed 21st November 2015].

Donlan, R. and Costerton, W. (2002) Biofilms: Survival Mechanisms of Clinically Relevant Microorganisms. *Clinical Microbiology Reviews*, 15(2) 167-193. Available from: http://www.ncbi.nlm.nih.gov/pmc/articles/PMC118068/ [Accessed 21st November 2015].

Dortet, L., Legrand, P., Soussy, C-J. and Cattoir, V. (2006) Bacterial Identification, Clinical Significance, and Antimicrobial Susceptibilities of *Acinetobacter ursingii* and *Acinetobacter schindleri*, Two Frequently Misidentified Opportunistic Pathogens. *Journal of Clinical Microbiology*, 44(12) 4471-4478. Available from: http://jcm.asm.org/content/44/12/4471.full [Accessed 21st November 2015].

Dosler, S. and Karaaslan, E. (2014) Inhibition and destruction of Pseudomonas aeruginosa biofilms by antibiotics and antimicrobial peptides. *Peptides,* 62(2014) 32–37. Available from: http://www.sciencedirect.com/science/article/pii/S0196978114002903 [Accessed 21st November 2015].

Durante-Mangoni, E., Del Franco, M., Andini, R., Bernardo, M., Giannouli, M. and Zarrilli, R. (2015) Emergence of colistin resistance without loss of fitness and virulence after prolonged colistin administration in a patient with extensively drug-resistant *Acinetobacter baumannii*. *Diagnostic Microbiology and Infectious Disease*, 82(3), 222–226. Available from http://www.sciencedirect.com/science/article/pii/S0732889315001030 [Accessed 21st November 2015].

Eaktasang, N., Kang, C., Jung Ryu, S., Suma, Y. and Kim, H. (2013) Enhanced Current Production by Electroactive Biofilm of Sulfate-Reducing Bacteria in the Microbial Fuel Cell. *Environmental Engineering Research*, 18(4) 227-281. Available from: http://kpubs.org/article/articleMain.kpubs?articleANo=E1HGBK_2013_v18n4_277 [Accessed 21st November 2015].

Eijkelkamp, B., Hassan, K., Paulsen, I. and Brown, M. (2011) Investigation of the human pathogen *Acinetobacter baumannii* under iron limiting conditions. *BMC Genomics*, 12(126). Available from http://www.biomedcentral.com/1471-2164/12/126 [Accessed 21st November 2015].

Eucast. (2003) Determination of minimum inhibitory concentrations (MICs) of antibacterial agents by broth dilution. *Clinical Microbiology and Infection*, 9(8) 1–7. Available from http://www.sciencedirect.com/science/article/pii/S1198743X14640635 [Accessed 23rd November 2015].

Falagas, M. and Kasiakou, S. (2005) Colistin: the revival of polymyxins for the management of multidrug-resistant gram-negative bacterial infections. *Clinical infectious diseases : an official publication of the Infectious Diseases Society of America*, 40(9) 1333–1341. Available from http://cid.oxfordjournals.org/content/40/9/1333.long [Accessed 19th November 2015].

Feng, X., Sambanthamoorthy, K., Palys, T. and Paranavitana, C. (2013) The human antimicrobial peptide LL-37 and its fragments possess both antimicrobial and antibiofilm activities against multidrug-resistant *Acinetobacter baumannii*. *Peptides*, 49(2013) 131–137. Available from: http://www.sciencedirect.com/science/article/pii/S0196978113003203 [Accessed 21st November 2015].

Fernando, D. and Kumar, A. (2012) Growth phase-dependent expression of RND efflux pump- and outer membrane porin-encoding genes in *Acinetobacter baumannii* ATCC 19606. *The Journal of antimicrobial chemotherapy*, 67(3), pp.569–72. Available from http://jac.oxfordjournals.org/content/67/3/569.long [Accessed 21st November 2015].

Ferre, R., Melo, M., Correia, A., Feliu, L., Bardaji, E., Planas, M. and Castanho, M. (2009) Synergistic effects of the membrane actions of cecropin-melittin antimicrobial hybrid peptide BP100. *Biophysical Journal*, 96(5) 1815–1827. Available from http://www.sciencedirect.com/science/article/pii/S0006349509002306 [Accessed 11th November 2015].

Gaddy, J., Arivett, B., McConnell, M., López-Rojas, R., Pachón, J. and Actis, L. (2012) Role of acinetobactin-mediated iron acquisition functions in the interaction of *Acinetobacter baumannii* strain ATCC 19606T with human lung epithelial cells, Galleria mellonella caterpillars, and mice. *Infection and immunity*, 80(3) 1015–24. Available from

http://www.ncbi.nlm.nih.gov/pmc/articles/PMC3294665/ [Accessed 21st November 2015].

Gaddy, J., Tomaras, A. and Actis, L. (2009) The *Acinetobacter baumannii* 19606 OmpA Protein Plays a Role in Biofilm Formation on Abiotic Surfaces and in the Interaction of This Pathogen with Eukaryotic Cells. Infection and Immunity, 77(8) 3150-3160. Available from: http://iai.asm.org/content/77/8/3150.full [Accessed 21st November 2015].

Giamarellou, H., Antoniadou, A. and Kanellakopoulou, K. (2008) *Acinetobacter baumannii*: a universal threat to public health? *International Journal of Antimicrobial Agents*, 32(2) 106–119. Available from http://www.sciencedirect.com/science/article/pii/S092485790800109X [Accessed 18th November 2015].

Goh, H., Beatson, S., Totsika, M., Moriel, D., Phan, M., Szubert, J., Runnegar, N., Sidjabat, H., Paterson, D., Nimmo, G., Lipman, J. and Schembri, M. (2013) Molecular analysis of the *Acinetobacter baumannii* biofilm-associated protein. *Applied and environmental microbiology*, 79(21) 6535–43. Available from: http://www.ncbi.nlm.nih.gov/pmc/articles/PMC3811493/ [Accessed 21st November 2015].

Gopal, R., Kim, Y., Lee, J., Lee, S., Chae, J., Son, B., Seo, C. and Park, Y. (2014) Synergistic effects and antibiofilm properties of chimeric peptides against multidrug-resistant *Acinetobacter baumannii* strains. *Antimicrobial Agents and Chemotherapy*, 58(3) 1622–1629. Available from http://www.ncbi.nlm.nih.gov/pmc/articles/PMC3957903/ [Accessed 21st November 2015].

Gordon, N. and Wareham, D. (2010) Multidrug-resistant *Acinetobacter baumannii*: mechanisms of virulence and resistance. *International Journal of Antimicrobial Agents*, 35(3) 219–226. Available from http://www.sciencedirect.com/science/article/pii/S0924857909005159 [Accessed 21st November 2015].

Gordon, Y., Romanowski, E. and McDermott, A. (2005) A review of antimicrobial peptides and their therapeutic potential as anti-infective drugs. *Current eye research*, 30(7) 505–515. Available from http://www.ncbi.nlm.nih.gov/pmc/articles/PMC1497874/ [Accessed 21st November 2015].

Guaní-Guerra, E., Santos-Mendoza, T., Lugo-Reyes, S. and Terán, L, (2010) Antimicrobial peptides: General overview and clinical implications in human health and disease. *Clinical Immunology*, 135(1) 1–11. Available from: http://www.sciencedirect.com/science/article/pii/S1521661609009127 [Accessed 27th November 2015].

Hall, B., Acar, H., Nandipati, A. and Barlow, M. (2014) Growth Rates Made Easy. Mol Biol Evol, 31(1) 232-238. Available from: http://mbe.oxfordjournals.org/content/31/1/232.full.pdf+html [Accessed 30th November 2015].

Harrison, J., Ceri, H., Yerly, J., Stremick, C., Hu, Y., Martinuzzi, R. and Turner, R. (2006) The use of microscopy and three-dimensional visualization to evaluate the structure of microbial biofilms cultivated in the Calgary Biofilm Device. *Biological procedures online*, 8(1) 194–215. Available from http://www.ncbi.nlm.nih.gov/pmc/articles/PMC1779619/ [Accessed 30th November 2015].

Høiby, N., Bjarnsholt, T., Givskov, M., Molin, S. and Ciofu, O. (2010) Antibiotic resistance of bacterial biofilms. *International Journal of Antimicrobial Agents*, 35(4) 322–332. Avaiable from http://www.sciencedirect.com/science/article/pii/S0924857910000099 [Accessed 24th November 2015].

Hou, K., Pan, H., Schlesinger, P. and Wickline, S. (2015) A role for peptides in overcoming endosomal entrapment in siRNA delivery-A focus on melittin. *Biotechnology Advances*, 33(6) 931–940. Available from http://www.sciencedirect.com/science/article/pii/S0734975015300045 [Accessed 22nd November 2015].

IBM Corp. (2012). IBM SPSS Statistics for Windows. [software] version 21.0. Armonk, NY: IBM Corp. Available from: http://www-01.ibm.com/support/docview.wss?uid=swg24032236 [Accessed 2nd December 2015].

Isa, L., Antunes, C., Visca, P. and Towner, K. (2014) *Acinetobacter baumannii*: evolution of a global pathogen. Pathogens and Disease, 71(3) 292-301. Available from http://onlinelibrary.wiley.com/doi/10.1111/2049-632X.12125/abstract [Accessed 21st November 2015].

Jenssen, H., Hamill, P. and Hancock, R. (2006) Peptide antimicrobial agents. *Clinical Microbiology Reviews*, 19(3) 491–511. Available from

http://www.ncbi.nlm.nih.gov/pmc/articles/PMC1539102/ [Accessed 21st November 2015].

Joo, SH. 2012 Cyclic Peptides as Therapeutic Agents and Biochemical Tools. Biomolecules and Therapeutics, 20(1) 19-26. Available from: http://www.ncbi.nlm.nih.gov/pmc/articles/PMC3792197/ [Accessed 28th April 2016].

Jurtshuk, P. and McQuitty, D. (1976) Use of a quantitative oxidase test for characterizing oxidative metabolism in bacteria. *Applied and Environmental Microbiology*, 31(5) 668-679. Available from: http://www.ncbi.nlm.nih.gov/pmc/articles/PMC291174/ [Accessed 23rd November 2015].

Kaemmer, S. (2011) Application Note # 133 Introduction to Bruker ' s ScanAsyst and PeakForce Tapping AFM Technology. *Bruker*, 1–12. Available from https://www.bruker.com/fileadmin/user_upload/8-PDF-Docs/SurfaceAnalysis/AFM/ApplicationNotes/Introduction_to_Brukers_ScanAsyst_and_PeakForce_Tapping_Atomic_Force_Microscopy_Technology_AFM_AN133.pdf [Accessed 21st November 2015].

Karageorgopoulos, D, and Falagas, M. (2008) Current control and treatment of multidrug-resistant *Acinetobacter baumannii* infections. *The Lancet Infectious Diseases*, 8(12) 751–762. Available from http://www.sciencedirect.com/science/article/pii/S1473309908702792 [Accessed 23rd November 2015].

Kassamali, Z., Rupali, J. and Danziger, L. (2015) An Update on the arsenal for multidrug-resistant Acinetobacter infections: Polymyxin antibiotics. *International Journal of Infectious Disease*, 30(2015) 125-132. Available from: http://www.sciencedirect.com/science/article/pii/S120197121401666X [Accessed 1st December 2015].

Lakshmaiah Narayana, J. and Chen, J. (2015) Antimicrobial peptides: Possible anti-infective agents. [in press] *Peptides*. Available from http://www.sciencedirect.com/science/article/pii/S0196978115001680 [Accessed 19th November 2015].

Lavertovich, O. (2012). Confocal Fluorescence Microscopy Optical Imaging and Spectroscopy. Characterization of Materials 2nd edition, 1-15. Available from: http://onlinelibrary.wiley.com/doi/10.1002/0471266965.com127/abstract [Accessed 13th November 2015].

Laverty, G., Gorman, S., and Gilmore, B. (2011) The Potential of Antimicrobial Peptides as Biocides. *International Journal of Molecular Sciences*, 12(12) 6566–6596. Available from http://www.mdpi.com/1422-0067/12/10/6566 [Accessed 12th November 2015].

Leica. (2015) Leica Application Suite X. Leica Microsystems. Available from: http://www.leica-microsystems.com/products/microscope-software/software-for-life-science-research/las-x-powerful-and-flexible/ [Accessed 11th November 2015].

Lewis, K. (2012) Recover the lost art of drug discovery. *Nature*, 485(7399) 439-440. Available from http://www.nature.com/nature/journal/v485/n7399/full/485439a.html [Accessed 22nd November 2015].

Li, A, Lee, P., Ho, B., Ding, J., and Lim, C. (2007). Atomic force microscopy study of the antimicrobial action of Sushi peptides on Gram negative bacteria. *Biochimica et biophysica acta-Biomembranes*, 1768(3) 411–418. Available from http://www.sciencedirect.com/science/article/pii/S0005273606004858 [Accessed 21st November 2015].

Li, J., Rayner, C., Nation, R., Owen, R., Spelman, D., Tan, K. and Liolios, L. (2006) Heteroresistance to colistin in multidrug-resistant *Acinetobacter baumannii*. *Antimicrobial agents and chemotherapy*, 50(9) 2946–50. Available from http://www.ncbi.nlm.nih.gov/pmc/articles/PMC1563544/ [Accessed 13th November 2015].

Li, Y., Xiang, Q., Zhang, Q., Huang, Y. and Su, Z. (2012) Overview on the recent study of antimicrobial peptides: Origins, functions, relative mechanisms and application. *Peptides*, 37(2) 207–215. Available from http://www.sciencedirect.com/science/article/pii/S0196978112003002 [Accessed 21st November 2015].

Loehfelm, T., Luke, N. and Campagnari, A. (2008) Identification and characterization of an *Acinetobacter baumannii* biofilm-associated protein. *Journal of Bacteriology*, 190(3) 1036–1044. Available from: http://www.ncbi.nlm.nih.gov/pmc/articles/PMC2223572/ [Accessed 21st November 2015].

Longo, F., Vuotto, C., Donelli, G. (2014). Biofilm formation in *Acinetobacter baumannii*. *New Microbiologica*, 37 119-127. Available from: http://www.newmicrobiologica.org/PUB/allegati_pdf/2014/2/119.pdf [Accessed 13th November 2015].

Longo, G. and Kasas, S. (2014). Effects of antibacterial agents and drugs monitored by atomic force microscopy. *Wiley Interdisciplinary Reviews: Nanomedicine and Nanobiotechnology*, 6(3) 230–244. Available from: http://onlinelibrary.wiley.com/doi/10.1002/wnan.1258/abstract [Accessed 14th November 2015].

Mah, TF., Pitts, B., Pellock, B., Walker, G., Stewart, P. and O'Toole, G. (2003) A genetic basis for Pseudomonas aeruginosa biofilm antibiotic resistance. *Nature*, 426 306-310. Available from: http://www.nature.com/nature/journal/v426/n6964/full/nature02122.html [Accessed 19th November 2015].

Manzini, M., Perez, K., Riske, K., Bozelli, J., Santos, T., Da Silva, M., Saraiva, G., Politi, M, Valente, A, Almeida, F., Chaimovich, H, Rodrigues, M., Bemquerer, M., Schreier, S. and Cuccovia, I. (2014) Peptide:Lipid ratio and membrane surface charge determine the mechanism of action of the antimicrobial peptide BP100. Conformational and functional studies. *Biochimica et Biophysica Acta-Biomembranes*, 1838(7) 1985–1999. Available from http://www.sciencedirect.com/science/article/pii/S0005273614001394 [Accessed 13th November 2015].

Maragakis, L. and Perl, T. (2008) *Acinetobacter baumannii*: epidemiology, antimicrobial resistance, and treatment options. *Clinical infectious diseases*, 46(8) 1254–1263. Available from http://cid.oxfordjournals.org/content/46/8/1254.long [Accessed 21st November 2015].

Maria-Neto, S., de Almeida, K., Macedo, M. and Franco, O. (2015) Understanding bacterial resistance to antimicrobial peptides: From the surface to deep inside. *Biochimica et Biophysica Acta (BBA) – Biomembranes*, 1848(11b) 3087-3088. Available from: http://www.sciencedirect.com/science/article/pii/S0005273615000577 [Accessed 21st November 2015].

Marumo, K., Komukai, D., Hirose, M., Nakamura, H., Tanaka, H., Ugajin, K., Nagashima, G., and Yoshimura, A. (2013) Evaluation in vitro of the efficacy of colistin methanesulfonate against biofilm-forming multidrug-resistant Pseudomonas aeruginosa (MDRP). *Journal of Infection and Chemotherapy*, 19(2), 348–351. Available from http://www.ncbi.nlm.nih.gov/pubmed/22872187 [Accessed 21st November 2015].

McConnell, M., Actis, L. and Pachón, J. (2013) *Acinetobacter baumannii*: Human infections, factors contributing to pathogenesis and animal models. *FEMS Microbiology Reviews*, 37(2) 130–155. Available from http://femsre.oxfordjournals.org/content/37/2/130.long [Accessed 21st November 2015].

Merritt, J., Kadouri, D. and O'Toole, G. (2005) Growing and analyzing static biofilms. Curr Protoc Microbiol, 1(2005) 1-29. Available from: http://www.ncbi.nlm.nih.gov/pubmed/18770545 [Accessed 25th November 2015].

Moffatt, J., Harper, M., Harrison, P., Hale, J., Vinogradov, E., Seemann, T., Henry, R., Crane, B., St. Michael, F., Cox, A., Adler, B., Nation, R., Li, J. and Boyce, J. (2010) Colistin resistance in *Acinetobacter baumannii* is mediated by complete loss of lipopolysaccharide production. *Antimicrobial Agents and Chemotherapy*, 54(12) 4971–4977. Available from http://www.ncbi.nlm.nih.gov/pmc/articles/PMC2981238/ [Accessed 21st November 2015].

National Center for Biotechnology Information. (2015) Crystal Violet. *PubChem Compound Database; CID=11057*. Available from http://pubchem.ncbi.nlm.nih.gov/compound/Crystal_violet [Accessed 1st November 2015].

Necas, D. and Klapetek, P. (2012) Gwyddion: an open-source software for SPM data analysis. *Central European Journal of Physics*, 10(1) 181-188. Available from: http://link.springer.com/article/10.2478%2Fs11534-011-0096-2 [Accessed 22nd November 2015].

Nguyen, L., Haney, E. and Vogel, H. (2011) The expanding scope of antimicrobial peptide structures and their modes of action. *Trends in Biotechnology*, 29(9) 464–472. Available from http://www.sciencedirect.com/science/article/pii/S0167779911000886 [Accessed 22nd November 2015].

Nuri, R., Shprung, T. and Shai, Y. (2015) Defensive remodeling: How bacterial surface properties and biofilm formation promote resistance to antimicrobial peptides. *Biochimica et Biophysica Acta (BBA)-Biomembranes*. Available from http://www.sciencedirect.com/science/article/pii/S0005273615001790 [Accessed 25th November 2015].

O'Neill, J. (2014) Antimicrobial Resistance : Tackling a crisis for the health and wealth of nations. *Review on Antimicrobial Resistance.* Available from http://amr-review.org/Publications [Accessed 18th November 2015].

O'Neill, J. (2015) Securing new drugs for future generations: the pipeline of antibiotics. *Review on Antimicrobial Resistance.* Available from http://amr-review.org/Publications [Accessed 11th November 2015].

Olson, M., Ceri, H., Morck, D., Buret, A., and Read, R. (2002) Biofilm bacteria: Formation and comparative susceptibility to antibiotics. *Canadian Journal of Veterinary Research* 66(2) 86–92. Available from http://www.ncbi.nlm.nih.gov/pmc/articles/PMC226988/ [Accessed 21st November 2015].

Peleg, A., Seifert, H. and Paterson, D. (2008) *Acinetobacter baumannii*: Emergence of a successful pathogen. *Clinical Microbiology Reviews*, 21(3) 538–582. Available from http://www.ncbi.nlm.nih.gov/pmc/articles/PMC2493088/ [Accessed 1st November 2015].

Potron, A., Poirel, L. and Nordmann, P. (2015) Emerging broad-spectrum resistance in *Pseudomonas aeruginosa* and *Acinetobacter baumannii*: Mechanisms and epidemiology. *International Journal of Antimicrobial Agents*, 45(6) 568-585. Available from http://www.sciencedirect.com/science/article/pii/S0924857915001041 [Accessed 21st November 2015].

Pott, T., Gerbeaud, C., Barbier, N. and Méléard, P. (2015) Melittin modifies bending elasticity in an unexpected way. *Chemistry and Physics of Lipids*, 185(2015) 99–108. Available from http://www.sciencedirect.com/science/article/pii/S000930841400067X [Accessed 21st November 2015].

Reeks, B., Champlin, F., Paulsen, D., Scruggs, D. and Lawrence, L. (2005) Effects of sub-minimum inhibitory concentration antibiotic levels and temperature on growth kinetics and outer membrane protein expression in *Mannheimia haemolytica* and *Haemophilus somnus*. Canadian Journal of Vertinary Research, 69(1) 1-10. Available from: http://www.ncbi.nlm.nih.gov/pmc/articles/PMC1142163/ [Accessed 1st December 2015].

Rhouma, M., Beaudry, F., Theriault, W., Bergeron, N., Laurent-Lewandowski, S., Fairbrother, J., Letellier, A. (2015) Gastric stability and oral bioavailability of colistin sulfate in pigs challenged or not with Escherichia coli O149: F4 (K88). *Research in Veterinary Science*, 102, 173-181. Available from:

http://www.sciencedirect.com/science/article/pii/S0034528815300370 [Accessed 29th April 2016].

Rice, L. (2008) Federal funding for the study of antimicrobial resistance in nosocomial pathogens: no ESKAPE. *The Journal of infectious diseases*, 197(8) 1079–1081. Available from http://jid.oxfordjournals.org/content/197/8/1079.long [Accessed 1st November 2015].

Rifflet, A., Gavalda, S., Téné, N., Orivel, J., Leprince, J., Guilhaudis, L., Génin, E., Vétillard, A. and Treilhou, M. (2012) Identification and characterization of a novel antimicrobial peptide from the venom of the ant *Tetramorium bicarinatum*. *Peptides*, 38(2) 363–370. Available from http://www.sciencedirect.com/science/article/pii/S0196978112003828 [Accessed 17th November 2015].

Robert, L. (2015) Size sensors in bacteria, cell cycle control, and size control. Frontiers in Microbiology, 6(515). Available from: http://www.ncbi.nlm.nih.gov/pmc/articles/PMC4448035/ [Accessed 16th November 2015].

Rodríguez-Rojas, A., Rodríguez-Beltrán, J., Couce, A. and Blázquez, J. (2013) Antibiotics and antibiotic resistance: A bitter fight against evolution. *International Journal of Medical Microbiology*, 303(6-7) 293–297. Available from http://www.sciencedirect.com/science/article/pii/S1438422113000192 [Accessed 21st November 2015].

Rolfe, M., Rice, C., Lucchini, S., Pin, C., Thompson, A., Cameron, A., Alston, M., Stringer, M., Betts, R., Baranyi, J., Peck, M. and Hinton, J. (2012) Lag Phase Is a Distinct Growth Phase That Prepares Bacteria for Exponential Growth and Involves Transient Metal Accumulation. *Journal of Bacteriology*, 194(3) 686-701. Available from: http://jb.asm.org/content/194/3/686.full [Accessed 1st December 2015].

Rossolini, G., Arena, F., Pecile, P. and Pollini, S. (2014) Update on the antibiotic resistance crisis. *Current Opinion in Pharmacology*, 18, 56–60. Available from http://www.sciencedirect.com/science/article/pii/S1471489214001052 [Accessed 21st November 2015].

RZ Lab. (2016) Helical Wheel Projects. *RZlab*, Available at: http://rzlab.ucr.edu/scripts/wheel/wheel.cgi?sequence=ABCDEFGHIJLKMNOP&submit=Submit [Accessed 25th April 2016].

Sauger, J., Rodriguez-Hernandez, M., De la Torre, B., Panchon-Ibanez, E., Fernandez-Reyes, M., Andreu, D., Pachon, J. and Rivas, L. (2006) Activity of Cecropin A-Melittin Hybrid Peptides against Colistin-Resistant Clinical Strains of *Acinetobacter baumannii*: Molecular Basis for the Differential Mechanisms of Action. *Antimicrobial Agents and Chemotherapy*, 50(4) 1251-1256. Available from: http://www.ncbi.nlm.nih.gov/pmc/articles/PMC1426946/ [Accessed 1st December 2015].

Schumann, P. and Pukall, R. (2013) The discriminatory power of ribotyping as automatable technique for differentiation of bacteria. Systematic and Applied Microbiology, 36(6) 369-375. Available from: http://www.sciencedirect.com/science/article/pii/S072320201300091X [Accessed 21st November 2015].

Seo, M-D., Won, H.-S., Kim, J-H., Mishig-Ochir, T. and Lee, B-J. (2012) Antimicrobial Peptides for Therapeutic Applications: A Review. *Molecules*, 17(10) 12276–12286. Available from http://www.mdpi.com/1420-3049/17/10/12276 [Accessed 21st November 2015].

Sharma, S., Sen, P., Mukhopadhyay, S. and Guha, S. (2003) Microbicidal male contraceptive—Risug induced morphostructural damage in E. coli. *Colloids and Surfaces B: Biointerfaces*, 21(1) 43-50. Available from: http://www.sciencedirect.com/science/article/pii/S0927776503001310 [Accessed 21st November 2015].

Shin, S., Kim, B., Park, S., Jo, S. and Lee, I. (2014) Haloganan: a novel antimicrobial peptide for treatment of wound infections. *Peptides*, 62(2014) 137–43. Available from: http://www.sciencedirect.com/science/article/pii/S0196978114002964 [Accessed 20th November 2015].

Silhavy, T., Kahne, D. and Walker, S. (2010) The bacterial cell envelope. *Cold Spring Harbor perspectives in biology*, 2(5). Available from http://cshperspectives.cshlp.org/content/2/5/a000414.full [Accessed 20th November 2015].

Song, J., Cheong, H., Noh, J, and Kim, W. (2015) In vitro Comparison of Anti-Biofilm Effects against Carbapenem-Resistant *Acinetobacter baumannii* : Imipenem , Colistin , Tigecycline , Rifampicin and Combinations. Infection and Chemotherapy, 47(1) 27–32. Available from: http://www.ncbi.nlm.nih.gov/pmc/articles/PMC4384457/ [Accessed 11th November 2015].

Soon, R., Nation, R., Harper, M., Adler, B., Boyce, J., Tan, C., Li, J. and Larson, I. (2011) Effect of colistin exposure and growth phase on the surface properties of live *Acinetobacter baumannii* cells examined by atomic force microscopy. *International Journal of Antimicrobial Agents*, 38(6) 493–501. Available from: http://www.sciencedirect.com/science/article/pii/S0924857911003311 [Accessed 11th November 2015].

Soon, R., Nation, R., Hartley, P., Larson, I. and Li, J. (2009) Atomic force microscopy investigation of the morphology and topography of colistin-heteroresistant *Acinetobacter baumannii* strains as a function of growth phase and in response to colistin treatment. *Antimicrobial Agents and Chemotherapy*, 53(12) 4979–4986. Available from: http://www.ncbi.nlm.nih.gov/pmc/articles/PMC2786353/ [Accessed 1st November 2015].

Souza, A., Díaz-Dellavalle, P., Cabrera, A., Larrañaga, P., Dalla-Rizza, M. and De-Simone, S. (2013) Antimicrobial activity of pleurocidin is retained in Plc-2, a C-terminal 12-amino acid fragment. *Peptides*, 45(2013) 78–84. Available from: http://www.sciencedirect.com/science/article/pii/S0196978113001411 [Accessed 21st November 2015].

Stocks, S. (2004) Mechanism and use of the commercially available viability stain, BacLight. *Cytometry Part A*, 61(August) 189–195. Available from http://onlinelibrary.wiley.com/doi/10.1002/cyto.a.20069/epdf [Accessed 23rd November 2015].

Stukalov, O., Korenevsky, A., Beveridge, T. and Dutcher, J. (2008) Use of atomic force microscopy and transmission electron microscopy for correlative studies of bacterial capsules. *Applied and environmental microbiology*, 74(17) 5457–65. Available from: http://www.ncbi.nlm.nih.gov/pmc/articles/PMC2546619/ [Accessed 2nd December 2015].

Subasinghage, A., O'Flynn, D., Conlon, J. and Hewage, C. (2011) Conformational and membrane interaction studies of the antimicrobial peptide alyteserin-1c and its analogue [E4K]alyteserin-1c. *Biochimica et Biophysica Acta - Biomembranes*, 1808(8) 1975–1984. Available from: http://www.sciencedirect.com/science/article/pii/S0005273611001179 [Accessed 19th November 2015].

Téné, N., Roche-Chatain, V., Rifflet, A., Bonnafé, E., Lefranc, B., Leprince, J. and Treilhou, M. (2014) Potent bactericidal effects of bicarinalin against strains of the *Enterobacter*

and *Cronobacter* genera. *Food Control*, 42(2014) 202–206. Available from http://www.sciencedirect.com/science/article/pii/S0956713514000954 [Accessed 18th November 2015].

The Global Health Network. (2013) Microbiology Standard Operating Procedure-Bacterial Identification using BioMerieux API Kits. Available from: https://globalhealthlaboratories.tghn.org/site_media/media/articles/Bacterial_Identification_API_Kits.docx [Accessed 17th November 2015].

ThermoFisher Scientific. (2015) LIVE/DEAD® BacLight™ Bacterial Viability Kit, for microscopy & quantitative assays. ThermoFisher Scientific. Available from: https://www.thermofisher.com/order/catalog/product/L7012 [Accessed 1st December 2015].

Toh, B., Paterson, D, Kamolvit, W., Zowawi, H., Kvaskoff, D., Sidjabat, H., Wailan, A., Peleg, A. and Huber, C. (2015) Species identification within *Acinetobacter calcoaceticus–baumannii* complex using MALDI-TOF MS. *Journal of Microbiological Methods*, 118(2015) 128–132. Available from http://www.sciencedirect.com/science/article/pii/S0167701215300610 [Accessed 21st November 2015].

Torcato, I., Hiang, YH., Franquelim, H., Caspar, D., Craik, D., Castanho, M. and Henriques, S. (2013) Design and characterization of novel antimicrobial peptides, R-BP100 and RW-BP100, with activity against Gram-negative and Gram-positive bacteria. *Biochimica et Biophysica Acta (BBA) – Biomembranes*, 1828(3) 944-955. Available from: http://www.sciencedirect.com/science/article/pii/S0005273612004270 [Accessed 21st November 2015].

Van Acker, H., Van Dijck, P. and Coenye, T. (2014) Molecular mechanisms of antimicrobial tolerance and resistance in bacterial and fungal biofilms. Trends in Microbiology 22(6) 326–333. Available from http://www.sciencedirect.com/science/article/pii/S0966842X14000249 [Accessed 21st November 2015].

Vaneechoutte, M., Dijkshoorn, L., Nemec, A., Kämpfer, P. and Wauters, G. (2011) Manual of Clinical Microbiology, 10th Edition. *American Society of Microbiology*. Available from: http://www.asmscience.org/content/book/10.1128/9781555816728.chap42 [Accessed 21st November 2015].

Velkov, T., Thompson, P., Nation, R. and Li, J. (2010) Structure—Activity Relationships of Polymyxin Antibiotics, *J Med Chem*, 53 1898–1916. Available from: http://www.ncbi.nlm.nih.gov/pmc/articles/PMC2907661/ [Accessed 26th April 2016].

Wadhwani, W., Strandberg, E., Van den Berg, J., Mink, C., Burck, J., Cirieloo, R., Ulrich, A. (2014) Dynamical structure of the short multifunctional peptide BP100

in membranes. *Biochimica et Biophysica Acta (BBA) – Biomembranes* 1838(3) 940-949. Available from: http://www.sciencedirect.com/science/article/pii/S0005273613003982 [Accessed 27th April 2016].

Webb, H., Khanh Truong, V., Hasan, J., Crawford, R. and Ivanova, E. (2011) Physico-mechanical characterisation of cells using atomic force microscopy-Current research and methodologies. *Journal of Microbiological Methods*, 86(2) 131-139. Available from: http://www.sciencedirect.com/science/article/pii/S0167701211002119 [Accessed 24th November 2015].

Wiegand, I., Hilpert, K. and Hancock, R. (2008) Agar and broth dilution methods to determine the minimal inhibitory concentration (MIC) of antimicrobial substances. *Nature protocols*, 3(2) 163–75. Available from: http://www.nature.com/nprot/journal/v3/n2/full/nprot.2007.521.html [Accessed 1st December 2015].

Zeng, X. and Lin, J. (2013) Beta-lactamase induction and cell wall metabolism in Gram-negative bacteria. *Frontiers in Microbiology*, 4(128) 1–9. Available from http://www.ncbi.nlm.nih.gov/pmc/articles/PMC3660660/ [Accessed 13th November 2015].

Zhou, W., Apkarian, R., Wang, Z. and Joy, D. (eds) (2007) *Scanning Microscopy for Nanotechnology,* Techniques and Applications. 1st Edition. New York. Springer.

8 Appendices

8.1 API 20NE Results sheet

(The Global Health Network, 2015)

TEST	REACTION	NEGATIVE	POSITIVE
$NO_3 \rightarrow NO_2$ $NO_2 \rightarrow N_2$	Reduction of potassium nitrate	Colourless Red/pink	Red (NIT1+NIT2) Colourless (Zn)
TRP	Indole production from tryptophan	Yellow	Pink
GLU	Glucose fermentation	Blue/green	Yellow
ADH	Arginine hydrolysis	Yellow	Orange/pink/red
URE	Urea hydrolysis	Yellow	Orange/pink/red
ESC	Aesculin hydrolysis	Yellow	Grey/brown/black
GEL	Gelatin hydrolysis	No pigment diffusion	Diffusion of black pigment
PNPG	p-nitrophenyl-βD-galactopyranoside hydrolysis	Colourless	Yellow
GLU	Glucose assimilation	Transparent	Opaque
ARA	Arabinose assimilation	Transparent	Opaque

MNE	Mannose assimilation	Transparent	Opaque
MAN	Mannitol assimilation	Transparent	Opaque
NAG	N-acetyl-glucosamine assimilation	Transparent	Opaque
MAL	Maltose assimilation	Transparent	Opaque
GNT	Gluconate assimilation	Transparent	Opaque
CAP	Caprate assimilation	Transparent	Opaque
ADI	Adipate assimilation	Transparent	Opaque
MLT	Malate assimilation	Transparent	Opaque
CIT	Citrate assimilation	Transparent	Opaque
PAC	Phenyl-acetate assimilation	Transparent	Opaque
Oxidase	Cytochrome oxidase	Colourless	Purple

8.2 Maximum dilutions per hour and which dilutions being spread plated.

Hour	Max Dilutions	Dilutions Spread
0	10^{-5}	10^{-3},10^{-4}, 10^{-5}
1	10^{-6}	10^{-4},10^{-5}, 10^{-6}
2	10^{-7}	10^{-5},10^{-6}, 10^{-7}
3	10^{-7}	10^{-5},10^{-6}, 10^{-7}
4	10^{-7}	10^{-5},10^{-6}, 10^{-7}
5	10^{-7}	10^{-5},10^{-6}, 10^{-7}
6	10^{-7}	10^{-5},10^{-6}, 10^{-7}
7	10^{-8}	10^{-6},10^{-7}, 10^{-8}
8	10^{-8}	10^{-6},10^{-7}, 10^{-8}
9	10^{-8}	10^{-6},10^{-7}, 10^{-8}
10	10^{-9}	10^{-7},10^{-8}, 10^{-9}
11	10^{-9}	10^{-7},10^{-8}, 10^{-9}
12	10^{-9}	10^{-7},10^{-8}, 10^{-9}
13	10^{-9}	10^{-7},10^{-8}, 10^{-9}
14	10^{-10}	10^{-8},10^{-9}, 10^{-10}
15	10^{-10}	10^{-8},10^{-9}, 10^{-10}
16	10^{-11}	10^{-9},10^{-10}, 10^{-11}
17	10^{-11}	10^{-9},10^{-10}, 10^{-11}
18	10^{-12}	10^{-10},10^{-11}, 10^{-12}
19	10^{-12}	10^{-10},10^{-11}, 10^{-12}

20	10^{-12}	10^{-10},10^{-11}, 10^{-12}
21	10^{-13}	10^{-11},10^{-12}, 10^{-13}
22	10^{-13}	10^{-11},10^{-12}, 10^{-13}
23	10^{-13}	10^{-11},10^{-12}, 10^{-13}
24	10^{-14}	10^{-12},10^{-13}, 10^{-14}
25	10^{-14}	10^{-12},10^{-13}, 10^{-14}
26	10^{-14}	10^{-12},10^{-13}, 10^{-14}
27	10^{-14}	10^{-12},10^{-13}, 10^{-14}
28	10^{-14}	10^{-12},10^{-13}, 10^{-14}
29	10^{-14}	10^{-12},10^{-13}, 10^{-14}
30	10^{-14}	10^{-12},10^{-13}, 10^{-14}